



Universidade do Minho  
Escola de Engenharia

Nelson Duarte Mendes Oliveira

Advanced in mould assembling  
technologies for high precision polymer  
based optical components



Universidade do Minho  
Escola de Engenharia

Nelson Duarte Mendes Oliveira

Advanced in mould assembling  
technologies for high precision polymer  
based optical components

Tese de Doutoramento  
Program Doutoral em Líderes para as Indústrias Tecnológicas

Trabalho efectuado sob a orientação do  
Professor Doutor António José Vilela Pontes

## STATEMENT OF INTEGRITY

I hereby declare having conducted my thesis with integrity. I confirm that I have not used plagiarism or any form of falsification of results in the process of the thesis elaboration.

I further declare that I have fully acknowledged the Code of Ethical Conduct of the University of Minho.

University of Minho, 11 de Outubro de 2014

Full name: Nelson Duarte Mendes Oliveira

Signature: \_\_\_\_\_



# ACKNOWLEDGEMENTS

---

I would like to take this opportunity to express my acknowledgment of the opportunity that has been given to me to perform this research. It has represented four years of intense experience, both scientific and personal, that has taken me through an incredible epic journey. My foremost thanks go to my supervisor, Professor Antonio Pontes, for his guidance, incentive, encouragement, availability and wisdom in helping me to perform my PhD studies. It has been a source of real satisfaction to be his student.

Furthermore, I would like to acknowledge Dr. Leite Pinto from Olesa and Dr. Rui Magalhães from PIEP for the support given on the development of this research project.

My gratitude also to Filipe Brito and José António from Olesa and to Engineer Carlos Azevedo from PIEP for their technical insights and their interest in helping me solve project problems arising and also to Professor Fernando Duarte and the student Valter Ferreira.

An acknowledgement of my thanks is owed to Renault and, more precisely, to Eng<sup>o</sup> Armindo de Almeida, Eng<sup>o</sup> Philippe Martz, Eng<sup>o</sup> Shohreh Tavakoli and many others, for the help given during my placement there. In particular, I wish to thank Eng<sup>o</sup> Armindo de Almeida for the help given on finding a place to stay during my internship in France.

I also want to express my gratitude for the financial support given by the InLaser project through the QREN program.

Finally, I would like to thank my family, my wife and my friends for their ongoing encouragement and support given during the entire PhD.



# Abstract

---

In recent years, the worldwide economic crisis and the continuing trend toward globalization have forced companies worldwide to seek to improve existing production systems or implement new manufacturing processes. So as to maintain a competitive edge in global markets, many companies have relocated their production facilities to countries where labor costs are lower. Compared to the optimization of existing production facilities and methods, relocation is a more complex process since it is invariably necessary to change existing suppliers for newer, more local sources, to construct new production facilities and to train new employees. To avoid these dislocations, a range of alternative solutions are available, for example the redesign of components or substitution of raw-materials. It was based on this problem that this project was initiated. This PhD had the objective of developing a new process capable of producing a functional automotive component in an optimized way and with a lower cost compared to existing processes. To achieve this objective intensive study was made into the concept of a manufacturing process utilizing established injection molding processes allied with the use of emergent laser welding technologies. These two processes were chosen mainly due to their capability of producing different components in a single process with a high rate of production and associated low cost.

To achieve the desired end, several tasks were undertaken. In the first instance a market research study was done so as to define which automotive component case study warranted particular examination. An in-depth appraisal of the state-of-the-art of the technologies involved in the projected manufacturing process was also undertaken. Following on identification of the optimal component case study to be produced by the hybrid production process, initial design of a mold and assembling process was undertaken, this ultimately leading on to the formulation of a business plan. This PhD was made in collaboration with PIEP and Olesa (Industrial partner).

A broad-brush market evaluation was made of the automobile and motorcycle market. This analysis was done to identify and evaluate the potential of possible component case studies. From this initial analysis two case studies were selected: a door trim and a rear lamp; after preliminary studies of the investment needed to produce

a complete door trim or a rear lamp, it was decided to focus on the rear lamp as the case study; the rear lamp chosen already exists on the market.

To adapt the existing rear lamp to be produced through this new process it was necessary to develop a new electric circuit and to change the resistive lamp to LEDs. To produce the electric conductive circuit, it was decided to use conductive polymers to increase the level of automation of the process. The modification made to the existing rear lamp was made according to legislation UNECE Vehicle Regulations - 1958 Agreement; Regulation No. 50 -Rev.2 - Position lamps, stop lamps, direction indicators for motorcycles. Based in this legislation and the chosen LEDs, it was necessary to use 11 LEDs, to emit the mandatory light flux. To ensure the success of the new electric conductive circuit, several conductive additives were mixed with PC and PP and then tested. These comparative conductive tests showed that the material that presented the best electric conductivity was PC with 5% of carbon nanotubes.

Another objective of this project was to examine the application of laser welding as the joining process. To study their viability in joining the different components of the rear lamp, several materials were studied - PC, PMMA and PP. As a corollary, the influence that commonplace additives such as talc and glass fibers have on the transmission of laser beam light was also examined. Laser welding of the different materials was characterized in terms of the resistance of the seams. According to the study results, the best combination of materials obtained would seem to be PMMA with PC while the best welding conditions are available with a minimum velocity of 20cm/min, a minimum power of 20W and a laser emitter 1mm in diameter. With the completion of these initial tests a preliminary hybrid manufacturing process using the two chosen technologies was identified and the design of the mold used to produce a functional rear lamp finalised.

The thesis, as structured, encompasses a comparative cost analysis examining and contrasting the comparable unit costs of production under the current manufacturing/ assembling process with those of the new hybrid process under study. The current process produces component subsystems with a lower cost when compared to the hybrid process for production batches smaller than 2800 units. After this batch size, the hybrid process produces subsystems with lower cost. In the thesis, a number of factors that influence the final price of the component subsystem were also studied and evaluated. In particular, the possibility to produce component subsystems with two injection machines in contra-cycle with one laser and robot was examined; this



production process seems capable of producing component subsystems with a lower cost and double the productive capacity when compared to the process initially studied.



# Sumário

---

A atual crise económica e a globalização têm levado a que muitas das empresas procurem otimizar os seus processos produtivos ou então deslocalizar a sua produção para países onde o custo de mão-de-obra é mais barata, de forma reduzir o custo final. Muitas das vezes, a deslocalização obriga à substituição dos atuais fornecedores, por fornecedores locais, construção de novas instalações e formação dos novos colaboradores o que torna esta solução muito dispendiosa. De forma a evitar os elevados custos de uma deslocalização, novas soluções podem ser desenvolvidas, tais como otimização do atual processo produtivo, otimização do componente ou modificação da matéria-prima. É neste sentido que este projeto de investigação se insere, ou seja, desenvolver um novo processo que permita produzir subsistemas completos de uma forma otimizada e com um custo inferior às soluções existentes no mercado.

De forma a obter o processo desejado várias tarefas foram realizadas, tais como estudo de mercado, estado da arte da tecnologia, o desenvolvimento técnico da ideia e finalmente a definição da estratégia de mercado. O trabalho foi realizado em colaboração com o PIEP e com a Olesa (parceiro industrial). Mais precisamente, o trabalho teve como objetivo, desenvolver uma célula de fabrico capaz de produzir subsistemas funcionais. Para isso foram utilizadas tecnologias como o laser e a montagem dentro do molde.

A primeira tarefa realizada consistiu em analisar o Mercado automóvel e de motociclos. Esta escolha deveu-se ao facto de serem estes os mercados, onde parceiro industrial já se encontra implementado. Para tal foram analisados vários mercados tais como o europeu, indiano, norte-americano e japonês. A pesquisa mostrou que a maioria dos mercados sofreu com a crise mundial excetuando o mercado indiano. Esta pesquisa permitiu definir dois casos de estudo possíveis, um painel de porta e um farol traseiro de um motociclo. Após a realização do estudo preliminar e alguns contactos com o parceiro industrial decidiu-se que caso de estudo a ser estudado seria o farol do motociclo.

Com a definição do caso de estudo, partiu-se para estado de arte das tecnologias definidas anteriormente e que serão utilizadas na célula de fabrico. O estado de arte revelou a existência de dois processos de soldadura por laser, um por transmissão e

outro direto. O processo de soldadura por transmissão necessita que um dos materiais seja transparente ao laser, enquanto o outro material deva ter a capacidade de absorver toda a energia emitida pelo mesmo. Neste processo são utilizados lasers de diodo e de Nd:YAG. A soldadura direta não tem os mesmos requisitos que o método anterior, uma vez que neste processo é utilizado laser de CO<sub>2</sub> que é absorvido por todos os materiais. A pesquisa sobre o processo de montagem dentro do molde demonstrou uma enorme variedade de processos. Mesmo assim, a maioria das técnicas baseia-se na utilização de variedade de processos. Mesmo assim, a maioria das técnicas baseia-se na utilização de placas rotativas nos moldes, robots ou então o processo de sobre-moldação.

O desenvolvimento do caso de estudo teve como primeira etapa a modificação do emissor de luz. O farol atual utiliza uma lâmpada incandescente, enquanto o novo farol utilizará LEDs (Diodo Emissor de Luz). Com a substituição do emissor foi necessário desenvolver estruturas refletoras de modo a que o farol cumprisse a legislação. O material condutor da corrente elétrica no interior do farol foi substituído por um polímero condutor. A última modificação realizada no farol consistiu na remoção das estruturas da soldadura por ultrassons, para superfícies lisas de modo a poder ser soldado por laser. Após analisar as modificações partiu-se para a definição do número LEDs necessários para cumprir a legislação, material condutor e as melhores condições de soldadura. Os estudos e os cálculos mostraram que são necessários 11 LEDs para cumprir a legislação. Em termos de condutividade elétrica o material que apresentou a menor resistividade foi o PC com 5% de nano tubos de carbono (CNT's). Em termos de soldadura a laser, a combinação de materiais que apresentou maior resistência mecânica foi a PMMA/PC. Para esta combinação de materiais, as melhores condições de soldadura são uma potência de 20W, uma velocidade de 20 cm/min e um diâmetro do laser de 1 mm. Para finalizar o estudo deste novo processo, foi efetuada uma análise financeira comparativa entre o processo atual e o novo. A análise demonstrou que a produção com esta célula de fabrico apresenta custos inferiores ao processo atual. O mesmo estudo demonstrou que utilizando duas injetoras em contra ciclo é possível aumentar a cadência de produção reduzindo ao mesmo tempo o custo final do farol traseiro. O edifício é o fator com maior peso no preço final do farol traseiro. Neste caso se em vez de adquirir o edifício existir a possibilidade de aluga-lo é possível reduzir o preço final do farol substancialmente em produções inferiores a 5000 unidades.

# Publications related with this Thesis

---

1. OLIVEIRA, N.; PONTES, A. J. - Advanced in mold assembling technologies for high precision polymer based optical components. Conference MIT Portugal, 2010.
2. OLIVEIRA, N.; PONTES, A. J. - Laser beam propagation through different polymeric materials; International Conference on Polymers and Molds Innovations 2012, Ghent, Belgium, 2012
3. OLIVEIRA, N.; PONTES, A. J. - Laser welding: effect of additives on the transparency and mechanical weld resistance of different polymeric materials; International Conference Portuguese Materials Society (SPM), Materiais 2013, Coimbra, Portugal, 2013
4. OLIVEIRA, N.; PONTES, A. J. - In mold laser welding for high precision polymer based optical components; International Conference on Polymer Processing Society 29, Nuremberg, Germany, 2013
5. OLIVEIRA, N.; PONTES, A. J. - Advanced in mold assembling technologies for high precision polymer based optical components. Conference MIT Portugal, Coimbra, Portugal, 2014.
6. OLIVEIRA, N.; PONTES, A. J. - Combination of laser welding with in-mold assembling into a single process. International Conference on Polymers and Molds Innovations 2014, Portugal, 2014

## Patent

OLIVEIRA, N.; MAGALHÃES, R., BRITO, F., PINTO, J., PONTES, A. J. – Sistema e método de injeção e soldadura, Patent Pending, 2014

# Table of contents

---

1	Introduction .....	2
2	Introduction .....	6
2.1	Market analysis .....	6
2.1.1	Motorcycle market .....	8
2.1.2	Automobile market .....	10
2.1.3	Optical component suppliers and manufactures .....	12
2.1.4	Daylights .....	16
2.1.5	Interior Door trim .....	17
3	State-of-the-art .....	22
3.1	Laser welding .....	22
3.1.2	Laser cut .....	33
3.1.3	Modeling the interaction between laser and matter .....	34
3.2	Non-conventional molding techniques .....	39
3.2.1	Overmolding .....	40
3.2.2	In-Mold operations .....	42
3.2.3	In-Mold-Decoration (IMD) .....	43
3.2.4	Injection welding process .....	43
3.2.5	“Ice Cold Trick” .....	45
3.2.6	Others techniques .....	45
3.3	Conductive polymers .....	46
3.4	Research method .....	47
4	New concept of the rear light .....	50
4.1	Introduction .....	50
4.2	Rear lamp design .....	51
4.2.1	LED (Light Emitting Diodes) .....	52
4.2.2	Electric circuit with conductive polymers .....	54
4.2.3	Preliminary tests of electric circuit .....	59
4.2.4	Secondary optics .....	66
4.3	Laser welding tests .....	70
4.3.1	Laser requirements .....	70
4.3.2	Transmittance analysis to the plastic materials .....	71
4.3.3	Preliminary welding tests and results .....	78

4.3.4	Test procedure .....	79
4.3.5	Mechanical tests results.....	82
4.3.6	Visual inspection results.....	94
4.4	Concluding remarks.....	100
5	Prototype tool for in-mold assembling .....	104
5.1	Simulation of the injection molding process.....	105
5.2	Mold concept .....	107
5.3	The manufacturing cell.....	109
5.3.1	The process tasks .....	114
5.4	Results and process validation .....	117
5.5	Concluding remarks.....	121
6	Cost analysis .....	124
6.1	Cost analysis .....	125
6.2	Conclusion .....	129
7	Conclusion .....	132
8	Future work .....	136
	Bibliography .....	138

# List of figures

---

Figure 1 USA market evolution [5].....	8
Figure 2 European market evolution [6] .....	9
Figure 3 Two wheel India market sales [7].....	9
Figure 4 Japanese motorcycle market sales [8].....	10
Figure 5 European automobile market [9] .....	10
Figure 6 The USA automobile market [10] .....	11
<b>Figure 7 The Indian automobile market [7] .....</b>	<b>12</b>
Figure 8 Japanese automobile sales [11].....	12
Figure 9 Laser welding by transmission [43].....	23
Figure 10 Laser welding methods [43] .....	24
Figure 11 Transmission Spectrum for major lasers types [43] .....	26
Figure 12 laser beam dimensions .....	29
Figure 13 transversal cut of a laser welding zone .....	30
Figure 14 Power intensity of a laser beam computed over a 1-mm-diameter hole [65]. .....	30
Figure 15 Set-up of hybrid-laser-MIG welding [67].....	31
Figure 16 local selectivity of the laser bonding (SBL) [68].....	32
Figure 17 laser cut process [54] .....	34
Figure 18 Snell's law (courtesy acousticslab.org).....	35
Figure 19 multi-material processes [84].....	40
Figure 20the IMD process [88] .....	43
Figure 21 The DSI process [89] .....	44
Figure 22the Foboha's TwinCube [91] .....	46
Figure 23 Conductivity of different materials [98] .....	47
Figure 24Research method.....	48
Figure 25Actual front view of the rear lamp.....	50
Figure 26 rear view of the rear lamp .....	51
Figure 27the number of LEDs according with lamp in use [115].....	54
Figure 28 configuration of the electric circuit.....	55
Figure 29the electric circuit for producing two types of lights [117].....	57
Figure 30the relative luminous flux versus electric current [118] .....	58
Figure 31 rear view of the electric circuit .....	58
Figure 32 frontal view of the electric circuit.....	59
Figure 33 mold for injecting the conductive material .....	59
Figure 34mold cavities.....	60
Figure 35 electric tension used to test the conductive material.....	60
Figure 36 light emission by the LED on the base section .....	61
Figure 37 POM mixed with 4% of CNT .....	62
Figure 38 Circuit test with PC with 4% of CNT .....	63
Figure 39 Circuit Test with PC with 5% of CNT.....	64
Figure 40 Final result of the PC with 5% of CNT.....	64
Figure 41 PP mixed with 5% (w/w) of CNT.....	65
Figure 42 PP mixed with 7% (w/w) of CNT.....	65



Figure 43 PP mixed with 9% (w/w) of CNT.....	66
Figure 44 Luminous intensity of the LEDs HPWT-MX [120] .....	66
Figure 45 The Secondary optics [120].....	67
Figure 46 factors that influence the built of the reflection parabolas [120] .....	67
Figure 47 different parabolas according with the different fs [120] .....	68
Figure 48 reflective cavities for the case study .....	68
Figure 49 the pillow optics factors [112] .....	69
Figure 50 geometry of the pillow optics [120].....	69
Figure 51 final design of the crystal with the optic pillows .....	70
Figure 52 specimen analyzed .....	73
Figure 53the transmittance analysis; PC and PMMA .....	74
Figure 54the transmittance analysis to PC and PC mixed with Glass Fiber .....	75
Figure 55 the Transmittance analysis of PP homopolymer and copolymer.....	76
Figure 56the transmittance analysis to PP mixtures.....	76
Figure 57 transmittance analysis of the mixture of PP with cellulose fibers .....	77
Figure 58 transmittance analysis of the mixture PP with Clearweld.....	78
Figure 59 specimen configuration.....	81
Figure 60 dimensions of the different specimens according with the final thickness .....	82
Figure 61 sample test welded by laser welding.....	82
Figure 62 Testing machine.....	83
Figure 63the Shear stress of the welded PC/PMMA specimens .....	84
Figure 64 Deformation of the PC/PMMA specimens .....	85
Figure 65 Shear Stress for the different amorphous materials .....	87
Figure 66 Deformation of the different amorphous materials.....	88
Figure 67 A new analysis to evaluate the Shear Stress of the PP/PP seam.....	89
Figure 68 Seam deformation for laser welding PP/PP .....	90
Figure 69 Comparison between PP / PP with additives .....	92
Figure 70 Deformation of the PP with different additives on their matrix .....	94
Figure 71 photos of the seam of the weld between PMMA with PC .....	95
Figure 72 photos of the weld made between PC with PC .....	96
Figure 73 specimen welded and injected with condition 1 .....	96
Figure 74 specimen welded and injected with conditions 2.....	97
Figure 75 specimen welded and injected with conditions 3.....	97
Figure 76 specimen welded and injected with conditions 4.....	98
Figure 77 specimen welded and injected with conditions 5.....	98
Figure 78 specimen welded and injected with conditions 6.....	99
Figure 79 specimen welded and injected with conditions 7.....	99
Figure 80 specimen welded and injected with conditions 8.....	100
Figure 81the final rear lamp. ....	104
Figure 82 crystal and housing prototypes .....	105
Figure 83 injection time for the fill the housing.....	105
Figure 84 volumetric shrinkage of the housing.....	106
Figure 85 injection time of the crystal .....	106
Figure 86 volumetric shrinkage of the crystal.....	107
Figure 87 the mold .....	108

Figure 88 the metallic ring (green lines) .....	108
Figure 89 mold concept.....	109
Figure 90 The Manufacturing cell.....	109
Figure 91 the manufacturing cell from a different perspective .....	110
Figure 92 laser head in more detail .....	110
Figure 93 Billion with the vertical unit and the laser protection.....	111
Figure 94the Piovan drying/dehumidifying unit .....	112
Figure 95 the laser and the NX100 robot control unit.....	112
Figure 96 the robot the laser head .....	113
Figure 97 robot control and robot console .....	113
Figure 98 different sections of the mold used on the process .....	114
Figure 99 Process Tasks (a: mold open; b: injection of all components; c: rotation of the plates; d: in-mold assembly).....	115
Figure 100 Laser Welding.....	116
Figure 101 ejection of the final subsystem (red part).....	117
Figure 102themold .....	118
Figure 103 ejection and transport of the crystal component .....	118
Figure 104the Crystal component .....	119
Figure 105 front and back side of the housing without the electric circuit .....	119
Figure 106 the housing with the electric circuit .....	120
Figure 107 the interaction between the PC and PP .....	120
Figure 108the final rear lamp .....	121
Figure 109assumption of the actual factory assembly layout .....	124
Figure 110the new production site .....	125
Figure 111 Comparison between the new and the old process .....	126
Figure 112 comparison between the process studied and variation .....	127
Figure 113 comparison between the old process with and without the rent .....	128
Figure 114 comparison between the new process with and without the rent.....	128
Figure 115 comparison between the new process variation with and without the rent.....	129
Figure 116 inputs for the new process .....	150
Figure 117 cost inputs for the old process.....	151

# List of tables

---

Table 1 Producers of optical components for cars and their products. ....	14
Table 2 Producers of optical components for motorcycles and their products .....	15
Table 3 Producers of door trims and their products. ....	18
Table 4 Different laser welding configurations [43-44].....	25
Table 5 Influence of the different additives on the final seam .....	27
Table 6 - processing conditions used on the injection molding tests of the conductive polymer	61
Table 7 injection molding conditions for POM.....	62
Table 8 injection molding conditions for the different materials tested.....	63
Table 9 Raw-materials analysed .....	72
Table 10 materials and additives studied .....	72
Table 11 Processing conditions of the amorphous polymers .....	73
Table 12 Processing conditions of the semi-crystalline materials.....	74
Table 13 Processing conditions of the semicrystalline material samples.....	79
Table 14 Processing conditions used to produce the PCs and PMMA samples .....	79
Table 15 Taguchi L8 table for PC with PMMA welding studies.....	80
Table 16 New Taguchi table for the PP .....	81
Table 17 DOE results for PMMA/PC .....	86
Table 18 DOE results for PP/PP .....	91



# Chapter 1

---

# 1 Introduction

In the highly competitive global automotive market, where each centime counts, the present global economic crisis has obliged companies to develop new strategies with the objective of reducing the final price of their products so as to remain competitive. To several companies the solution has been relocating their production facilities to other countries where labor cost are much lower when compared to European countries. Relocation has had particular impact within the ranks of TIER1 (supplier ranking) automotive component producing companies. For example, molds that in the past were produced in Europe are now made in mold-making companies in China, where comparative labor cost are lower. Another example is in the production of many plastic automotive components; hitherto, production was centered near to the automotive assembly plants. Now, dependant on the requisite batch size, these components can be produced in Colombia, Europe or China [1]. For that reason, if automotive component suppliers want to continue production of tools or components to TIER 1 companies, they need to constantly innovate and improve their production processes so as to further reduce unit costs.

The research presented in this thesis, is part of a continuing effort to develop a new process capable of diminish the lead time and consequently the cost of the final component. To be more specific, this new process stems from the needs of the mold-making company, Olesa. The company has found that if they want to maintain their competitive edge and retain major clients, they need to provide innovative solutions capable of producing products at highly competitive prices so as avoid losing out to lower labour cost countries or to more competitive lower cost suppliers. To maintain their competitiveness, Olesa is endeavoring to develop a manufacturing process capable of producing a complete subsystem such as a motorcycle lamp or a door trim in the same production cycle. After a brainstorming session between PIEP and Olesa, the idea to combine in-mold assembly and laser welding in the same process emerged. Based on this initial aim, several research objectives were identified:

1. Which component subsystems can be assembled using this combination of technologies?
2. How can this integration be made?
3. Are conductive polymers appropriate for use in this process?

4. Which are the best laser welding properties for joining the different components of the subsystem?
5. Is it possible to produce components with a lower cost compared to the current production and assembling process?

For achieve these objectives, a state-of-the-art appraisal was made of the two main technologies, laser welding and in-mold assembling. After this initial task, market research was undertaken with the support of Olesa to identify and define prospective component subsystems capable of being built by the new hybrid process. The third task entailed defining the necessary processes requisite for the production of the case study component identified. This focused mainly on defining which materials are best welded by laser, their optimal dimensions and the material to be used as well as examining the underlying characteristics of different lasers. The lasts three tasks of the research were focused on determining optimal laser welding properties and processes, the development of the mold and, finally, the business model for the new process. The business model analysis had the prime objective of defining the best sales strategy but was also structured to examine whether or not the new process had the capability to produce components with a lower cost when compared to existing production processes.

Component competitiveness aside, the research work underpinning this thesis is fundamentally a scientific contribution designed to enhance understanding of the interaction between a laser beam, a polymer and the admixture of conductive additives - set within the context of an industrial process. It is to be hoped that some scientific contribution to the area of polymer and mold development will also arise following on the innovations that were implemented to achieve the main objective.





## Chapter 2

---

## 2 Introduction

This chapter presents the results of a market analysis designed to decide which component case studies are best suited to the hybrid production process under study.

### 2.1 Market analysis

The main objective of the analysis was to find components suitable for production through a combination of a non-conventional molding technique and a laser welding technique. The secondary objective was to appraise the underlying competitiveness of components so produced vis-à-vis components produced using conventional production processes. With the support of an industrial partner, Olesa, market research was initiated with the objective of evaluating possible case studies. Two prime paths were followed, analysing the several automotive markets.

The global automotive market (cars, trucks, buses and motorcycles), is one of the most competitive, not only because of the large number of manufactures but also because of the enormous number of automotive component suppliers. Traditionally, these were mainly to be found in countries where automobile assembly factories were centered. Nowadays, this is not so important, lower ocean transportation costs progressively enhancing the importance of lower labor costs.

In this highly competitive market, eight major groups exist, the OEM's (Original Equipment Manufacturer) of the automotive world. The main groups are General Motors and Ford in the USA, Toyota and Honda in Japan, PSA (Peugeot Citroen) and Renault in France, Fiat in Italia, Hyundai in South Korea and the Volkswagen group in Germany. Other brands have a much lower market share. [2]

The Original Equipment Manufacturer motorcycle market is not markedly different from the car sector of the automotive market. According to Wikipedia there are 26 countries with at least one motorcycle manufacturer although much of the global production remains centered on a relatively small number of producer countries and companies. The Japan Automobile Manufacturers Association (JAMA) indicates that the major builders of motorcycles are China, India, Indonesia, Brazil, Japan, Taiwan, Thailand and Vietnam. Despite the large numbers of small-scale manufacturers, the

companies with enhanced market share are Honda, Yamaha, Kawasaki and Suzuki in Japan, Aprilia and Ducati in Italy, Triumph in the UK, Harley-Davidson in the USA and Guangzhou Motors, Zongshen Motorcycle and Shanghai Feiling Motorcycle in China. [3]

Underlying these numerous automobile and motorcycle manufacturers, it is possible to identify an extremely complex and constantly evolving supply chain. This chain goes from the raw material producer to the subsystem assembler. This supply chain is divided into different levels/ranks that normally are called TIER(s) denoting the ranking of individual suppliers according to the degree of commercial distance in the relationship between the OEM (Original Equipment Manufacturer) and supplier. At the end of the chain is the OEM, for example Ford. At the beginning of the chain are the TIER3 companies. These companies produce and supply the raw material and tools. TIER2 suppliers are the companies that define the standards for a particular component, for example, the dimensions of the tires on a vehicle. The TIER1 suppliers are the companies that produce and supply discrete components, such as armrests or door panels. They also can supply complete component systems or subsystems for assembly directly on-line within the factories of the OEM, for example, head light assemblies or a complete door trim. [4]

The product focus for this research study centered on the products produced by TIER1 companies since these companies supply the subsystems to the OEM companies. Global production data for the main subsystems, such as a head lights, rear lights or door trim are not available, year-on-year but reliable data is available for the vehicles produced worldwide. For that reason it was decided to use an approximation, between the number of vehicles (cars and motorcycles) sold and accompanying subsystem production volumes. The market research analysed Europe, the USA, Japan and India production. The Indian and European markets were chosen because Olesa is already implemented therein. The other two were chosen owing to their OEM brand status, and the relatively large size of their respective markets.

The first market research analysis was undertaken for the motorcycle market, followed by the automobile market.

### 2.1.1 Motorcycle market

The worldwide economic crisis and the high price of oil has affected the consumption of all durable goods. The research presented in this section seeks to analyse the impact on global motorcycle production volumes.

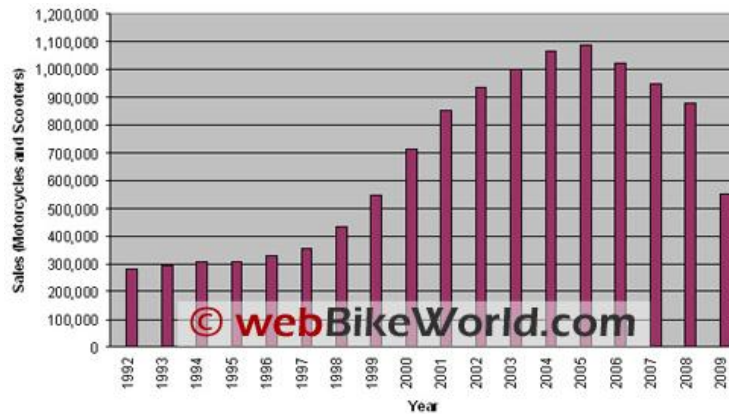


Figure 1 USA market evolution [5]

The first market analyzed was the United States of America. This market was analyzed between 1992 and 2009, Figure 1. The American market presented a behavior similar to a normal curve over the 11 year period 1999/2009. The market saw an augmented demand for motorcycles between 1992 until 2005 but, thereafter, demand started diminishing until reaching a minimum in 2009. The major fall in demand occurred between 2008 and 2009, a consequence of the rapid downturn in the pace of US economic production (and confidence) then current. All in all, US demand for motorcycles in 2009 was broadly similar to the level of demand in 1999

The European market was the second market analyzed. This market was analyzed between 2002 and 2007, Figure 2. In Europe the demand for two wheel transportation remained stable between 2002 and 2004. After that year, demand increased until it reached a maximum in 2006. The following year, demand started diminishing, to levels below those of 2005. The data gathered showed that the motorcycle has a higher share market than the moped. Overall, when compared to the US market the European market for two wheeled vehicles is seen to be almost double the size. Another difference between the two markets, is in the year when the demand started to fall off; in Europe this occurred in 2007 and in American in 2006.

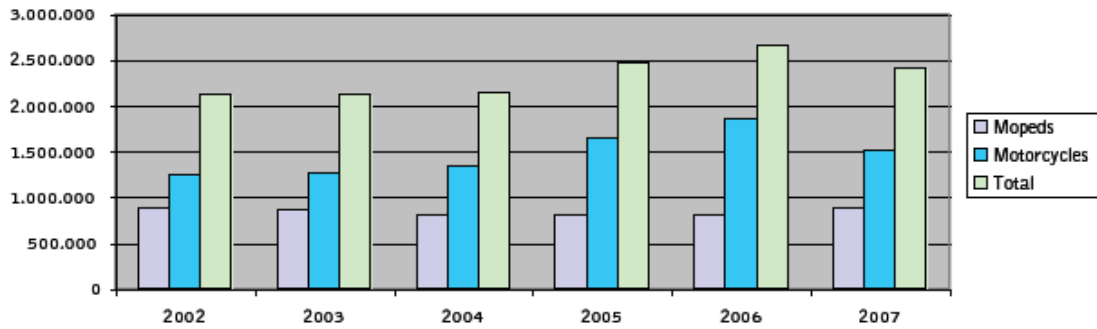


Figure 2 European market evolution [6]

The Indian market was the third market analyzed. This huge market was analyzed between 2005 and 2012, figure 3. Compared to the US and European markets, Indian two wheeled vehicle sales did not show any marked diminution in volume throughout the period of study. To be more specific, during the period analysed the demand for motorcycles decreased slightly over 2007/08 but has grown consistently in the study period thereafter, initially after a period of stabilization in demand over 2008/09. After 2009, it is possible to discern a linear growth behavior on the part of demand for two wheeled vehicles in India between 2009 and 2012.

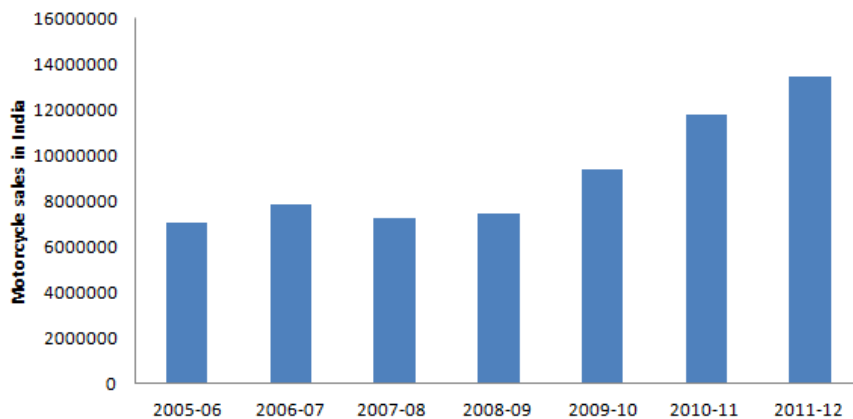


Figure 3 Two wheel India market sales [7]

The last market evaluated was the Japanese market. Figure 4 presents data as to the evolution of motorcycle demand within the major Japanese market over the course of the past 10 years. The market presented a relatively stable behavioral pattern, until the second semester of 2007; the first semester of 2008 then showed a large reduction in demand for Japanese motorcycles and the following semesters have seen a continuing decline in demand through the last semester of 2009. As can be seen, during the first

semester of 2010 some small growth in aggregate Japanese motorcycle demand was registered.

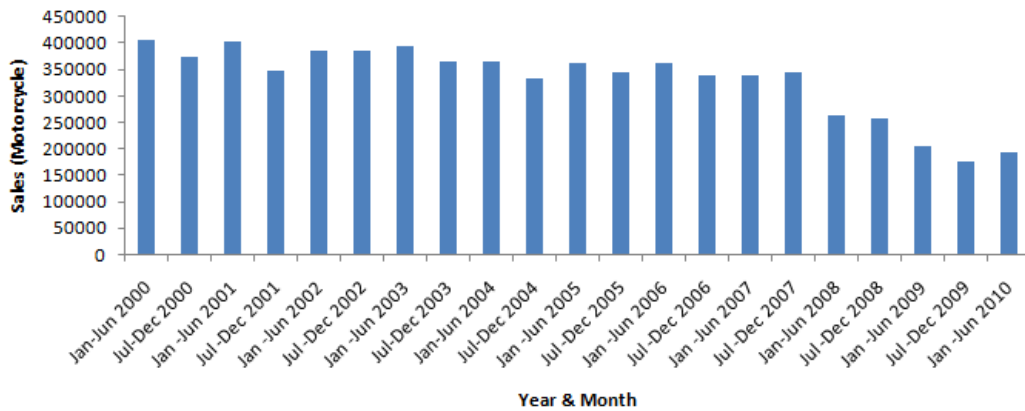


Figure 4 Japanese motorcycle market sales [8]

### 2.1.2 Automobile market

Crisis impacted sales volumes have also been a prominent feature within the global automobile industry over much of the recent past, although some signs of improvement have manifested of late.

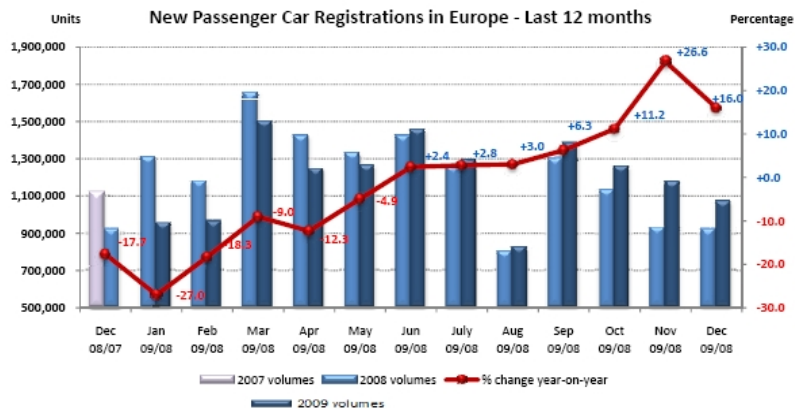


Figure 5 European automobile market [9]

The European market is the first market analyzed. Figure 5 presents data on the variation in automobile demand for the European market between 2008 and 2009. As presented, this analysis serves to bring out the underlying seasonality of automobile sales within the European market. The number of sales registered shows that August was always the month with the lower sales with March the month with the higher

number of sales. The market exhibits at least three very pronounced sales seasons, the first running from March to May, the second from June to August and the third season from September to December. In each case is possible to record an initial peak in vehicle demand at the beginning of each season with sales volumes decreasing progressively thereafter. Notwithstanding these interesting variations, the first four months of 2009 saw far fewer automobiles sold within Europe when compared to the corresponding period one year earlier in 2008.

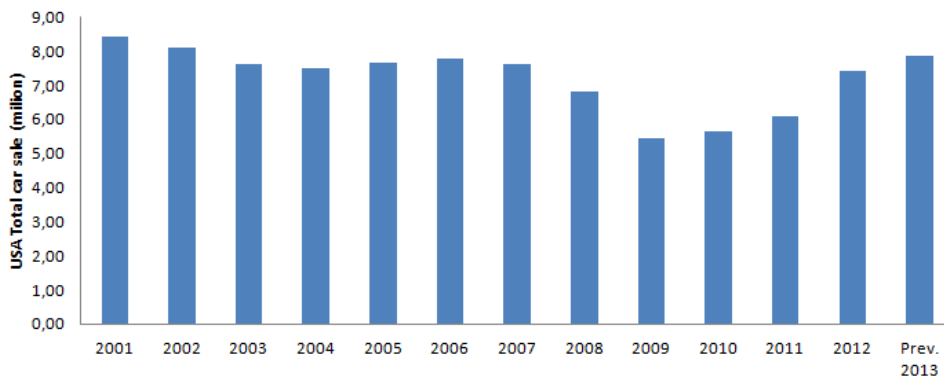
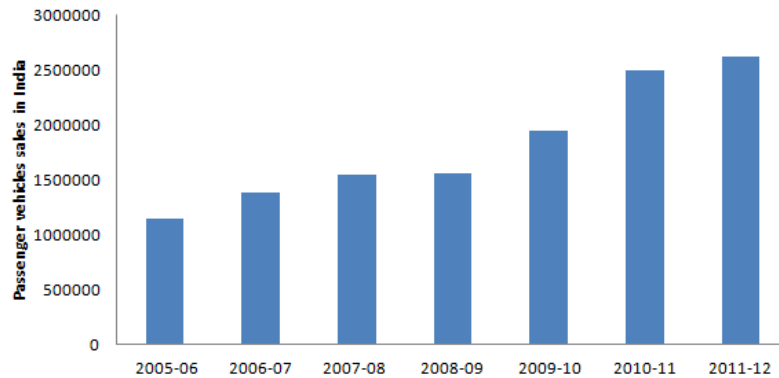


Figure 6 The USA automobile market [10]

The second market analyzed was the United States of America. In figure 6 is presented the evolution in car demand in the USA over the period 2001/2012. As can be seen, automobile sales between 2001 and 2007 did not show any marked degree of variation, remaining relatively stable at or near the 8 million vehicle mark during the entire period. In the following year, 2008, sales fell away quite steeply with the situation worsening further in 2009, the decreasing sales being explicable in light of the financial crisis then affecting the market. In the following year, demand for new vehicles started growing again and in 2012 demand had continued to improve such that sales levels approximately the same as those existing before the economic crisis were registered. This may mean that the US automobile market has recovered from the financial crisis.

The Indian market was the third market analyzed. The evolution on the demand for new vehicles is presented in figure 7. The analysis of this market was made for vehicles sold between 2005 and 2012. During this period, the Indian market showed a relatively rapid linear growth in the demand for new vehicles. The constant year-on-year growth has resulted in the virtual doubling of demand over the period of analysis. Indian automobile demand in 2011-12 was nearly double that registered in 2005-06. The continuing rapid pace of Indian GDP development attendant on sustained domestic

economic growth has largely obviated the impact of the global economic crisis which has clearly had minimal effect in this market. The data collected showed only a small stabilization in the demand during the period of the crisis (2007-2009).



**Figure 7 The Indian automobile market [7]**

Developments in recent Japanese automobile market demand are analyzed between 2000 and 2011 and presented in figure 8. During the period of analysis, the market exhibited two distinct phases, growing fairly steadily over 2000/2006 and declining fairly steadily thereafter. The only exception was in 2010, when demand picked up momentarily to the level of 2007. In 2011, the demand for new vehicles again exhibited a negative tendency. It is possible to conclude that the level of Japanese demand for new vehicles is presently running at a level comparable to that registered in the late '80's.

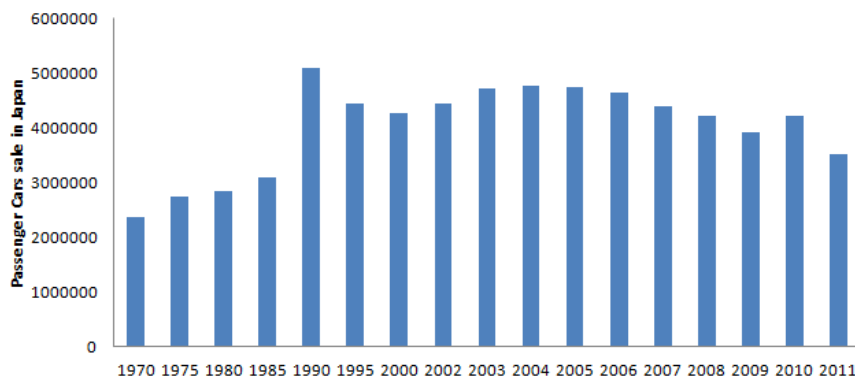


**Figure 8 Japanese automobile sales [11]**

### 2.1.3 Optical component suppliers and manufactures



In this section is presented analysis of the main suppliers of optical components for automobile and motorcycle OEMs. This research was made on the markets previously analyzed, in this case European, USA, Indian and Japanese.

The research showed that in Europe, the main optical component suppliers for the automotive industry are Hella KGaA Hueck & Co. and Aspöck System in Germany, Valeo Cibie in France and Wipac Limited in England. In the USA, some of the main suppliers of head and rear lamps are Anzo USA, IN. PRO. CAR WEAR INC., RECON Truck Accessories, Visteon Corporation and Taiki USA. For the two other markets analyzed, the research showed the existence of two major suppliers in Japan - Toyoda Giken Co. Ltd and Luminus Japan and one in India - the company Pankaaj Motors.








The research also discovered a number of other major suppliers outside the four markets analysed, for example, in China Mingzhen Electronic Ltd. and the Jiangsu Tianju Lamp Industrial Co., Ltd. While primarily focused on the automobile sector, most of the companies presented above, can also supply to motorcycle OEMs.

The study showed that the main motorcycle suppliers of optic components are Acerbis of Italy and Moto Lume of the USA. Other companies, with the capability of producing optical components were also found, these companies including Polisport Plásticos, S.A. and Paulo Mendes S.A. in Portugal, Ufoplast from Italy and RAPTOR II, Moose Racing Species and Rinder SL from Spain. Further afield in China suppliers like Changzhou Xufengzhixiu Vehicle Lamp Co., Ltd. were found while, outside of the main market, companies specializing in customized solutions like the Arlen Ness company in the US were discovered.

Interestingly, the study reveals that many of the above named companies produce and market their own products besides the products they supply to the OEM companies.






In the following tables 1 and 2 are presented some of the optical components produced by the companies presented in this chapter.

Table 1 Producers of optical components for cars and their products.

Company	Optical component
<i>Hella</i> KGaA Hueck & Co. [12]	
Valeo Cibié [13]	
Wipac Limited [14]	
Anzo USA [15]	
In. Pro.Car Wear inc. [16]	
Mingzhen Electronic LTD. [17]	
Jiangsu Tianju Lamp Industrial Co., Ltd. [18]	

In the following table 2 are presented some of the products produced by the companies that produce lamps for motorcycles.

Table 2 Producers of optical components for motorcycles and their products

Brand	Optics
Acerbis [19]	
Moto Lumé [20]	
Moose Racing [21]	
Polisport Plásticos, S.A. [22]	
RAPTOR II [23]	
Ufoplast [24]	
Rinder SL [25]	
Changzhou Xufengzhixiu Vehicle Lamp Co., Ltd. [26]	

#### 2.1.4 Daylights

The selection of a headlamp or a rear lamp as a component case study requires some study of illumination specifications. One of these specifications refers to the utilization of daylights in the case of motorcycles. In the case of automobiles this is not mandatory except in the north European countries such as Denmark, Sweden, Finland and Iceland where the utilization of these daylights is now mandatory. In others countries where utilization is not obligatory it is normal to find two types of systems, automatic or manual. The automatic system turns on daylights when the car ignition is on, and turns them off correspondingly. In the manual system, the decision rests with the driver. Despite not yet being mandatory, utilization of daylights has increased steadily in recent years. Several major automotive producers have already implemented the fitting of daylights to production vehicles - General Motors, Lexus, Mercedes Benz, Saab, Subaru, Suzuki, Volkswagen, Volvo, etc. More will undoubtedly follow as recent studies have demonstrated that the utilization of these lights improves the safety of the driver and pedestrians by increasing visibility [27] [28].

In recent years several studies have been undertaken to determine the advantages and disadvantages of these lights in countries like Australia, Japan, etc. A number of these studies have concluded that the use of this system can decrease the number of accidents, mainly because of increased visibility, lowered reaction times and improved perception of the distance between vehicles [29]. On the contrary, the use of these lights has been held to increase fuel consumption, decrease the lifetime of the lamps, mask other lights and cause glare (dependent on the power of the light used). [30]

There are three types of daylights presently available on the market:

- Low-intensity lights that turn on when the car starts (lights immediate).
- Dimmed high intensity lights (the voltage of the high intensity light is set so as to reduce its intensity)
- Dedicated lights with a standard intensity

These daylights normally uses a filament lamp bulb as the standard emitter although in recent years LED's (Light Emitting Diodes) have steadily increased their market share. While the use of LED technology decreases the power needed to produce

the same amount of light emitted through common bulbs, the emission of a restricted spectrum of white light together with relatively poor heat conduction characteristics have both been cited as major disadvantages. [28] [30].

### **2.1.5 Interior Door trim**

The door trim component subsystem was the other case study to be analyzed. This section presents a conceptual appraisal of door trim and looks at the main companies that supply this subsystem to OEMs.

Door trim is a plastic subsystem that is assembled in the inner part of the car door; it is the plastic subsystem that enters into contact with passengers and is used to guard water bottles, maps, reading glasses and other personal travel-orientated products. It is normally built with six components, but the number is dependent on car model and price as well as the laws of different countries. In general, the Door trim is comprised of a panel, an armrest, a bottom compartment and a component that absorbs prospective side impact energy - the absorber. The components that are visible to passengers, e.g. the armrest can be covered with fabric or PVC film. In some of the components it is possible to impart in-mold decorative effects giving the appearance of metal or wood to the plastic component.

The development process of Door Trim, starts in the OEM (Audi, Mercedes, Opel, etc.). These companies define the design of different components, make an initial choice of raw-material, color and how the different components will be connected. After this initial development, the OEM companies make a business call to several TIER 1 companies. The TIER1 companies that enter in this business call must conduct their own studies on the components. These studies normally have the objective of changing the initial raw material and the assembling process. The winner of the business calls produce and assemble the complete door trim. The major door trim producers are companies such as Antolyn, Tramico, Omnion Plastique, Faurecia and other major producers of plastic components.

Table 3 presents a selection of these major door trim companies together with samples of their door trim products.

Table 3 Producers of door trims and their products.

Company	Door trim
Faurecia [31]	
Magna International Inc. [32]	
Johnson Controls [33]	
Peguform [34]	
Antolin-Irausa, S.A. [35]	
Visteon Corporation [36]	
Draexlmaier [37]	
Kasai Kogyo Co. Ltd. [38]	

Trim Masters, Inc. [39]	
Röchling-Group [40]	
International Automotive Components Group [41]	
Simoldes Plastic Division [42]	





## Chapter 3

---

### **3 State-of-the-art**

This chapter presents an appraisal of the state-of-the-art of each of the technologies under study. The first technology analyzed was laser welding/cutting. The second technology analyzed was the different non-conventional molding techniques that exist on the market.

#### **3.1 Laser welding**

Laser welding is one of the most recent processes used to join different plastic components. Besides this process, it is possible to find a wide variety of other processes for joining and welding plastic/metal components on the market. In this case it is possible to find fifteen different techniques and their variants; the main competitors to laser welding are hot gas welding, extrusion welding, ultrasonic welding, linear vibration welding not to mention processes such as resistive implant welding and dielectric welding. [43-45]

As a joining process, laser welding is a technology suitable for joining plastic sheet, plastic films, molded thermoplastics and textiles [43]-[46]. In this process, it is possible to use different type of lasers - gaseous, solid and liquids lasers - for joining the same plastic components. The difference between the three lasers comes from the material used for producing the laser. The lasers most commonly used in industrial processes are the Diode, fiber, Nd:YAG and CO<sub>2</sub> lasers [47-49]. The Diode, fiber and Nd:YAG are solid lasers and are normally used in transmission laser welding. The CO<sub>2</sub> laser is used only in cutting and direct laser welding [50]. The impossibility of using this laser in transmission laser welding is due to the wavelength of the CO<sub>2</sub> laser beam which is readily absorbed by plastic polymers components.

Compared to the other processes, the main advantages of laser welding are the non-contact, non-contaminant nature of the process, its inherent flexibility and ease of control, its amenability to easy automation and its ability to yield a high quality, relatively stress free seam. Only small mechanical stresses arise in the seam zone, the low mechanical stress on the seam being due to the highly localized energy deposition. The process also produces minimum heat affected zones [43-44] [46]; this is extremely important for biological probes handled within micro-fluidic biochips where, typically, the thermal gradient should not exceed 45°C to 70°C. [50-51].

The disadvantage of the process is the necessity of having a perfect contact between components so as to maximize heat exchange between the two. When the objective is welding by transmission it is not possible to use carbon black or a high percentage of talc on the transparent component part. In transmission laser welding the component with the lower thickness should be on top. This will reduce the laser power needed to weld the two parts. The area where the weld will be made must be larger than the laser beam diameter. Plastics with a difference on their melting temperatures greater than 50°C cannot be joined by this process since the material with the lower melting temperature will start to degrade before the other material begins to melt. Neither is it practicable for use with semi-crystalline transparent materials, because of the reflection of the laser beam provoked by the spherulites within the material.

Welding by transmission is the most used process. It works best on the transparency that polymeric materials have when a laser beam with a wavelength in the near-infrared region (830–1064 nm) is applied. The joining of the two parts is made accordingly with the component on the top transparent to the laser beam and the component on the bottom capable of absorbing the near infra-red laser beam. Considering that many common polymers are normally transparent to the laser beam it is oftentimes necessary to add additives such as carbon black, Clearweld® and Lumogen® to the component that will be on the bottom so as to better promote laser absorption. To overcome problems arising from polymer transparency it has also proved possible to employ CO<sub>2</sub> lasers since the wavelength of the beam (10600 nm) emitted by this laser is rapidly absorbed by all plastic polymers [50]. In figure 9 is presented a diagrammatic representation of laser welding by transmission.

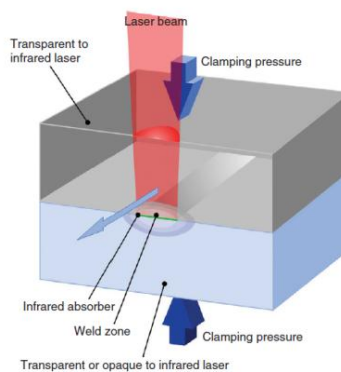


Figure 9 Laser welding by transmission [43]

As can be adduced from figure 9, the absorption of laser beam energy by the plastic component is particularly important in the case of organic polymers where the efficient absorption of incident laser radiation combined with low thermal conductivity and thermal diffusivity imply a complete conversion of incident laser radiation into heat.

During welding these thermal and optical characteristics are of singular importance having great influence on the interaction between the laser and the polymer; the heat generated between the laser beam and the absorber material is transmitted to the transparent plastic part by conduction while the laser beam can be reflected, absorbed, or scattered during transmission laser welding.

Laser welding efficiency is clearly strongly dependent on the materials' properties. In this case, to obtain a high-quality seam, it is necessary to have a good understanding of the interaction between the material and the laser. Since the interval of absorbance of the wavelength of the laser beam by the material is very small, even to CO<sub>2</sub> lasers [52], materials with a low percentage of carbon black tend to let the laser energy pass through the material. The accompanying low level of energy absorption presents a problem for the process since only a small percentage of the delivered energy will contribute to the creation of the seam. In image 10, following, a variety of different laser beam configurations are presented.

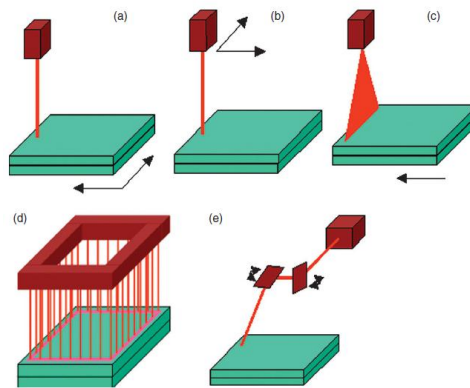
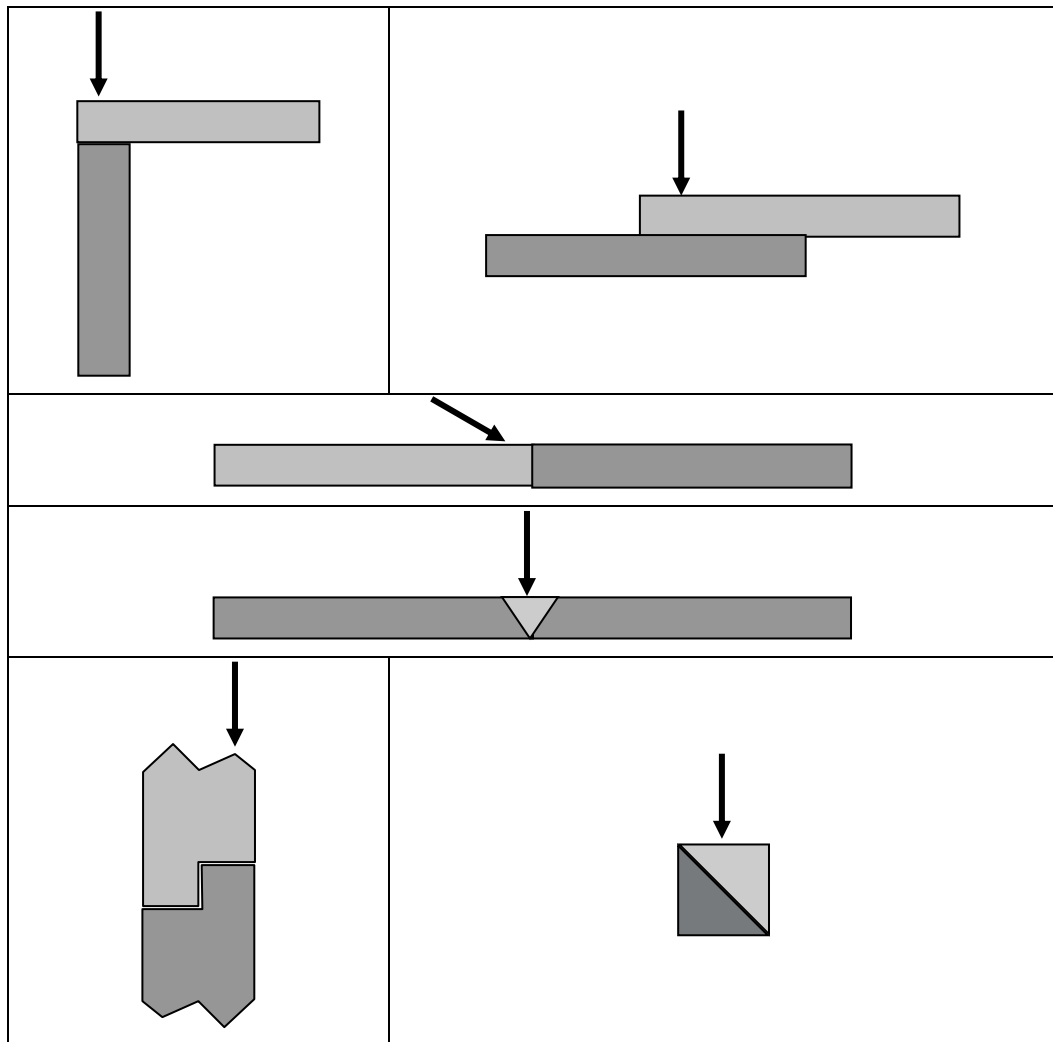


Figure 10 Laser welding methods [43]

In the following table 4 a number of different joining configurations for laser welding are presented.

Table 4 Different laser welding configurations [43-44]



Thermoplastics can be separated according to their molecular structure into two classes: amorphous and semi crystalline polymers. All of them are highly transparent to the laser beams that are emitted in the near infrared spectrum. The amorphous polymers (e.g., Polycarbonate (PC), Polystyrene (PS), and Poly (methyl methacrylate, PMMA) does not significantly affect the course of the beam [51] [53]. On the contrary, the semi-crystalline polymers (e.g., PA, PP) have the capability to scatter the beam due to their crystalline structures [51] [54-56]. In the following, figure 11 is presented the transparency of a 0.5mm thick sheet of PC to different lasers.

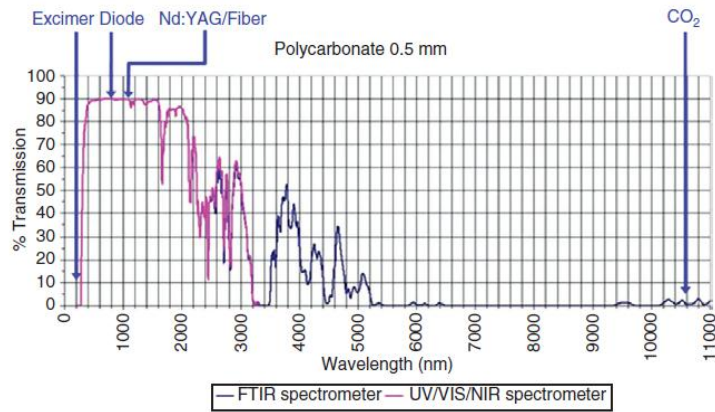


Figure 11 Transmission Spectrum for major lasers types [43]

As noted earlier, to improve the quality of a seam it is necessary to mix additives with the polymer. These additives can be carbon black or special additives such as Clearweld. According to the company that produces Clearweld, this additive has very little visible green color and does not affect the appearance of components, even in transparent component parts. [46]

It is also possible to weld plastics without additives; in this case the laser needs to emit a laser beam with a wavelength between 1900 nm to 2000 nm. This wavelength creates an intrinsic heating effect throughout the whole of the illuminated plastic material. [57]

Besides carbon black, Clearweld, etc. other additives can also influence the final quality of the seam. These additives normally work as a mirror; one example of reflection of the laser beam is seen when additives such as glass fiber and talc are present in the polymer. In particular, glass fibers show a very pronounced effect on the distribution of the power flux along the seam path [58-59].

Materials present on the surface of the components to be welded are also capable of reflecting the laser beam. These materials are;

- Glues with high percentage of mineral additives,
- Metallic paints placed on the welding path.
- Oils with mineral charges

Table 5 examines the influence that each additive has on the final quality of the seam. [43-44].

Table 5 Influence of the different additives on the final seam

	Matrix	Additive	concentration	Quality of the seam		
	Absorbent	PP/PC	Talc	Low	↑	
high				↓		
Glass fiber			Low	↑		
			High	↓		
Clearweld additive			Low	↓		
			High	↑		
BASF lumogen			Low	↓		
			High	↑		
Carbon black			Low	↓		
			High	↑		
Oxide of titanium			Low	↑		
			High	↓		
			Matrix	Additive	Concentration	Quality of the seam
			Transparent	PP/PC/PMM A	Talc	Low
High						↓
Glass fiber					Low	↑
	High	↓				
Clearweld	Low	X*				
	High	X*				
Lumogen	Low	X*				
	High	X*				
Black carbon	Low	X*				
	High	X*				
Oxide of titanium	Low	X*				
	High	X*				

X\*- must not be used on the matrix

These additives are not the only structures that influence the propagation of the laser beam through the transparent component. Crystalline structures such as spherulites that are present within the polymer matrix also have the capability of influencing light transmission characteristics. This influence is mainly due to the average diameter (5–1000 nm) of these structures that are near the wavelength of the laser beam. The similar dimension between the beam wavelength and the crystalline structure will provoke reflection and refraction of the beam. In this case, the higher the size of the spherulites the higher the laser power needed to join the different components. The increase in laser power will lead to a global increment in the degree of crystallinity at the seam zone - the higher the temperature at the seam zone, the higher the degree of crystallinity. It is possible to obtain up to 90% of crystallinity during the welding process when high laser power and moderate scanning speeds [60] are applied. It is also possible to delineate different zones within the seam cross section, the crystalline morphology of each zone being related to a specific thermal cycle. The growth of the degree of crystallinity leads also to the augmentation of scattering of the laser beam.

### **3.1.1 Laser beam behavior**

Clearly, before starting the development or the adaptation of a product to the laser welding process, it is necessary to consider the nature and thickness of the transparent and absorptive materials that are to be employed, the type of materials and the additives present within the matrix of the polymers.

Besides these factors, it is also necessary to take into consideration the diameter of the laser beam which can increase or decrease in accordance with the distance between the laser head and the part to be welded. In this case the laser beam has two zones: the focusing and the defocusing area. In the focus area it is possible to measure the minimum diameter that is near zero; the point where the diameter is zero is known as the focalization point (FL); after this point the diameter of the laser increases, this zone of expansion being known as the defocusing length (BL). Normally the diameter increases and expands in angles between 2° and 4° [61]. In the following figure 12 a diagrammatic representation of laser beam behavior is shown.



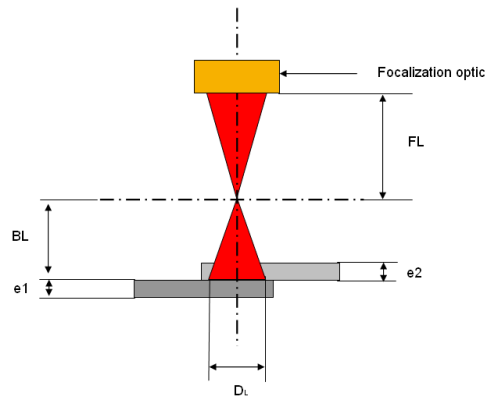


Figure 12 laser beam dimensions

To ensure a good bond between the two components, the zone where the welding will occur, must not have irregularities, and the gap between the parts should be near zero. Besides the welding zone it is necessary to take into consideration the clamping zone. This zone of pressure has the objective of maintaining in close contact the two components during the welding process. One example of the influence that clamping force has on the final quality of the seam can be seen in welding PVC. In this case, it is necessary to produce a clamping pressure between 0.5 MPa and 4.0 MPa to obtain a seam with a good quality [62-63].

Designing a good quality laser welding zone means following certain rules; one of them is related to the marks of the extractors [43-44]. In this case extractors must not be located on the welding path, and the welding path should be smooth. Roughness of the surface can also affect the transmission and absorption of the laser beam, since the increase of this property will increase the diffusion reflection of the beam.

### 3.1.1.1 Mechanical and dimensional properties of the seams

Comparing to the welding of metallic materials, the welding of plastic has some restrictions in terms of size; welding paths higher than 250x400 mm should be welded with lasers that work in pulse mode and not continuous. Conversely, lasers are free of restrictions in terms of seam width.

To obtain the best mechanical resistance of the seam, the laser beam must have an angle of 90° between the laser beam and the surface to be welded. In case of the impossibility in using this angle, the structure should be designed such that a minimum

angle of  $70^\circ$  be attained between the laser and the surface. The following figure 13 presents an examination of a transversal section of a seam. [60] [64].

**Definition:**

- $e_1$  : zone where heat propagation exists
- $e_2$  : seam
- $D_L$  : Laser beam diameter
- $S_D$  : Laser beam deviation zone

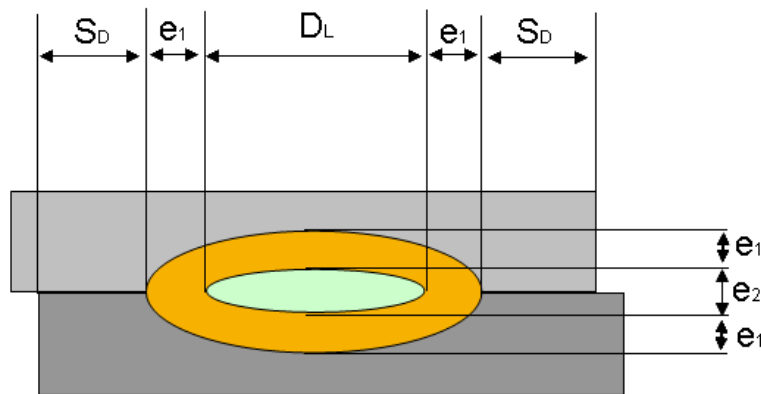


Figure 13 transversal cut of a laser welding zone

Visualizing the welding zone from the top it is possible to determine the temperature distribution along the seam width; this is presented in the following figure 14. [65]

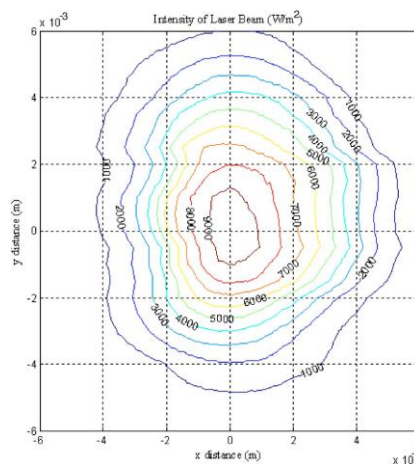


Figure 14 Power intensity of a laser beam computed over a 1-mm-diameter hole [65].

### 3.1.1.2 Other variants of laser welding

Direct laser welding, is another variant of laser welding and normally is used to join plastics with a thickness lower than 0.5mm. This technique cannot be used at high speeds, except if the joint is made directly by the laser beam.

Laser welding can also be used with coating techniques such as Cathodic arc physical vapor deposition (CA-PVD) and electron beam evaporation (EB-PVD). These methods are special techniques employed to impart a metal appearance to plastic components. The influence of these techniques - CA-PVD and EB-PVD - in the final properties of the seam created by laser welding have been studied by Sultana [66]

He studied mainly the transmission laser welding of micro-joints of titanium-coated glass and polyimide. According to his studies, the coating made by CA-PVD technique have a lower influence on the laser beam. For that reason it is possible to obtain seams with four times greater resistance than with the other technique. The use of EB-PVD has moderately influence in the final quality of the seam, due to poor initial adhesion to the substrate, its very smooth surface characteristics and a propensity to generate hotspots which can lead to local film decohesion. On the other hand, CA-PVD was more effective since the deposited film provided enhanced robustness with improved adhesion and a rougher substrate all of which had contributed to the improved seam strength noted. [66]

#### **3.1.1.2.1 Hybrid process**

Laser welding is a technique with a considerable potential for joining different materials and components of all sizes. In the following topical review some of the studies done in combining laser welding with other welding techniques are presented.

Due to the high level of automation that it is possible achieve with laser welding, its use in combination with other welding processes has attracted credible interest. One such study appraised the combination between laser welding and metal inert gas (MIG) processes. According to the authors of this study, this combination results in a high productivity rate, low deformation, and the prevention of porosity formation. In the following figure15 is presented the hybrid MIG technique. [67]

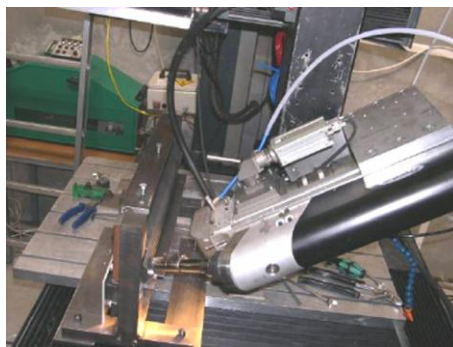


Figure 15 Set-up of hybrid-laser-MIG welding [67]

The Local selectivity of the laser bonding (SBL) is a technique developed by M.J. Wild [68]. This technique has the objective of joining silicon wafer with glass wafer using a laser beam. SBL is a technique that was developed based on the transmission laser welding process. In this case is necessary that one of the components of the joining must to be transparent to the laser beam and the other capable of absorbing the laser beam energy. Figure 16 details the local selectivity technique used for laser bonding.

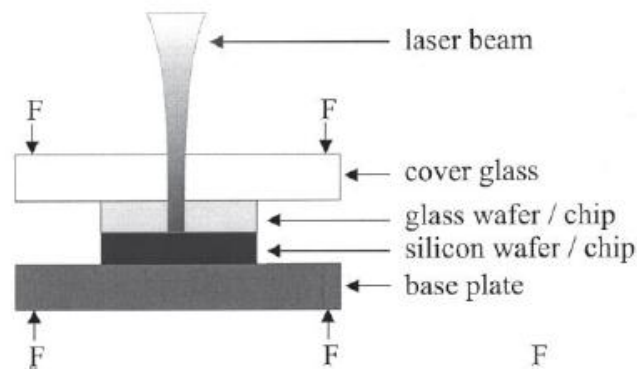


Figure 16 local selectivity of the laser bonding (SBL) [68]

According to the author, the main advantages of this technology are the bond achieved in geometries with a thickness below 300 nm, a tolerance to high temperature loads over long periods and a locally and temporally restricted hot zone. [68]

Another technique of joining, where a laser is used is called Transmission Welding by an Incremental Scanning Technique (TWIST). This technique has the capability to weld components with a width near 100 mm. With this it is possible to achieve welding velocities near the 300 mm/s. TWIST is based on the overlapping of a high velocity movement of a laser beam over the seam zone. This highly dynamic movement can be circular, linear, etc. The seam is achieved by the path of a laser beam over the material several times in a circular movement and by a certain overlapping of the laser spot.

According to the Boglea Andrei et al. [69], TWIST has some significant differences in comparison to the other well established thermal joining approaches, even when compared to the normal laser welding. The heat affected zone (HAZ) has a significantly reduced depth compared to the usual laser weld seam achieved; this effect is achieved because of the high dynamic circular movement which leads to a uniform energy deposition over the cross-section of the weld seam. In the case of normal laser

contour welding, the energy deposition is stronger in the middle of the weld seam and decreases to the sides causing a deeper HAZ. [69]

### 3.1.2 Laser cut

Besides welding, lasers can also be used to cut plastic materials. Compared to welding, the cutting of polymers presents much the same problem as the welding process. This is due to the transparency of the plastic to the beam when lasers working in the near infrared (NIR) spectrum are employed. To overcome this disadvantage, CO<sub>2</sub> lasers are widely used. The main advantage of this laser lies in the wavelength emitted, which is 10600 nm. This wavelength is outside of the NIR spectrum and for that reason is more prone to be absorbed by all plastics. This laser also has other advantages - low cost and the capability of using high velocities for cutting different materials. As with welding, it is possible to use NIR spectrum lasers by overcoming transparency difficulties by using additives such as carbon black, Clearweld® or Lumogen® all of which can be admixed with the polymer. In comparison to the CO<sub>2</sub> laser, solid state lasers such as the Nd:YAG have inherently higher precision and produce a smaller burn area.

The cutting of plastics follows the following procedure. A laser beam is applied to the cutting zone and emits the necessary energy to melt the material. During the process an air flux is deployed so as to clean the melted material from the cut section. Depending on the material used, one of two behaviors can be detected - fusion cutting or melt shearing. Polymer materials such as PVC and PMM do not present fusion cutting behavior. In the case of PVC, during the cutting process chemical degradation normally occurs with the release of toxic vapors off the material. PMM and its derivatives normally vaporize during the cutting process but when this does not happen a thin liquid layer appears on the cut surface. For that reason it is necessary for a light flux of air to be employed so as to clean the layer away – as well as any other waste material impurities or material that has solidified. [70-72]. In the following figure 17, the major variables influencing laser cutting are presented.

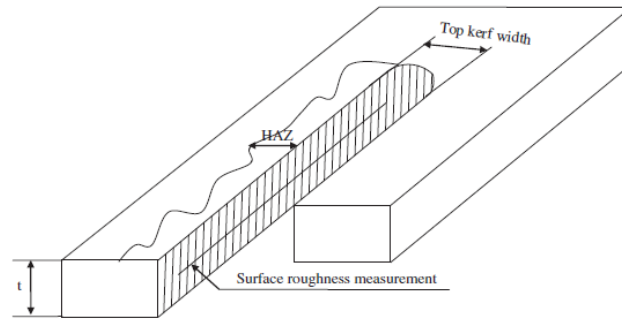


Figure 17 laser cut process [54]

Factors needing to be taken into account before and during the process.

- Heat affected zone, (HAZ)
- Roughness
- Dimensional precision
- Width of the Kerf (width of laser beam).

The quality of the cut is influenced by:

- Laser power
- Type of the Laser
- Cut velocity
- Operation mode (beam emitted in continuous or pulse),
- Gas used as a cut auxiliary
- Thickness and roughness of the part that will be cut

### 3.1.3 Modeling the interaction between laser and matter

Understanding how the laser beam interacts with the matter to hand is a crucial point, to produce a good seam in the welding or a good cut. This understanding can be obtained through practical tests or by the development of mathematical models. In the following paragraphs the main mathematic models that are capable of describing the interaction between the laser and matter are examined.

The first interaction between the laser and the matter occurs when the beam enters into contact with the surface of the matter. This initial interaction provokes a reflection of a fraction of the beam energy. This interaction is explained by Snell's law,

present in figure 18. According with Snell's (equation 1), the reflection of the light occurs when the light passes from an optically "thin" medium to an optically dense medium. [73]

$$\frac{\sin\varphi_A}{\sin\varphi_B} = \frac{n_A}{n_b} \quad (1)$$

Where  $\varphi_A$  is the incidence angle and  $\varphi_B$  the angle of reflection, and the  $n_A$  and  $n_B$  are the index of reflection of material A and B. In the following figure18 it is presented the light behavior according with Snell's law.

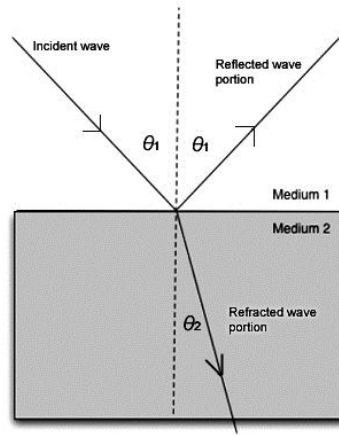


Figure 18 Snell's law (courtesy acousticslab.org)

Another interaction that occurs between the laser and the matter happens when the energy of the laser beam is transformed into heat. During the process of cutting or during direct welding is important to consider the diminishing of intensity of the laser beam when it enters in an optically dense medium. To this phenomenon is given the name of damping factor. This can be modeled by a Gauss shaped (equation 2) heat source whose intensity and shape varies with the penetration depth and radius.

$$QP = Q_0 e^{-\frac{r^2}{r_0^2}} \times QR_0 \quad (2)$$

Where is

$$QR_0 = e^{-\alpha z_s} \quad (3)$$

And

$$r = \sqrt{x_s^2 + y_s^2} \quad (4)$$

$Q_0$  is the maximum source intensity,  $r_0$  is the Gauss parameter (radius of the Gauss function curve),  $\alpha$  is the attenuation coefficient and  $Z_s$  is the distance from the surface.

In the transmission welding process, another interaction occurring between laser and matter is known as refraction. In this case, the laser beam is refracted along the thickness of the dense medium. This occurs due to the existence of additives as talc, glass fiber or crystalline structures. These materials and molecular structures have the capability of interacting with the beam, through the change of the path of the beam along the thickness. Depending on their concentration in the main material, this interaction can influence the final quality of the seam, since refraction of the beam will diminish the quantity of energy available in the welding zone. To understand this interaction, it is necessary to apply the Monte Carlo method and the Mie theory to evaluate the total radioactive interchange occurring within the system.

Mie theory also called Lorenz–Mie theory or Lorenz–Mie–Debye theory is an analytical solution of Maxwell’s equations for the scattering of electromagnetic radiation by spherical particle with a dimension comparable to the wavelength. This theory depends on the expanding coefficients of the incident wave, the scattered wave and the order of convergence of the series [74]. The equations are used to determinate the radioactive properties of particles and to determine just how much energy is being scattered on the matter. In the case of the laser, it is normal to use the GLMT (Generalize Lorenz–Mie theory) analysis. This allows the determination of the amount of scattering when the focal waist of the laser beam is incident to the sphere. [75-76]. In this case when a laser beam interacts with a sphere it is split into two components, one that crosses and another that intersects the particle forming a probe volume containing a number of interference fringes. The fraction of the energy that is scattered in any given direction, is defined by a scattering angle  $\gamma$  that is given by Scattering Phase Function presented in equation 5: [76-78]

$$\varphi_{(\gamma)} = 2 \frac{i_1 + i_2}{x^2 Q_{sca}} \quad (5)$$

Where  $i_1$  and  $i_2$  are the non-dimensional polarized intensities,  $x$  is the coordinate direction and  $Q_{sca}$  is the efficiency factor for scattering, presented in the following equation 6. [75]



$$Q_{sca} = \frac{2}{x^2} \sum_{n=1}^{\infty} (2n + 1)(|A_n|^2 + |B_n|^2) \quad (6)$$

Where  $A_n$  and  $B_n$ , are

$$A_n = i(-1)^n a_n \quad (7)$$

$$B_n = -i(-1)^n b_n \quad (8)$$

$a_n$  and  $b_n$  are the Mie scattering coefficients.

Where

$$n=1.2x+9 \quad (9)$$

With determination of the quantity of light scattering through the Mie theory, the next step consists of determining the quantity of energy necessary to melt the absorber material. The determination of this energy will be made through Beer–Lambert law. According to this theory, the laser spot is considered to have a circular shape with a radius  $R_0$  (m). The temperature field in the two components of the material assembly is determined through the general heat transfer equation. These calculi are made in a stationary mode using for that a density  $\rho$ , a thermal conductivity  $k$ , a specific heat (at constant pressure)  $C_p$ , a temperature  $T$ , and a time  $t$ . In the case of three dimensional assemblies equation 10 is normally used. [51] [55] [58] [61]

$$q_0 = \rho C_p \frac{\delta T}{\delta t} + \vec{\nabla}(-k\vec{\nabla}T) \quad (10)$$

The heat absorbed by the semi-transparent media is given by equation 11. [79-80]

$$q_0 = \frac{P}{\pi R_0^2} (1 - R_T) \alpha_T e^{-\alpha_T z_T} \quad (11)$$

Where  $R_T$ ,  $\alpha_T$  are the reflectivity and the absorptivity of the transparent part. It must be pointed out that only a very small part of the energy of the beam is absorbed by the transparent part and this occurs due to the presence of additives. For that reason the main quantity of the available beam energy continues arriving at the welding zone. To determine the amount of energy that arrives to the absorber part it is normal to use equation 12. [79-80]

$$q = \frac{P_{int}}{\pi R_0^2} \alpha_A e^{-\alpha_A Z_A} \quad (12)$$

Where  $R_A$ ,  $\alpha_A$  are the reflectivity and the absorptivity of the laser-absorbent parts,  $P_{int}$  represents the power density of the beam that can be obtained by equation 13 [51] [58].

$$P_{int} = P(1 - R_A)(1 - R_T)e^{-\alpha_T Z_T} \quad (13)$$

In amorphous polymers, the scattering and the reflection of the beam is neglected. The extinction of the beam is determined by the absorption. To finalize the welding process, it is necessary to determine the amount of heat that is transferred between the absorber and the transparent part. To determine the amount of heat exchange occurring it is necessary to take into account the heat that is transferred by convective, conductive and radioactive means. The exchange of heat between the two parts can be determined by using the equation 13. [54-55]

$$\vec{\nabla}(-k\vec{\nabla}T) = h(T - T_{ext}) + \varepsilon\sigma(T_{amb}^4 + T^4) \quad (13)$$

Where  $h$  is a global heat transfer coefficient.  $\varepsilon$  is the material emissivity and  $\sigma$  is the black body emission coefficient.

The energy distribution of the beam along the welding path has been already examined in figure 14. Understanding how the energy is delivered per unit length is important to obtain a good seam. This is also called the line energy (equation 14) and is held to be equal to the ratio between the laser power  $P$  (in Watts) and the welding velocity  $V$  (in m/s). Line energy is denoted by  $\Lambda$  (J/m). [43] [58]

$$\Lambda = \frac{P}{V} \quad (14)$$

Equation 15 below can be used as a first approximation, to determine the needed laser power (P) for welding the two materials.

$$P = \frac{\omega R W a (\rho c T_m + \Delta H_m)}{0.484} \quad (15)$$

Where  $\omega$  is the rotational speed in rad/s, R is the radius of the rotational trajectory, W is the weld width, a is the penetration depth, c is the specific heat capacity,  $T_m$  is the melting temperature, and  $\Delta H_m$  is the latent heat. [52]

### 3.2 Non-conventional molding techniques

A non-conventional molding technique was applied to this project. This technology was based on the concept of assembling different plastics components inside of the same mold. In the following paragraphs are described the technique and the several in-mold assembly variants.

The growing complexity in the designs of cars has pressured the OEM companies into developing new assembly processes that are capable of producing in a fast way complex subsystems. The research on new processes has led, in the case of mold making companies, to the development of an enormous variety of molds that are capable of assembling subsystems. In this case, it's possible to find in the molds market, molds with rotary cavities or with more complex movements. Research to understand which solutions are more suitable to be implemented in this project was undertaken. This state-of-the-art research showed that the most innovative techniques are molds with multiple partition lines or rotary plates capable of changing their configuration during the injection process. The most common technique in in-mold assembling is the use of robots or similar solutions to effect exchange between the cavities and the different parts to be assembled [81-85].

As an assembly process this technique presents the following advantages.

- Production of the product occurs inside of mold and obviates the need for stock between processes.

- This process avoids the need to utilize more than one mold or other tool, lessening with this, the work space necessary.
- Assures the exact alignment of the different components
- Reduces lead time
- Allows the production of parts with characteristics that in conventional processes would be impossible.

The most common processes are Ice Cold Trick, overmolding, IML, IMI and DSI. Each technique will be described in the following topics [81-85]. In figure 19 is presented the different multi-materials processes.

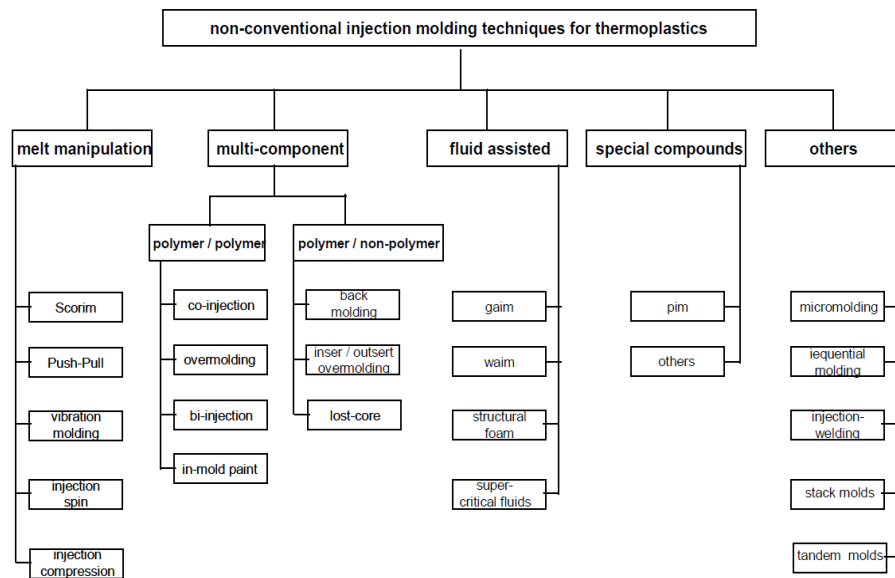


Figure 19 multi-material processes [84]

### 3.2.1 Overmolding

The Overmolding process is a technique whereby different plastics are injected over other materials. The most common process is the injection of a plastic over metallic parts. With this process it is possible to obtain a strong connection between plastic/plastic and metal/plastic without utilizing glues to maintain the connection between the materials. This technique has two variants: over-molding over an insert and multi-material injection. Insert over molding is used for low production volumes while the multi-material injection technique is used for high production rates or when the production cost is forbidden. [81-85].

### **3.2.1.1 Rotating Mold**

The use of rotating molds is a technique with great potential due to the high degree of freedom that is achieved in the geometric solutions for the molding. The process involves the independent injection of the different materials in the impressions (two or more) and is developed in two stages: after the injection of material A in cavity 1, the mold opens and the cavity rotates in order to place the preform inside of cavity 2. In the second stage a second material is injected over the initial preform, generating the desired part. The process can be achieved by using a rotating plate fitted to the moving platen of the injection molding machine in which the ejection side of the mold is assembled. These plates can be hydraulically or electrically operated. They allow for the selection of the rotating angle, and they have rotating joints enabling the connection to the fluids (water or oil) that control the mold temperature. Rotating plates are widely used and can be considered a very reliable solution. However, operational problems may occur in very high and heavy molds, due to the eccentricity of the mechanical loads on the rotating plate. It should also be noted and considered in the mold design that the filling of the second material occurs under unbalanced conditions as the polymers flows in a geometry confined by a the steel walls of the mold and the plastic surface of the preform. Furthermore, within the second cavity cooling from the core side will be affected by the lower thermal conductivity of the plastic wall of the preform. [85].

### **3.2.1.2 Rotary Central Block**

Another complex but flexible technique is the so-called rotary central block or horizontal rotary module. This process is suited to large volume series production (e.g., packaging) or for molding panels with large areas (e.g., automotive glazing).

The rotation of the central block defines the sequential stages of the process, namely the injection of the selected material and eventually an intermediate stage for assembling or cooling. Different design solutions may be used, in some cases requiring special closing units [85].

Plasdan, a Portuguese company, has developed a similar process called C-frame. The process has the capability to produce complex plastic parts [92].

### **3.2.1.3 Insert over-molding**

Injection over an insert is the most-used process of all overmolding processes. This process starts by attaching a pre-form to a mold cavity. After that, the injection process starts by filling the remains of the cavity with a melt polymer. With this technique conventional tools as well as conventional molds and a single injection unit can be used to obtain a multi material component. The use of conventional tools makes this process much more affordable when compared to multi-material processes. [81-85]

### **3.2.1.4 Multi-material injection molding**

Multi-material injection processes are also called bi-injection or multi-injection molding processes. To produce components through this technique it is necessary to develop a special mold. At the same time, this process only works if it used in a multi injection unit.

When employed, this technique has the capability of reducing mold cycle time, improving the final quality of the parts and reducing process costs. [81-85].

## **3.2.2 In-Mold operations**

### **3.2.2.1 In-Mold-Labeling (IML)**

In-Mold-Labeling (IML) is a process used mainly in the packaging industry as an alternative to print. This process is used when the design requires flexibility or when it is necessary to print directly on the part. The labels are normally printed on a film of Polypropylene with a thickness of tenths of a millimeter. The major advantage of this process is the integration of the processes downstream with the injection molding process. The major disadvantage of this process is the thermal resistance of the label and the slight increment of the cycle time.

The label is placed in the mold cavity by a worker or a robot and fixed in place by vacuum or by magnetic charge.

IML is mainly used in injecting parts with a small thickness. [84][86-87]

### 3.2.3 In-Mold-Decoration (IMD)

IMD is a polyvalent technology used in decorating plastic parts. The process is compared to a simple transference of paint from a polyester film to the part. This process does not need large changes in the mold.

The factors with more influence in the process are the mold design, the decorative films and the automation of the process.

Despite of the factors presented before, this process needs a good control system capable of controlling the temperature, the injection pressure and the course of the spindle. The IMD process makes it possible to inject parts with low injection pressure, or using the compression process. In the following figure 20 is presented a component made through the IMD process [83-85] [88].

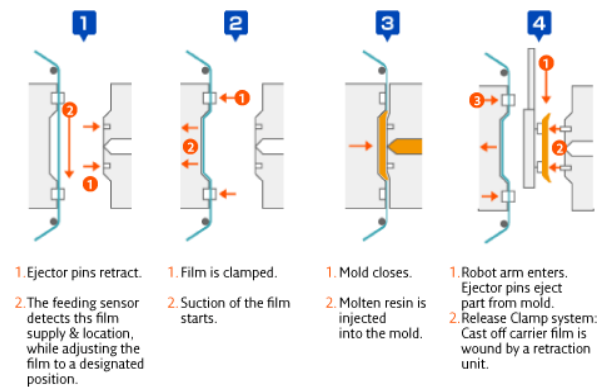


Figure 20 the IMD process [88]

### 3.2.4 Injection welding process

The injection welding process or Die Slide Injection (DSI) is a technology developed by Japan Steel Works, Ltd., with the objective of producing laminate structures and halo parts. This new technique has two variants the DSI-2M e M-DSI.

DSI-2M process has the capability of producing halo components. The production of halo parts occurs according to a strict procedure. Initially the different components are injected in different cavities. After that, one of the cavities of the mold rotates, until it is centered with the other cavity. Following this, the two components enter into contact by closure of the mold. The joining between the two components is obtained through the injection of a material in the contact zone of the two so as to effect a permanent connection.

The M-DSI was developed with the objective of producing laminate structures. The production of these structures is accomplished, through the use of a sliding mechanism that exists inside of the mold cavity. This process needs two injection machines, for producing the laminate structure.

The major advantages of the DSI processes are:

- Post-processing techniques such as assembling or gluing are not necessary
- Thickness variation is lower comparing to blow-injection
- The dimensional precision and visual aspects are excellent
- Freedom of the design
- The DSI-2M can be applied in 3D connections, even if the contact areas are irregular.
- Over-molding is allowed by adding inserts inside of the cavity.[83][89]

In the following figure 21 is presented the different steps of the DSI process.

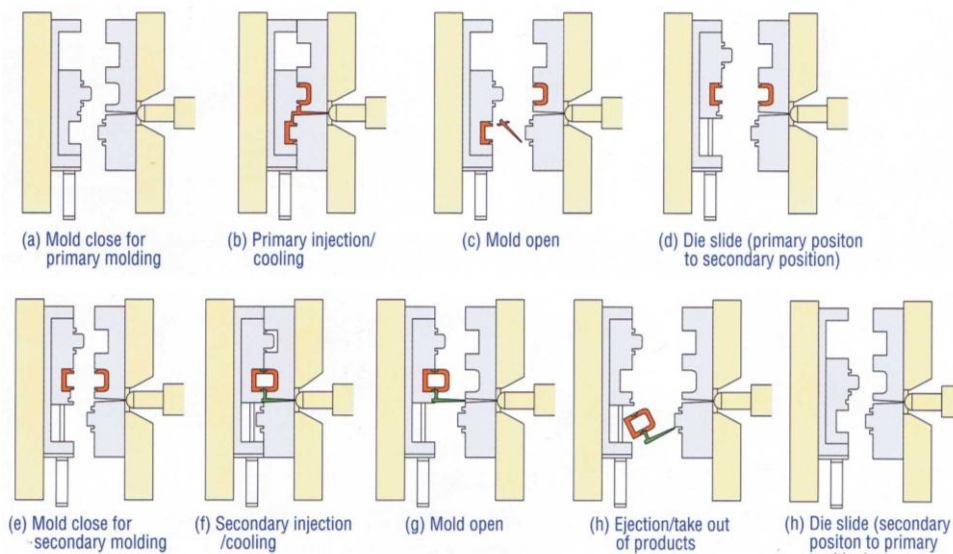


Figure 21 The DSI process [89]



### **3.2.5 “Ice Cold Trick”**

“Ice cold Trick” technique is a variant of the over-molding process, developed by Ferromatik Milacron in 1995. With this process it is possible to achieve a higher degree of freedom of movement compared to conventional over-molding process. Plus, it only needs one injection machine.

The augmentation of movements is achieved through an ultra-fast cooling of the first injected component. With the ultra-fast cooling it is possible to erase the mixture of molecular chains between the different components, even if they are made from the same material. The main requirement of this technique is the temperature control system since is necessary to use water close to the solidification temperature. In this process, the material to be used must be semi-crystalline and highly charged to support the volumetric contraction after the first injection. [83]

### **3.2.6 Others techniques**

Ferromatik Milacron and Foboha have developed a mold capable of combining over-molding and snap fits in one injection cycle. This technique/system has the name of Foboha’s TwinCube. The system is implemented between the halves of the mold plates and uses synchronization between two cubes in a counter-rotating movement. The cube has the capability of creating two distinctive molds, operating from a single injection machine. The production of a subsystem occurs at three levels, where each level is separated from the other. A driving mechanism controls and coordinates the opening and closing of the mold. With this technique is possible to add another injection machine if required. The main advantages of the process are the high efficiency in multi-component injection, the reduced cycle time, the insertion of labels, assembling of multi-components and the ejection of the finish parts. In figure 22 is presented the Foboha’s TwinCube system. [83][91]



Figure 22the Foboha's TwinCube [91]

The rotating mold Spin Stack is another in-mold assembling technique proposed by Gram Technology. In this case, the mold is divided into four index cores, positioned between the fixed and mobile plates of the mold. Each core has the capability of rotating 90°. The main application of this technique is the production of the spheres used in roll-on deodorants. [83]

### 3.3 Conductive polymers

Until relatively recently, one of the main applications of polymers was the protection of electrical wires and other electrical systems. Recent developments in polymer science have created materials with the capability of transporting electricity. Examples of these new materials are Polyaniline (PANI) and Polypyrrole (PPy). As is natural with most new materials they are still very expensive, making their consumption in common applications almost impossible at present [98]. To overcome this problem, other solutions have appeared on the market in recent years, in the shape of masterbatch. Here, different mixtures using conductive materials such as micro fibers of steel or carbon nanotubes with common polymers have been developed and tested [99-100] [101-102].

This second lower cost solution presents some challenges, mainly during the injection process. The major challenge of these mixtures is to obtain a good even distribution of the conductive particles in the mixture immediately prior to injection. [100] [103-104]. Poor mixing is visible at a microscopic level where the concentration of the fibers is oftentimes seen to be higher in the core than the skin of the part [105].

This higher concentration occurs due to the distribution of the particles which are very sensitive to injection speed, melt temperature and thickness [106-108]. For example, the application of high melt temperature and high injection speeds resulted in a non-uniform distribution of electrical conductivity across the specimen thickness. This result also showed higher electrical conductivity at locations father away from the injection gate [106] [109]. These outcomes will lead on to difficulties in the transport and distribution of electricity throughout the part. The polymers processed by hot compression molding present better electric conductivity when compared to parts produced by injection molding [106] [110-111].

Despite the disadvantages of these materials, they are being used in several applications. It has proven possible, in accordance with the correct concentration of these additives, to use these materials in electrostatic discharge dissipaters, electromagnetic interference (EMI) shielding, printed circuit board writing and transparent conductive coatings [106]. Figure 23 presents data showing the typical conductivity of these different materials.

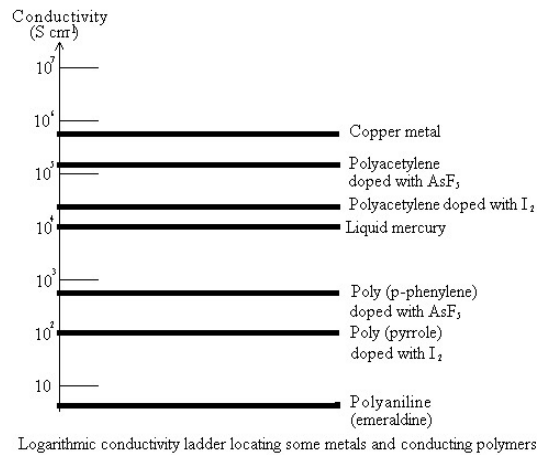


Figure 23 Conductivity of different materials [98]

### 3.4 Research method

Defining a research method is a critical point to achieve initial objectives and answer all of the research questions posed. Based on this purpose and considering the main objective, of combining laser welding and in-mold assembling, a research strategy was developed with the primary aim of establishing a definitive case study and, secondly, defining which type of light emitter should be used. Considering the advantages of

LEDs, it was decided to use this type of light emitter. In turn, this entailed defining the number of LEDs necessary to ensure compliance with legislative requirements as well as selecting the conductive material to be employed in the electric circuit. Design of the different components of the case study followed on. The first component designed was the electric circuit followed by the housing and the crystal. The material selection of these two components was made in parallel, finishing with selection of the material with the best laser welding properties. To accomplish this task it was necessary to develop another parallel task, in this case the cost model. This model had the objective of comparing the production cost of the new process with the existing process and also to supply necessary input to the laser welding study.

The second part of the research consisted initially in defining the manufacturing cell and mold requirements, followed by the preparation of a series of Moldflow® simulations. These simulations had the objective of understanding if all the components designed are able to be produced by injection molding and to define the best injection points. They also served to give some process inputs to the cost model. The final task related to the injection molding process, was the production of a complete rear lamp. For this final task all the knowledge acquired in previous tasks was brought together.

The last task completed was the business model which included the formulation of a business marketing strategy for selling the process to future clients.

The organizational chart for the research undertaken is presented in figure 24 below.

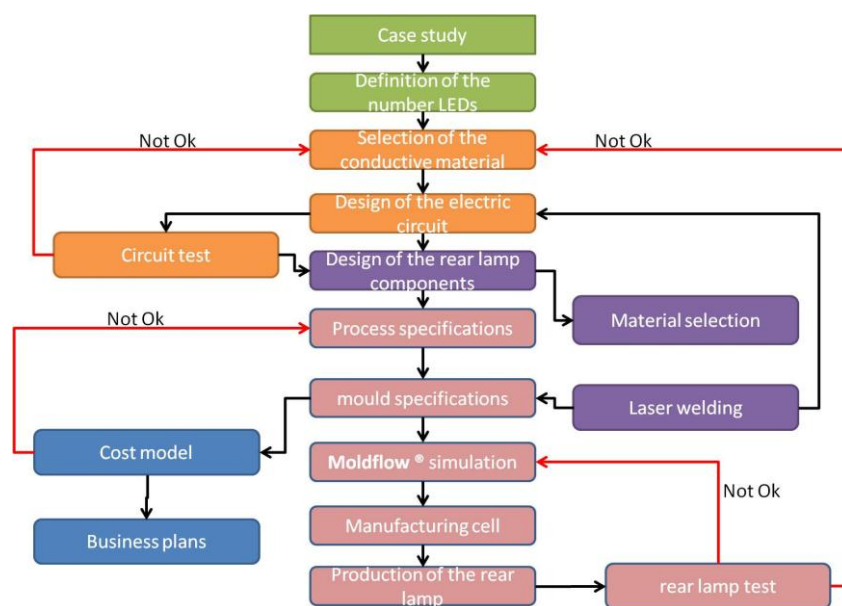


Figure 24 Research method

# Chapter 4

---

## 4 New concept of the rear light

This chapter will present the case study - the Rear Light - together with an outline of the various pre-production modifications needed. These modifications were made to the electric circuit, the reflective cavities and the light emitter.

The chapter is divided into two parts. In the first introductory part, an exposition of the different technologies used to produce the rear lamp is presented. In the second part the main modifications made to the rear lamp are detailed.

### 4.1 Introduction

In the previous chapter, two possible component case studies were looked at and the demand for them was analysed in four markets. Considering that the head and rear lamp can be applied to automobiles and motorcycles alike, this particular case study was selected. The rear lamp selected is an existing lamp, produced by Rinder SL, Spain.

The rear light (figure 25 and 26) is constituted by three components, an incandescent light bulb, a crystal lens and a housing. Taking into consideration similar products, this rear light is capable of working as both a stop and presence light. The actual housing is made from PC, and the lens is made from PMMA.



Figure 25 Actual front view of the rear lamp

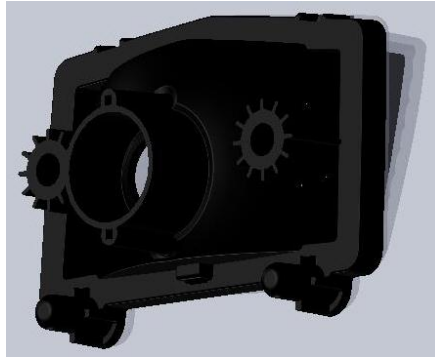


Figure 26 rear view of the rear lamp

With the presentation of the case study, it is necessary to make the requisite changes needed to turn this subsystem into one capable of being produced by in-mold assembling process and laser welding. The most important modifications were made on the light emitter, on the electric circuit and on the way they are joined together.

In the case of the light emitter, the main change was the replacement of an incandescent light bulb with LEDs (light-emitting diode). On the new rear lamp conductive polymers were used so as to reduce the time of assembling and the time of production. The third modification was made on the assembly process centering on the joining process. In the new process laser welding was used instead of ultrasound.

## 4.2 Rear lamp design

In this section, the modifications that were made to the case study so as to enable production through the chosen process will be detailed. In figures 25 and 26 the rear lamp under development is shown. This existing lamp is comprised of a crystal housing, a lamp bulb, a rubber gasket and an electric circuit. The lamp bulb, the rubber and the electric circuit are not shown in the above two figures.

Before adapting the existing rear lamp to the new production process it was necessary to know and understand the legislation regulating this type of product. This is important because is essential to understand if it is technically possible to implemented the modifications to the product needed. One of the technologies that were used was LEDs, which will be responsible to emit the light. In this case, it was essential to know the minimum number of LEDs needed to ensure compliance with the relevant

legislation - the UNECE Vehicle Regulations - 1958 Agreement; Regulation No. 50 - Rev.2 - Position lamps, stop lamps, direction indicators for motorcycles [112-114].

#### 4.2.1 LED (Light Emitting Diodes)

The use of LED's has been increasing rapidly in the last few years in different brands of automobiles and motorcycles. Since 2004 approximately 40% of all new vehicles and small trucks produced worldwide have used LED's as the center brake light [93]. Besides this application, they have been applied in the lights used for changing direction, fog light, daylights, internal vehicle light and rear lights [94]. According to several studies, the main advantages of this type of emitter are the savings of energy and fuel, and the enhancement of battery life. This is due to the lower voltage requirement putting less stress on the alternator and battery. This solution also gives more freedom in design, making the product more appealing to the driver. It is also possible to combine high performance with flexibility and reliability. [95-96].

The LED is a semiconductor chip that uses a material doped with impurities for emitting light. This chip is a p-n junction. This means that the electric current only goes in one direction, in this case from the p-side (anode) to the n-side (cathode). It is through this flux that is emitted the light [97].

In the following paragraphs is presented the procedure used to determine the number of LEDs and the dimensions of the electric system.

Considering the legislative requirements, the proposed number of LEDs to be used in the lamp was established made using the following equations [115].

$$\Phi_{V\ real} = \left( \frac{\Phi_{v\ spec}}{T_{signal}} \right) F_{guard} \quad (16)$$

Where  $\Phi_{V\ real}$  is the light real flux required,  $\Phi_{V\ spec.}$  is the light flux according with the legislation.

$$T_{signal} = (T_{filter})(T_{glass})(1 - L_{pattern}) \quad (17)$$

Where  $T_{filter}$  is the optical transmission of the filter,  $T_{glass}$  is the optical transmission of the glass.

$$\Phi_{LED} = \Phi_{cat} \times (T_{LED+optic}) \quad (18)$$



Where  $\Phi_{LED}$  is the light flux emitted by the LED,  $\Phi_{cat}$  is the minimum light flux emitted by the LED,  $T_{LED+optic}$  is the total loss of the light flux associated with the light emitter and with the secondary optics ( $0 \leq T_{LED+optic} \leq 1$ ).  $T_{optic}$  is the optical transmission of the secondary optics.

$$T_{LED+optic} = \left( \frac{\Delta\phi}{\Delta T_a} \right) \times [\phi(I_f, \theta_{ja}) \times (\phi_{collected}) \times (T_{optic})] \quad (19)$$

Where  $\Phi(I_f, \theta_{ja})$  is the normalized light flux versus electric resistance,  $\Phi_{collected}$  is the percentage of light flux collected by the secondary optic based on the angle of the secondary optic,

$$\frac{\Delta\phi}{\Delta T_a} = e^{-k(T_a - 25)} \quad (20)$$

Where  $\Delta\Phi/\Delta T_a$  is the reduction of the light flux according with the temperature, for accomplishing the minimal requirements, and  $K$  is the temperature coefficient. The right number of LEDs was obtained by using the equation 21. [115]

$$N = \frac{\phi_{V\ realista}}{\phi_{LED}} = \left( \frac{\phi_{V\ spec}}{\phi_{cat}} \right) \left( \frac{F_{guard}}{(T_{signal})(T_{LED+optica})} \right) \quad (21)$$

The values used in these equations were obtained from the LED's characteristics provided by the supplier. Accordingly, we used a  $T_{filter}$  of 0.9 (red), a  $T_{glass}$  of 1, a  $L_{pattern}$  of 0.3 and a  $F_{guard}$  of 1.25, a  $\Phi(I_f, \theta_{ja})$  of 0.56 and a light transmission of the secondary optic of 40%.

The chosen LED - HPWT-MD00-F4000 - was supplied from the company Lumileds. After manipulating the equations from 16 to 21, the minimum number of LEDs needed was 11. The result obtained is in the acceptable interval according to this type of lamp. The number of LEDs according with the type of lamp is presented in the following figure 27.

LED P/N	$\Phi_{cat}$ , lm	Signal ECE Cat 1 Front Turn $\Phi_{spec} = 15,9$ lm	Signal ECE Cat 2a Rear Turn $\Phi_{spec} = 4,7$ lm	Signal ECE Cat S1 Stop $\Phi_{spec} = 5,5$ lm	Signal ECE Rear Fog $\Phi_{spec} = 12,4$ lm
HLMP-C100	$\approx 0,375$			60 to 120	132 to 264
HPWA-M/DH	C, 1,5			15 to 30	33 to 66
	D, 2,0			12 to 24	25 to 50
HPWT-M/DH	E, 2,5			9 to 18	20 to 40
	F, 3,0			8 to 16	17 to 34
	G, 3,5			7 to 14	14 to 28
	H, 4,0			6 to 12	13 to 26
	I, 4,5			5 to 10	11 to 22
	J, 5,0			4 to 8	10 to 20

Intervalo do numero de LEDS

Figure 27 the number of LEDs according with lamp in use [115]

#### 4.2.2 Electric circuit with conductive polymers

After defining the number of LEDs needed, the next step was to determine the main dimensions of the electric circuit. Calculations were made for the two sections of the circuit, for the section that connects the different LEDs and for the section that controls the light intensity. Paramount in these calculations was the consideration that the main objective of this research is the production and assembling of all components in the same mold. To achieve this objective it was decided to use conductive polymers rather than metallic wiring since it is faster to produce a complete electric system by injection than by assembling wiring by hand.

It was decided to maintain polycarbonate as the main raw material of the housing. This was an important point to consider, since the circuit will be over molded by a material with a high processing temperature. For that reason it was decided to use a similar material so as to minimise the occurrence of deformations in the circuit. Market research was undertaken on material availability, this leading to the selection of a conductive material produced by RTP Company, the EMI 362 Polycarbonate (PC) Stainless Steel Fiber Electrically Conductive EMI/RFI/ESD Protection. The main reason for selecting this material was its low volumetric electric resistance, about 1 ohm.cm.

During the development of the circuit it was also necessary to take into consideration the legislative requirements of ECE 50. This legislation indicates the minimum and maximum voltage that the circuit is obliged to support without losing properties. According to the legislation, the circuit needs to support two different electrical

voltages, 13.5 and 6.5 volts [109]. In our circuit the design was optimized for a fixed voltage of 13.5 volts, this decision to use just one voltage being taken based on the the common motorcycle battery that normally operates at this level of electrical tension.

Besides the legal requirement, it is necessary to take into account the LED requirements in terms of maximum and minimum voltages so they can work with their full capability. The chosen LEDs have a maximum current of 70 mA and a voltage of 2.5 volts. However, as with other similar LEDs, this type of light emitter has problems in releasing the heat they produce. According to the design guidelines, this necessitates placement of each LED with a minimum distance between centers of 15 mm [116].

Taking in consideration these requirements and the number of LEDs needed, it was decided to use the configuration presented in the following figure 28.

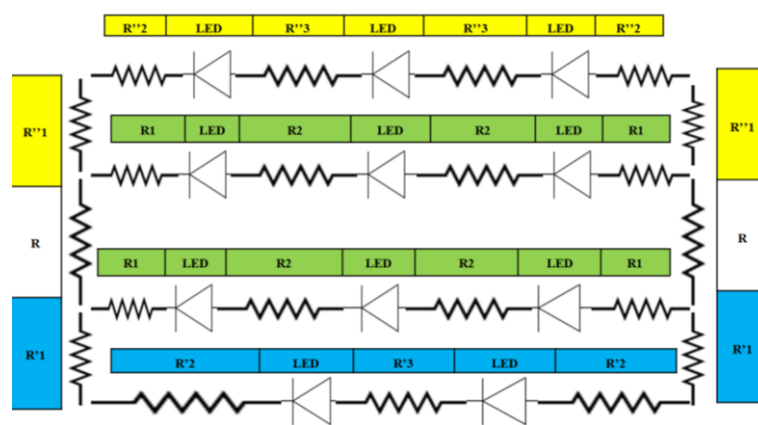


Figure 28 configuration of the electric circuit

The conductive section (in green) was the initial section to be designed after determination of the circuit was assessed. This was undertaken according with equation 22, using a voltage of 12.3V in all circuits.

$$V = R_1 I + V_{LED} + R_2 I + V_{LED} + R_2 I + V_{LED} + R_1 I \Leftrightarrow$$

$$\Leftrightarrow \frac{V - 3 \times V_{LED}}{I} = 2 \times R_1 + 2 \times R_2 \Leftrightarrow \frac{13,5 - 3 \times 2,5}{2 \times 70 \times 10^{-3}} = R_1 + R_2 \Leftrightarrow \quad (22)$$

$$\Leftrightarrow 42,86 = R_1 + R_2$$

Considering the large number of unknown parameter values in the equation and to keep manageable the complexity of the calculation, the values of width and thickness to obtain the optimal dimensions were calculated. The other dimensions such as distance between centers and the maximum width of the path were fixed (LED width). The optimal width and thickness of the circuit were obtained using the following equation 23.

$$R = \rho \times \frac{L}{A} \quad (23)$$

In equation 23 the  $\rho$  is the material resistivity, which in this case is 0.01 Ohm.m. L is the length between LEDs, and A is the cross section area of the conductive path. After manipulation of equation 23 the final dimensions of the circuit were obtained. In this case, for the section  $R_1$ , the following dimensions were obtained: thickness of 1.5 mm, width of 2 mm, length of 3 mm.

In the case of the section  $R_2$ , a width of 1.5 mm, a thickness of 1.5 mm and a length of 7.5 mm was obtained.

The electric circuit with the yellow color was designed with the same procedure used in the previous circuit. To determine the electric resistivity of the different parts in this circuit, equation 24 was used.

$$V = R_1''I + R_2''I + V_{LED} + R_3''I + V_{LED} + R_3''I + V_{LED} + R_2''I + R_1''I \Leftrightarrow$$

$$\Leftrightarrow \frac{V-3 \times V_{LED}}{I} = 2 \times R_1'' + 2 \times R_2'' + 2 \times R_3'' \Leftrightarrow \frac{13,5-3 \times 2,5}{2 \times 70 \times 10^{-3}} = R_1'' + R_2'' + R_3'' \Leftrightarrow \quad (24)$$

$$\Leftrightarrow 42,86 = R_1'' + R_2'' + R_3''$$

Besides equation 24, equation 23 was used to determine the final dimensions of this circuit. After manipulation of these two equations, the following values were obtained for  $R_1''$ , a length of 15mm and a width of 3.5mm. For  $R_2''$  the values obtained were a length of 3mm and a width of 4.4 mm. For  $R_3''$  the values obtained were a length of 7.4 mm and width of 5.3 mm. In this section of circuit the same thickness obtained in the previous circuit - 1.5 mm – was maintained.

The blue electric circuit section was the last circuit designed. In this circuit, equation 25 was used to determine the electric resistivity of the different parts constituting this section of circuit.

$$V = R'_1 I + R'_2 I + V_{LED} + R'_3 I + V_{LED} + R'_2 I + R'_1 I \Leftrightarrow$$

$$\Leftrightarrow \frac{V - 2 \times V_{LED}}{I} = 2 \times R'_1 + 2 \times R'_2 + R'_3 \Leftrightarrow \frac{13,5 - 2 \times 2,5}{70 \times 10^{-3}} = 2 \times R'_1 + 2 \times R'_2 + R'_3 \Leftrightarrow \quad (25)$$

$$\Leftrightarrow 121,43 = 2 \times R'_1 + 2 \times R'_2 + R'_3$$

The same procedures were used as in the sections above. Based on this, the values obtained for R''1 were a length of 15mm and a width of 3.5 mm, for R''2 a length of 10.5 mm and a width of 3.1 mm. For R''3 a length of 7.4 mm and a width of 2.7 mm was obtained. Again, in this last section of the circuit it was decided to maintain the same thickness of the previous section - 1.5 mm.

To finalize the design phase of the circuit it was necessary to insert additional electrical resistance. This had the objective of creating the capability of having in the same rear lamp two types of lights. In this case the objective is to accommodate the position light and the stop light. According to the literature, the position light must have 20% of the intensity of the stop light. This can be obtained, by adding more electric resistance in one section than another. This can be seen in the following figure 29.

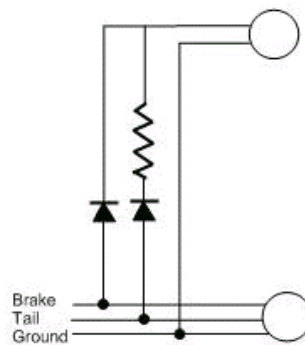


Figure 29 the electric circuit for producing two types of lights [117]

To obtain the 20% light intensity level it was necessary to analyse the data shown in figure 29. The figure presents the variation of the relative luminous flux with forward current for different thermal resistances. The LED that was used in the electric circuit

has a thermal resistance of 125°C/W. In figure 30 the curve for this thermal resistance is not shown. For this reason an approximation to the nearest curve available was made, in this case a thermal resistance of 200°C/W. Using this data, it was possible to determine the necessary current at which the LED will emit 20% of total luminous flux [118].

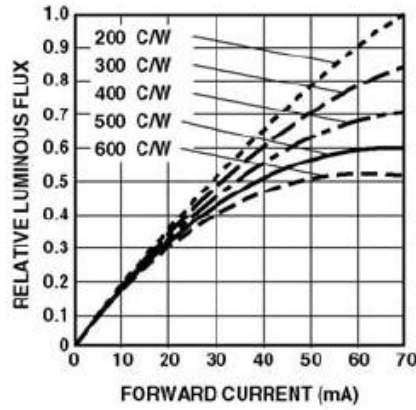


Figure 30 the relative luminous flux versus electric current [118]

According to figure 30 a current of 15 mA is needed to ensure having the necessary luminous flux required for the presence light. The remaining electric current will flow through the section of the circuit that controls the stop light. In this case an electric current of 55 mA was needed. Considering the requirements of these two electric currents it became necessary to add new structures to the circuit. These structures have the capability of controlling the current and subsequently the light that will be emitted in the rear lamp. After manipulating equation 23 the final dimensions of these structures was obtained. The structure that controls the presence light has a sectional dimension of 1.5x1.5 mm and a length of 6.5 mm. The structure that controls the stop light has a length of 3 mm with a sectional area of 1x4 mm<sup>2</sup>. The different lights connections and the final design of the electric circuit are presented in the following figures - 31 and 32.

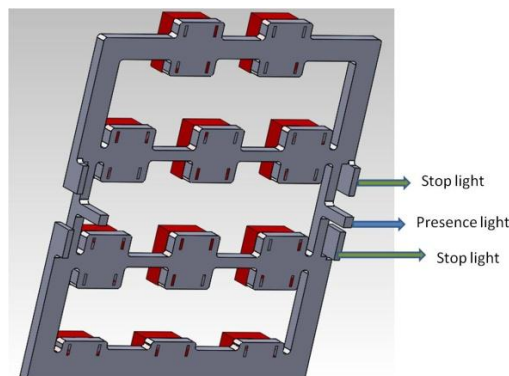


Figure 31 rear view of the electric circuit

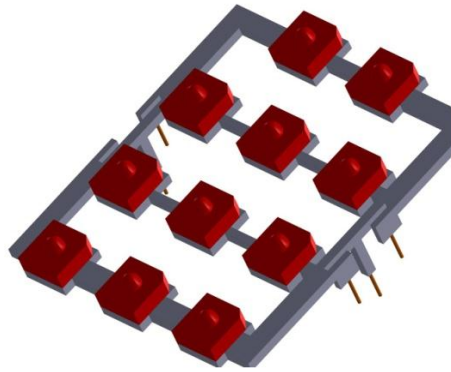


Figure 32 frontal view of the electric circuit

### 4.2.3 Preliminary tests of electric circuit

In this section the results of the experimental tests made to the design of the electric circuit presented previously are presented. The tests made had the objective of validating the data of the material used in previous calculus. Since the electric properties of this type of material are influenced by the level of dispersion of the fibers in the matrix it was necessary to determine the best injection parameters capable of maximizing the electric conductivity of the material. For that purpose a mold was built to produce the electric circuit.

The mold developed to inject the conductive polymer is presented in the following figure 33.

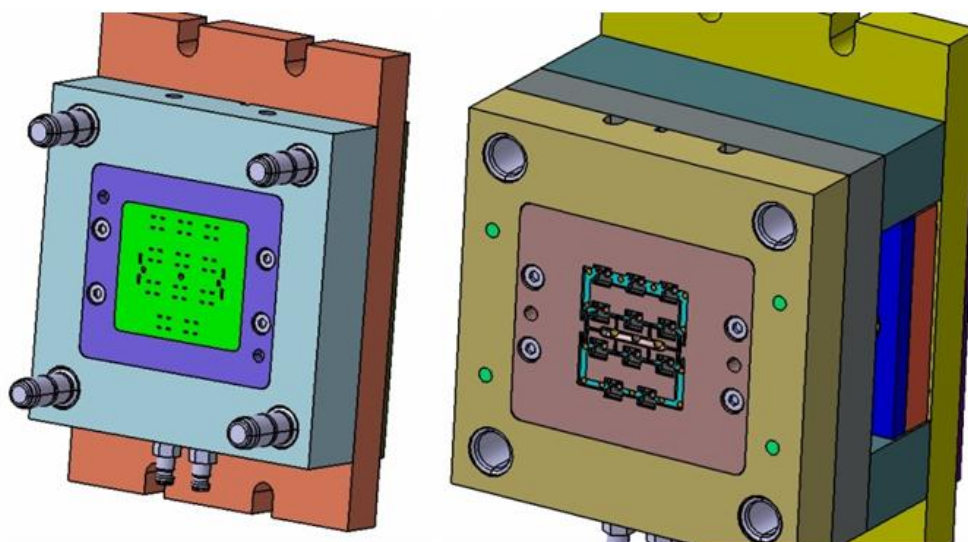


Figure 33 mold for injecting the conductive material



The mold had the dual purpose of evaluating the conductive properties of the material after injection and also validation of the chosen LED's – in particular, whether or not they could support the temperature and pressure parameters of the injection process. Figure 34 shows the mold cavities used to inject the different materials.

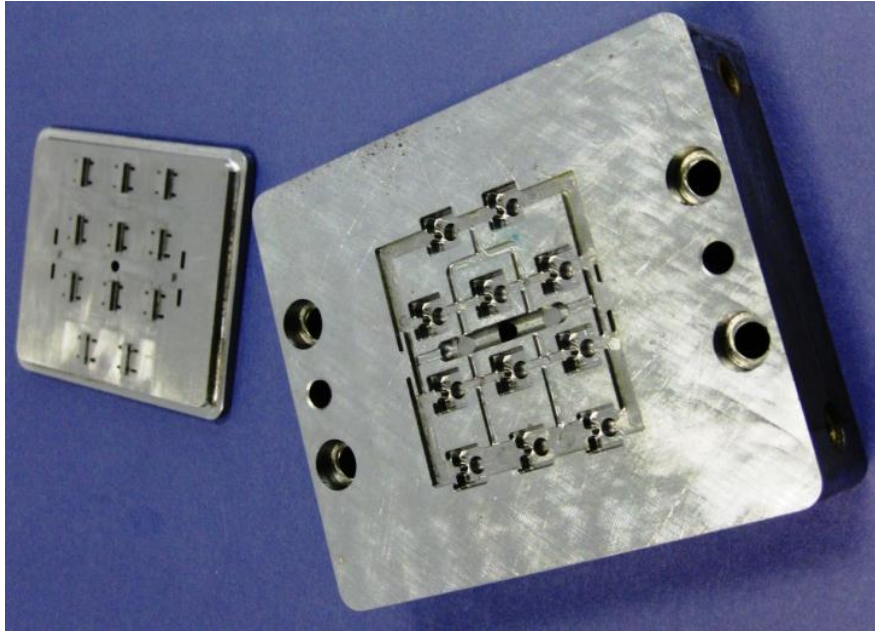


Figure 34 mold cavities

An electrical source - TTI EX752M Multi-mode PSU 75V/150V 300W – was used to test and validate all the injected electrical circuits. The tests were set up with a voltage of 12.5 V. Figure 35 shows the equipment and the voltage used.



Figure 35 electric tension used to test the conductive material



Initially the material used for the designed circuit was tested - EMI 362 Polycarbonate (PC) Stainless Steel Fiber Electrically Conductive EMI/RFI/ESD Protection. This material is supplied in two separate packages containing the metallic fibers and the polycarbonate. Since the final properties of the molding are depended on the distribution of the fibers, the two materials were mixed using an extrusion machine Coperion co-rotating twin screw extruder. The extruded material was injected in a Microinjection molding machine, Boy 12A. The injection molding processing parameters used are presented in the following table 6.

Table 6 - processing conditions used on the injection molding tests of the conductive polymer

Temperature (°C)		2 <sup>a</sup> Pressure		Velocity of injection
nozzle	Mold	Time	Pressure	
310	80	1s	25 Bar	120 mm/s

The first specimen analyzed was the specimen presented in figure 41. The specimen presented a high electric resistance and none of the LED's worked. To overcome the high resistance existent on the surface of the circuit it was decided to connect the wires of the electric source directly to the pins of the LEDs. All sections of the circuit were then analyzed; as can be seen, the LEDs that are in middle section and in the 2 LED section didn't emit light. The only section where it was possible to see light was on the bottom row of the circuit (Figure 36)..

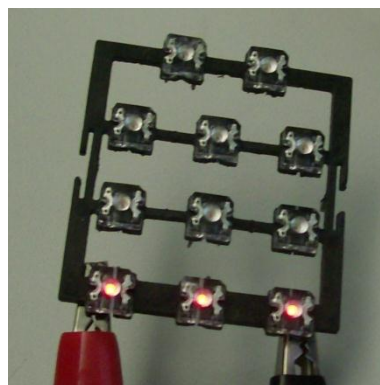


Figure 36 light emission by the LED on the base section

The results obtained in this initial test were not as expected. Rather than seeing all the LEDs emitting light, as expected, only the LEDs that are in the section with the wider width at the bottom are working.

To achieve the objective of having all the LEDs emitting light it was decided to analyze the properties of other material capable of conducting electricity. The materials considered are produced by Nanocyl S. A. and are supplied in Masterbatches. The materials selected were POM (Polyoxymethylene), PC and PP mixed with carbon nanotubes. Accordingly, the second material analyzed was the POM with 4% CNT. The injection conditions used are presented in Table 7.

Table 7 injection molding conditions for POM

Temperature (°C)		2 <sup>a</sup> Pressure		Injection velocity
Nzl	Mold	Tempo	Pressure	
200	80	1s	25 Bar	50 mm/s

The specimens produced with this new material presented better results. In this case it was possible to see at least two LEDs emitting light in each section; the light intensity was also higher compared to the first material analyzed.

However this material presented an unexpected behavior; for voltages higher than 12V the material started to melt. The results for different specimens are presented in figure 37.



Figure 37 POM mixed with 4% of CNT

Because of the melting of the material it was decided to study other matrices - PC and PP. In this new research it was also decided to study several percentages of carbon nanotubes for each matrix. In the case of the PC, two formulations were

selected, one with 4% CNT and the other with 5%. In the case of the PP three formulations were selected for examination, with 5% CNT, 7% and 9%. The processing conditions for each material are presented in the following table 8.

Table 8 injection molding conditions for the different materials tested

Material	Temperature (°C)		2 <sup>a</sup> Pressure		Velocity of injection
	Nzl	Mold	Time	Pressure	
PC4%	305	80	1s	40 Bar	50 mm/s
PC5%	290	80	2s	30 Bar	50 mm/s
PP5%	240	60	2 s	50 Bar	25 mm/s
PP7%	240	60	2 s	50 Bar	25 mm/s
PP9%	240	60	2 s	50 Bar	25 mm/s

The first material to be analyzed was PC mixed with 4% of CNT. The use of PC had the objective of decreasing the risk of losing electric properties and avoiding deformation when in contact with the material (PC) of the housing. Based on the good results obtained with the POM the same percentage of CNT, 4%, was used for the initial tests. However the PC mixed with 4% of CNT did not present the expected results. The injected circuit showed lower luminous intensity when compared to the POM at the same voltage although the number of LEDs seen to be emitting visible light was higher. This material also presented a higher electric resistance on the skin. Comparing the two - PC and POM – it was verified that PC does not melt with comparable increases in voltage. The results obtained are presented in the figure 38.

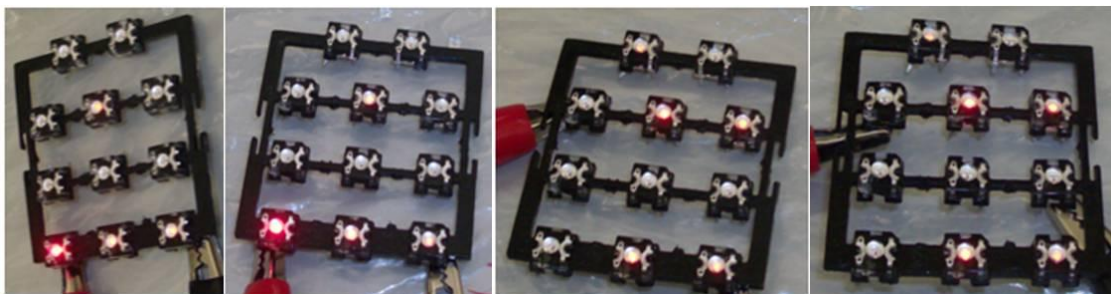


Figure 38 Circuit test with PC with 4% of CNT

Despite the lower light intensity emitted by the LEDs, the material showed an interesting result - the amount of LED that were emitting light was higher for the same

voltage. For that reason it was decided to increase the percentage of CNT by 1%. With this increase it was deemed possible to decrease the resistance of the electric circuit and this proved to be the case. The specimens with 5% of CNT presented better results compared to the specimens with 4% of CNT. However, despite the good results obtained, it was not possible to see all LEDs working at the design voltage; it was necessary to increase the voltage higher than 13 V to see all LED's working. The first results obtained for this material are presented in the figure 39.

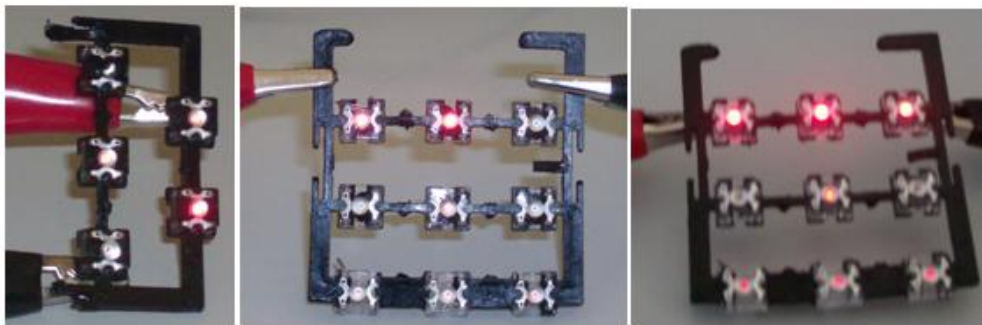


Figure 39 Circuit Test with PC with 5% of CNT

To overcome the high surface resistivity and taking into consideration that the majority of the CNTs are within the core it was decided to introduce metallic wiring in the connections. These wires have the primary objective of overcoming the high resistivity presented in the skin of the material used for the circuit. After this approach was adopted the results expected were obtained; it proved possible to turn on all the LED's at the designed voltage. The result obtained is presented in the figure 40.

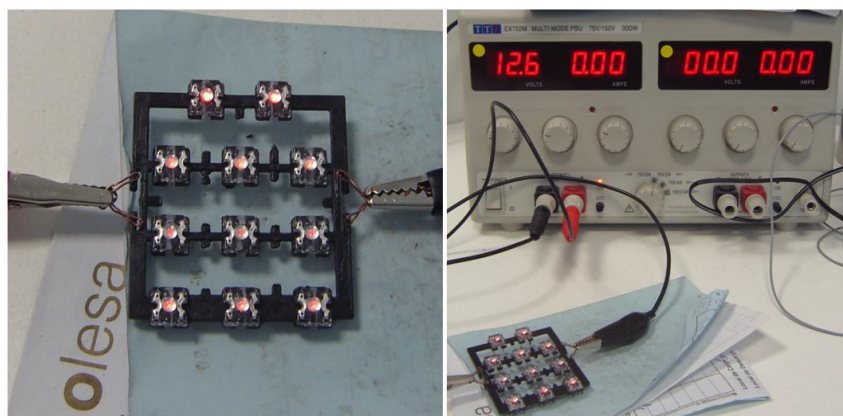


Figure 40 Final result of the PC with 5% of CNT

After the conclusion of this test it was necessary to understand if the electric circuit had the capability of working 24/7 with the same voltage and without losing luminous intensity. Accordingly, the electric circuit was tested continuously 24 hours daily for



one week at ambient environment temperature at a voltage of 12.6V. Throughout the test the circuit kept the same dimension without presenting any deformation and at the same level of luminous light intensity.

The last material to be tested was the PP. This material was selected due to its lower price and processing temperature in comparison with PC. The material chosen for study was PLASTICYL™ PP 2001 with 20% of CNT. According to the supplier, this material needs a higher percentage of CNT to obtain the same conductivity as PC. For the purposes of this study, three percentages of CNT, 5%, 7% and 9% were analysed.

The PP mixed with 5% of CNT was tested. When the design voltage of 12.6V was applied, none of the LEDs turned on. When the voltage was increase to 29.4 Volts the LED's turned on as presented in the following figure 41.



Figure 41 PP mixed with 5% (w/w) of CNT

The PP mixed with 7% of CNT was tested next. With this material some of the LEDs emitted light when the design voltage of 12.4V was supplied as can be seen in the following figure 42.

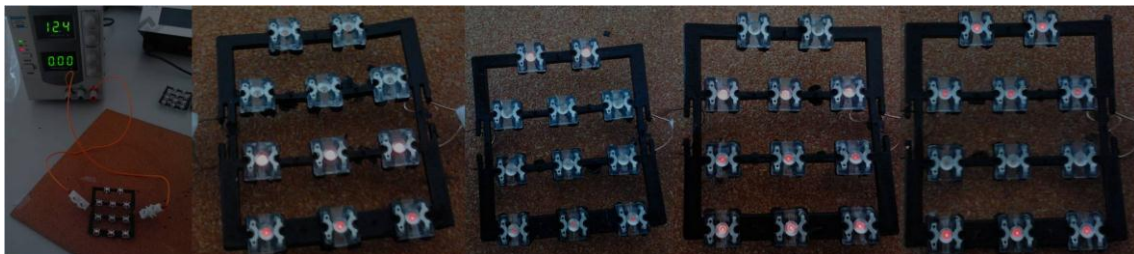


Figure 42 PP mixed with 7% (w/w) of CNT

The PP mixed with 9% of CNT was the material that presented the best results. In this case, it was possible to see all the LEDs emitting light at 12.5 V with a good intensity.

The electric circuit test showed all the LEDs emitting light as can be seen in figure 43.

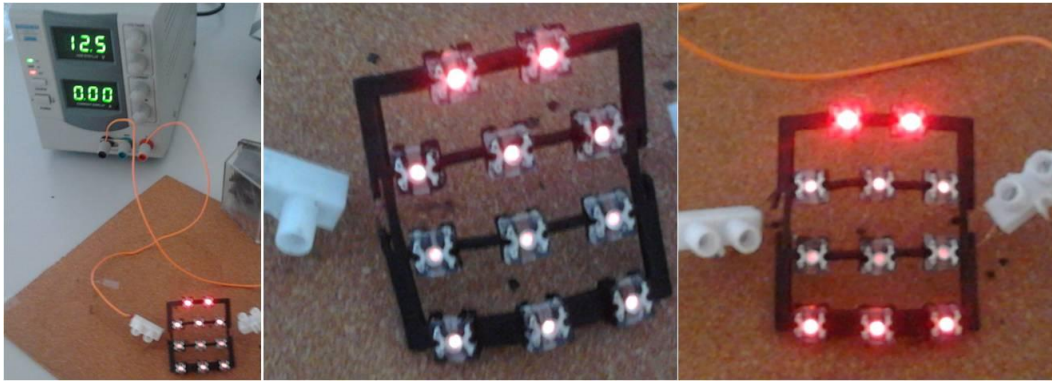


Figure 43 PP mixed with 9% (w/w) of CNT

#### 4.2.4 Secondary optics

When designing a rear lamp or a head lamp, it is always necessary to consider the view angles. These angles are the angles where the lamp must be visible to others – motorcycle and automobile drivers, pedestrians, etc. during the day and at night. According with regulation number 50 of ECE, every rear light of a motorcycle must have a horizontal view angle of  $-80^{\circ}/+80^{\circ}$  and a vertical angle between  $-15^{\circ}/+15^{\circ}$ . Based on the information gathered from this legislation it was necessary to verify if the chosen LED is compliant with these requirements. The chosen LED has an open vertical and horizontal angle of  $-35^{\circ}/35^{\circ}$ . After this angle, the luminous intensity is reduced to zero and other drivers cannot see it. The open angles of the LED are given shown in figure44 [120].

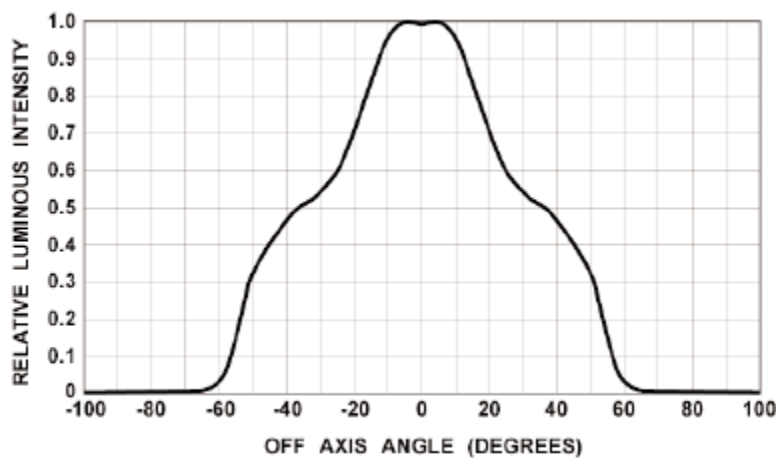


Figure 44 Luminous intensity of the LEDs HPWT-MX [120]

In the case of the vertical angle the chosen LED overcomes the limit required. In relation to the horizontal angle the luminous intensity is not enough. For that reason it was necessary to design structures capable of orienting the light according to the legislation. These structures are the pillow lens and reflective cavities. The pillow lens has the objective of increasing the horizontal angle while the reflective cavities serve to reduce the vertical angle. The reflective cavities are present in the following figure 45.

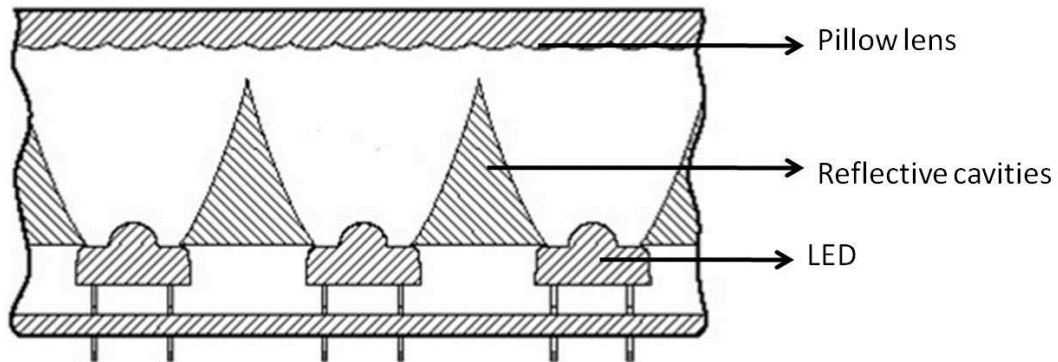


Figure 45 The Secondary optics [120]

The procedures used to design the reflective cavities - the equations and the calculi needed – so as to comply with legislative requirements are set out below.

To calculate the dimensions of the reflective cavities it was necessary to consider several factors – the distance between the centers of the LEDs (15 mm), the diameter of the crystal of the LED and the position where the light will be emitted. In this case an F value of  $0,99 \approx 1\text{mm}$  was used.

The different fs and the other factors needed to do the calculus are presented in the following figures 46 and 47.

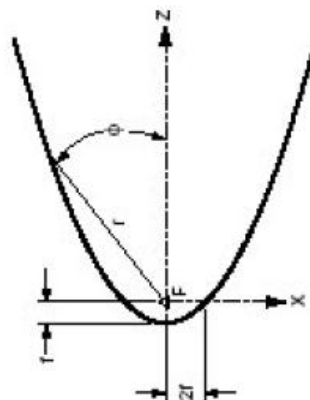


Figure 46 factors that influence the built of the reflection parabolas [120]

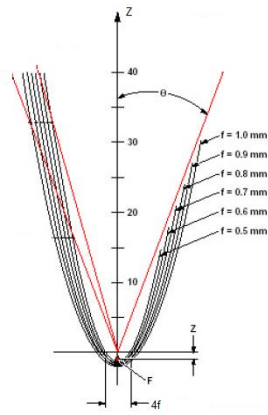


Figure 47 different parabolas according with the different fs [120]

So as to determine f equation 26 was used.

$$2f < \frac{1}{2} \times \text{diameter of the crystal of the LED} \quad (26)$$

For the chosen LED, the ideal f was 0.8, but because of the distance between the centers of the LEDs it was decided to use an  $\underline{f}$  of 0.66; with this value an open angle of  $20^\circ$  was obtained. To decrease this to the angle required by law  $-15^\circ/+15^\circ$  - it was necessary to create a negatively sloped structure of  $-5^\circ$  to comply with the legislation. The redesigned reflective cavities are shown in the following figure 48.

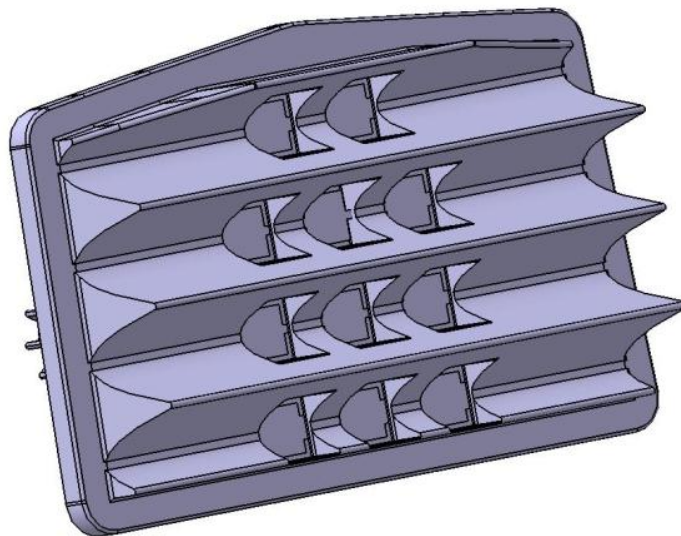


Figure 48 reflective cavities for the case study



Below are presented the calculus made to determine the final dimensions of the optical pillows. The supplier of the LEDs recommended the values presented in figures 49 and 50 to design the pillow lens.

Application	LED Type	Collimating Optic	$A_h$ (deg)	$A_v$ (deg)	$R_h$ (mm)	$P_h$ (mm)	$R_v$ (mm)	$P_v$ (mm)
CHMSL	HPWA-MHOO	Fresnel Lens (B = 5°)	22	22	5.3	4	5.3	4
CHMSL	HPWT-DHOO	None (B = 20°)	5	5	17	3	17	3
RCL/FTS	HPWT-MxOO	Fresnel Lens (B = 7°)	30	20	4.0	4	8.9	5.7
RCL/FTS	HPWT-MxOO	Reflector Cavity (B = 20°)	5	5	17	3	17	3

Figure 49 the pillow optics factors [112]

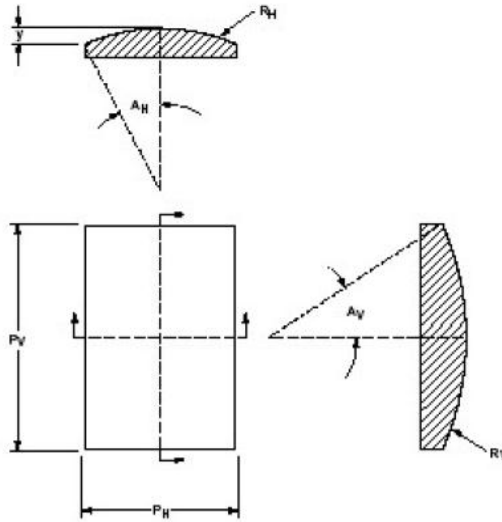


Figure 50 geometry of the pillow optics [120]

To finalize the design of the pillows it was necessary to determine the thickness of the pillow,  $y$ , used in the equation 27.

$$y = R_h(1 - \cos A_h) \quad (27)$$

After manipulating equation 27, a pillow thickness value of 0.065 mm was obtained. The final design of the crystal, is presented in the following figure 51.

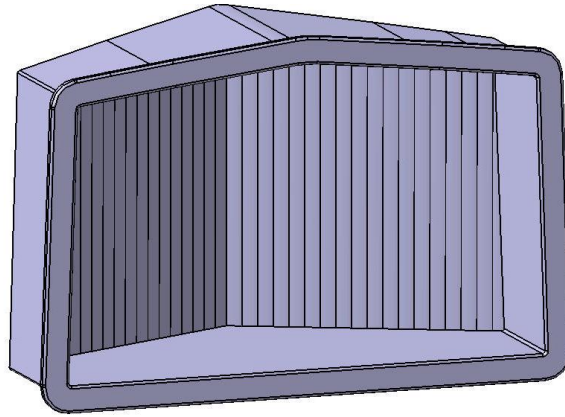


Figure 51 final design of the crystal with the optic pillows

### 4.3 Laser welding tests

With the design of the component case study approaching finalisation, the next step consisted of defining the best prospective welding procedure. This entailed consideration of defining the laser requirement as well as further study of the different materials to be used.

#### 4.3.1 Laser requirements

The definition of the laser requirement is of overriding importance to the project. In moving toward this definition the following requirements were considered:

- the thickness of the parts
- the materials and the specifications of the robot (motorman) – particularly the maximum load that it can support
- The capability of the laser to weld by transmission. This means that the beam wavelength must be in or near the infrared area, namely with a wavelength between 800 and 1080 nm

The power necessary to weld the two parts of the case study has not been defined. To determine the power needed Equation 15 was used (page 44), which was developed by Casalino G. and Ghorbel E [52]

Considering the materials under study and the requirements of the transmission welding process, it was decided to input the material property parameters of PC into equation 15 in the first instance. This material was chosen first due to its high melting temperature and due to the possibility of its being used as the absorber material. The parameters entered were  $\rho$  1220 kg/m<sup>3</sup>,  $T_m$  300 ° C (573 K) and  $c$  1300 J / (kgK). Since the material is amorphous the Hm factor was not considered and a thickness of 0.25 mm of molten material was entered. For the purposes of the calculation, a robot speed of 5 m / min (0.083 m / s) was used (but this speed can increase up to 12 m / min – the maximum speed of the robot). An initial laser beam diameter of 2 mm was also assumed. Working this through equation 15 a laser power requirement 77.9 W was obtained.

The equation used does not take into account power losses occasioned by laser reflectivity when welding transparent material. Making allowance for this, it was decided to increase the laser power requirement to 100W since normally of the order of 5% of the power is reflected by transparent material.

#### **4.3.2 Transmittance analysis to the plastic materials**

To achieve a good seam is necessary that all the energy from the laser arrives at the welding zone. In order to analyze the interactions occurring between the light and the polymer through a non-destructive method, four polymers (PMMA, PP Homopolymer, PP Copolymer and PC) were studied in terms of their salient characteristics - reflection, absorbance and transmission.

These interactions can be variously analysed through spectroscopy as FTIR (Fourier transform infrared) and/or UV-Vis (Ultra violet – visible) or near infrared spectroscopy. Considering the characteristics of the process it was decided to use near-infrared spectroscopy because this analytical method uses much the same spectrum as the laser chosen to do the welding. Through the tests undertaken it was possible to establish the amount of energy that was lost when the beam enters in contact with the transparent part. Table 9 following, details the materials and additives that were selected for analysis.

Table 9 Raw-materials analysed

Material	Additive	Supplier
Lexan PC 123R		Sabic®
Lexan PC3412R	20% glass fiber	Sabic®
PLEXIGLAS PMMA 8N		Evonik®
PP Moplen 348U		LyondellBasell ®
PP 579S		Sabic ®
PP 15T1020	20% talc	Sabic ®
Domolen P1-302-V30-N	30% talc	Domolen
	LWRPP267	Clearweld ®
	230 44 LBS 042407	interfibe®

In subsequent tests on the above materials the influence that glass fibers and talc have on the transmission of the laser beam through the specimen material were evaluated. In table 10, all the materials and additives selected for study are presented.

Table 10 materials and additives studied

Materials	Additives	Total weight
PMMA	Without	0%
PP (Homopolymer)	Without	0%
	Glass fiber	10%
		20%
	Talc	10%
		20%
PP (Copolymer)	Without	0%
	Clearweld	10%
	Wood fibers	10%
PC	Without	0%
	Glass fibers	10%
		20%

For the near-infrared spectroscopy a Spectrophotometer Shimadzu UV-3101PC UV-VIS-NIR equipped with an integrated sphere and a temperature control system Peltier® was used.

The test subjects used were injection molded discs of the various material/additive combinations with a nominal dimension of 2.1 mm thick and a diameter of 60 mm. Figure 52 details one such.

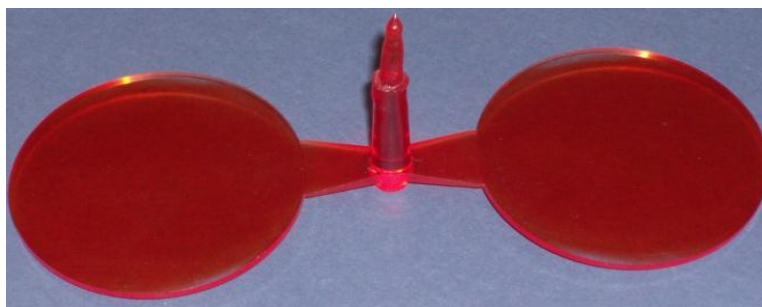


Figure 52 specimen analyzed

The discs were produced in an injection molding machine with 45 ton of clamp force – an Engel 45T. The processing characteristics for the different materials analysed are shown in Tables 11 and 12, for amorphous and semi-crystalline materials respectively.

Table 11 presents data as to the different processing conditions adopted for PC and PC with glass fibres and PMMA.

Table 11 Processing conditions of the amorphous polymers

Material	Temperature (°C)	Holding Pressure		Injection velocity
	Nzl*	Pressure	Time	
PC 123r	280	80 bar	30s	120 mm/s
PC 123r + PC 3412R	295	65 bar	6 s	25 mm/s
PC 3412R	295	80 bar	6 s	100 mm/s
PMMA	255	110 bar	32s	120 mm/s

\*Nzl=nozzle

In table 12 the different processing conditions for the different PPs and the PPs mixed with talc, glass fibres and with special additives as Clearweld® and wood fibres.

Table 12 Processing conditions of the semi-crystalline materials

Material	Temperature (°C)	2 <sup>a</sup> Pressure		Injection Velocity
	Nzl	Pressure	Time	
PP 348U (cop)	215	50 bar	30 s	120 mm/s
PP 579S (homo)	215	60 bar	12 s	150 mm/s
PP579S+ P1-302-V30-N	215	60 bar	12 s	120 mm/s
PP527S +PP15T1020	215	60 bar	12 s	120 mm/s
PP15T1020	215	65 bar	12 s	120 mm/s
PP 348U +LWRPP267	215	50 bar	30 s	120 mm/s
PP 348U +230 44 LBS042407	215	55 bar	12 s	100 mm/s

\*Nzl=nozzle

The processing conditions were unchanged for similar materials; in some mixtures it was necessary to adjust the second pressure or the injection velocity to achieve a good distribution of the additives.

The first comparison made on the NIR spectroscopy study, was done between the two amorphous materials, PMMA and PC, as can be seen in figure 53.

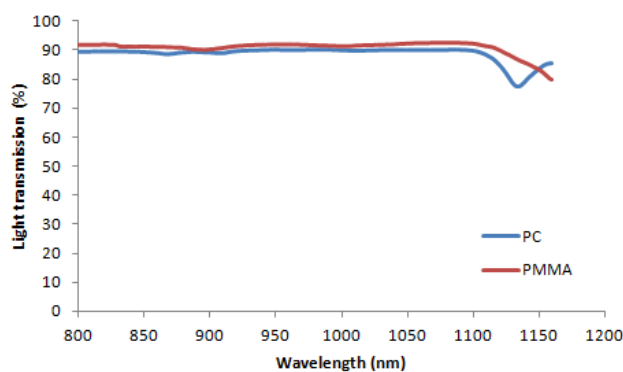


Figure 53 the transmittance analysis; PC and PMMA

The results registered by these two amorphous materials showed a high degree of transparency in all NIR spectra, indicating that these two materials are not suitable for use as the absorbent material. The difference between them occurs when a beam with wavelength of 1150 nm passes through them, this result showing that for these amorphous polymers the molecular chain does not affect the transmittance of the laser beam.

Figure 54 presents transmittance analysis results for PC with difference percentages of glass fiber admixed.

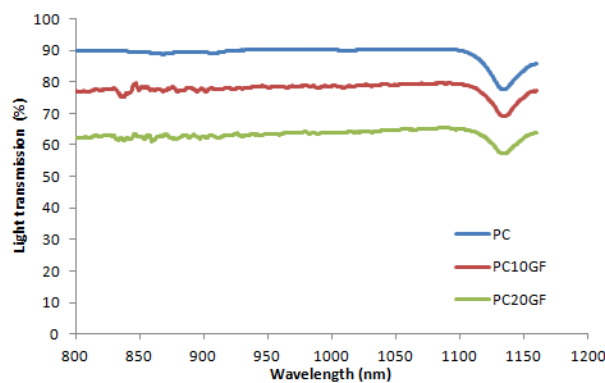


Figure 54 the transmittance analysis to PC and PC mixed with Glass Fiber

The NIR spectroscopy results for PC with and without glass fiber illustrates the extent that the glass fibers influence the light transmission. Transparency is seen to be progressively reduced with increases in the percentage of glass fiber - across the entire spectra analyzed.

The test showed that an increase of 20% of glass fiber was accompanied by a reduction of 30% in light transmittance - along the entire spectrum analyzed. The PC showed a peculiar behavior at wavelength of 1150 nm, where the transparency tends to diminish by 10% or so independent of the quantity of glass fiber added. Considering that the discs tested did not present any visible defect or deformation nor had any other additive, further study is needed to explain this behaviour. In any event, at a wavelength of 940 nm a light transmittance of 63% was determined for the PC sample with 20% glass fiber.

In figure 55 the results obtained with the PP homopolymer and copolymer are detailed.

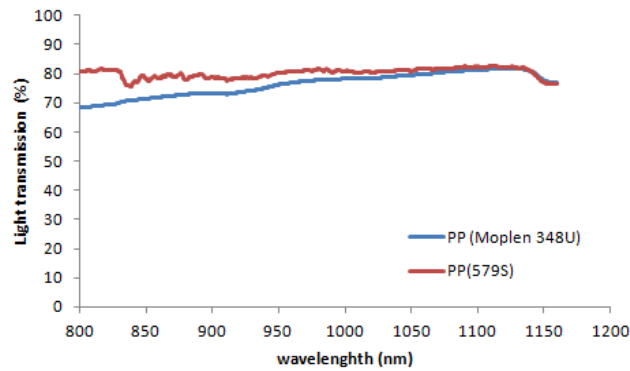


Figure 55 the Transmittance analysis of PP homopolymer and copolymer

The two materials present broadly similar transmittance values between the wavelength of 1000 and 1200 nm although the Moplen 348U (PP copolymer) spectrum exhibits slightly less transparency to light when compared with the PP 579S (PP homopolymer). This behavior could be explained through the different morphology of these materials. It is well known that in semi-crystalline materials the crystalline structures have the capability to reflect the light. Some reduction in transparency is visible between 800 and 1000 nm; more importantly, at the wavelength of the laser the PP579S showed a transparency near 80% and the Moplen near 75%.

In figure 56 the NIR results obtained from the different PP additive mixtures are presented. In these tests varying percentages of talc and glass fiber were mixed with PP 597S.

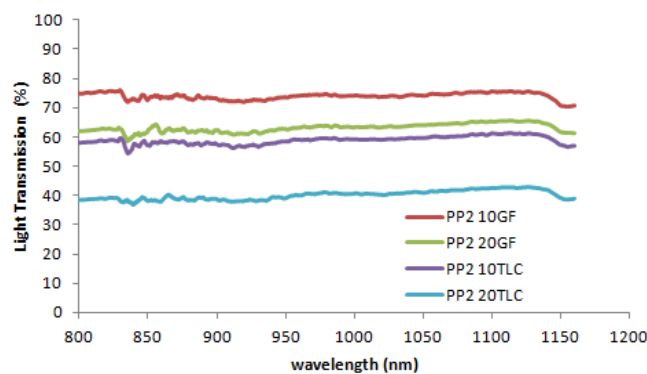


Figure 56 the transmittance analysis to PP mixtures



The results obtained showed some correspondence with those posted by the PC samples, the PP samples with the higher percentage of additives having a lower transparency to light. It was also observed that talc (TLC) was the additive with the most powerful influence on light transmittance. The results demonstrate that it is necessary to double the percentage of glass fiber to obtain a similar reduction in the transparency to light obtained with talc.

The results obtained with the PP mixed with two special additives - wood fibers and Clearweld - are presented in figure 57 and 58, respectively. The reason for studying cellulose/wood fibers was due to their recent increased utilization in the automotive industry.

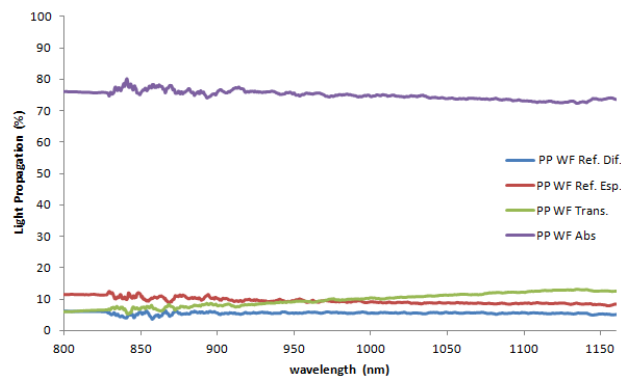


Figure 57 transmittance analysis of the mixture of PP with cellulose fibers

The results obtained demonstrated that the addition of 10% of wood fibers in PP showed a good capability for absorbing light emissions across the entire NIR spectrum. As measured, the material proved capable of absorbing near 80% of all the light emitted; the absorbance was calculated by measuring the differences between the light emitted, the light that crosses and the light that is reflected in either diffuse or specular form. With the result obtained it is possible to conclude that wood fibers can be a good substitute for special additives such as Clearweld, that are more expensive.

The NIR results of the mixture of PP Moplen 348U with the masterbatch supplied by Clearweld® are presented in figure 58. In this case 10% of the total weight of the PP/masterbatch mixture was comprised of masterbatch. The main reason for choosing the Clearweld masterbatch was due to its capability of absorbing light of the same wavelength as that of the chosen laser beam..

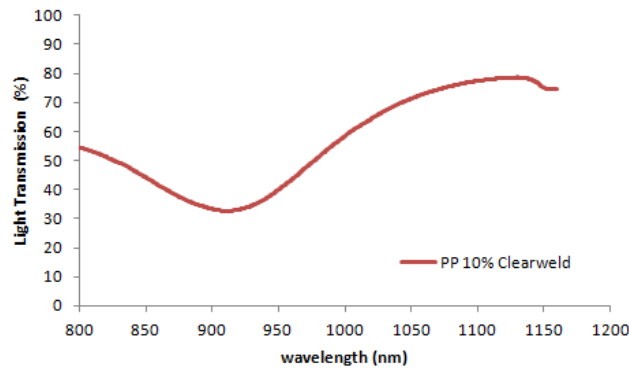


Figure 58 transmittance analysis of the mixture PP with Clearweld

As it was expected the additive supplied by Clearweld, presented a high level of absorbance of the light emitted between 900 and 950 nm. The results also demonstrate that the percentage of this additive used is not high enough since 30% of the light emitted with a wavelength of 947 nm crosses the material. Despite this result, a good mechanical resistance of the seam is to be expected since 70% of the light was absorbed by the material.

### 4.3.3 Preliminary welding tests and results

In this item will be presented and discussed the mechanical tests made to the different materials analyzed previously. The mechanical tests were made according with standard EN 12814-3:2000: Testing of welded joints of thermoplastics semi-finished products.

#### 4.3.3.1 The moldings

In these tests rectangular plates with nominal dimensions of 150x80 mm with a thickness of 2 mm. were used; the plates were produced in an injection molding machine - Ferromatik Milacron- K85 S 2F.

Tables 13 and 14 present the processing conditions used for PPs and PCs/PMMA, respectively in these tests.

Table 13 Processing conditions of the semicrystalline material samples

Material	Temperature (°C)	Holding pressure		Injection velocity
	Nzl	pressure	Time	
PP	215	23 bar	12 s	40 mm/s

A mold temperature of 40°C was used to produce the PP plates.

Table 14 Processing conditions used to produce the PCs and PMMA samples

Material	Temperature (°C)	Holding Pressure		Injection velocity
	nzl	Pressure	Time	
PC	280	23 bar	12 s	40 mm/s
PC GF	280	50 bar	12 s	40 mm/s
PMMA	255	23 bar	12 s	40 mm/s

To produce the PC and PMMA plates a mold temperature of 80°C was used.

#### 4.3.4 Test procedure

In order to obtain the best welding properties a DOE (table 16) was undertaken using as variables the width of the welding path, the welding velocity and the laser power. Four specimens were used for each condition. The intervals of values used to weld the amorphous materials are listed below;

- Velocity: maximum: 40 cm/min, minimum 20 cm/min
- Diameter: maximum 2 mm, minimum 1 mm
- Power: maximum 40 Watts, minimum 20 Watts

For these studies it was decided to use initially the materials that are commonly used on rear lamps and head lamps - namely PC mixed with 3% w/w carbon black as the absorber (housing), and PMMA as transparent to the laser beam (crystal). Since the two materials chosen have similar glass transition temperatures (T<sub>g</sub>) the welding possibilities are favourable.

In the following table15, the values used to construct the Taguchi L8 table are presented .

Table 15 Taguchi L8 table for PC with PMMA welding studies

	Laser Diameter	Laser Velocity	Laser Power
E1	1	1	1
E2	1	1	2
E3	1	2	1
E4	1	2	2
E5	2	1	1
E6	2	1	2
E7	2	2	1
E8	2	2	2

Apart from the use of PC and PMMA, other possibilities were studied, such as PP. This material was considered since PP has a lower cost compared to both PC and PMMA. This lower cost is of great advantage for mass production of components for the automotive industry. To weld the PP material the same procedure used in the PC/PMMA test was adopted. The difference between the first and the second test was the addition of one more material. In this case two transparent materials were used - a PP homopolymer and a PP copolymer. .As an absorber a PP admixture with 3% (w/w) of carbon black was used. This analysis had the objective of understand how these materials can be joined under a laser beam.

The preliminary results obtained in the mechanical tests performed on the PP samples showed a large standard deviation and a great number of specimens separated without being tested. Based on these pre-analysis results it was decided to repeat the tests.

For the second analysis the same materials - PP 579 (level 2) and PP Moplen RP348U (level 1) – were used. However, in comparison to the first analysis two injection parameters were changed - the mold temperature and the cooling time. These particular parameters were chosen because of the influence that they have on the growth of crystalline structures. For the mold temperature parameter it was decided to use a temperature of 40°C for level 2 and 25°C for level 1. For the cooling time parameter a time of 30 s for level 2 and 15 s for level 1 was used. In terms of welding conditions, a laser power of 30 W and 15 W was used, a welding velocity of 40 cm/min and 20

cm/min and a beam diameter of 2 mm and 1 mm. The higher values correspond to level 2 and the lower values to level 1.

The Taguchi table used to test the combination PP with PP is presented on the table 16.

Table 16 New Taguchi table for the PP

	Material	mold temperature	cooling time	Laser Power	welding velocity	Laser diameter
1	2	2	2	2	2	2
2	2	2	2	1	1	1
3	1	2	1	2	2	2
4	1	2	1	1	1	1
5	2	1	1	2	1	1
6	2	1	1	1	2	2
7	1	1	2	2	1	1
8	1	1	2	1	2	2

To test the mechanical resistance of the different transmission welded seams it was decided to use the standard EN 12814-3, testing of welded joints of thermoplastics semi-finished products- Part 3: Tensile creep test. This standard defines the procedure and the nominal dimensions of the specimen according to the thickness of the final components. The various different material specimens used in these tests all had a nominal thickness of 2 mm, which gave a final thickness ( $a_n$ ) of 4 mm. The specimen configuration used on the mechanical tests is presented in figure 59.

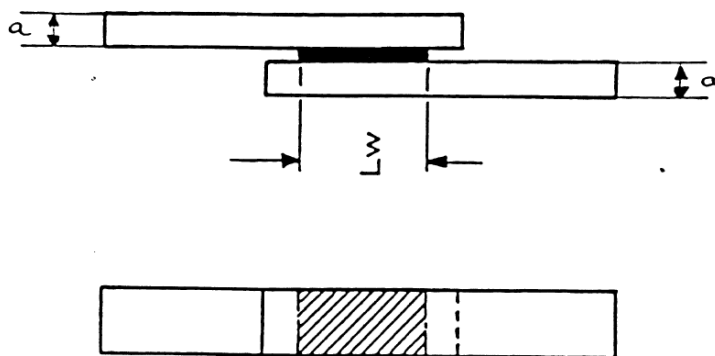


Figure 59 specimen configuration

Based on the final thickness of the case study, the standard indicates the use of a nominal width ( $b$ ) of 15 mm, a  $L_0$  120 mm and  $L$  170 mm. For these tests it was decided to use specimens with a width of 30 mm  $L_0$  120 mm and  $L$  170 mm. The use of these

dimensions was due to the existence of a mold with these same dimensions. The dimension of the specimens used in these tests is presented in the figure 60.

$D_n$ or $a_n$	$b$	$L_0$	$L$
$20 \leq D_n < 50$	$a_n + \frac{D_n}{10}$	80	$\geq 120$
$50 \leq D_n < 100$	$a_n + \frac{D_n}{10}$	120	$\geq 170$
$D_n \geq 100$ or flat assemblies : $a_n < 10$	15	120	$\geq 170$
$10 < a_n \leq 20$	30	120	$\geq 170$
$a_n > 20$	$1,5 \times a_n$	$3 \times a_n + L_w$ with 120 min.	$\geq L_0 + 80$

Figure 60 dimensions of the different specimens according with the final thickness

With the definition of the materials, the dimensions of the specimens and the test procedure established, the welding process was initiated. In the following figure 61 a specimen welded with the diode laser used is shown. The image presented is of a specimen welded where PMMA is the transparent material and the PC (black) the absorbent material. The specimen presented in figure 61 was welded using welding condition number 4 of table 15.

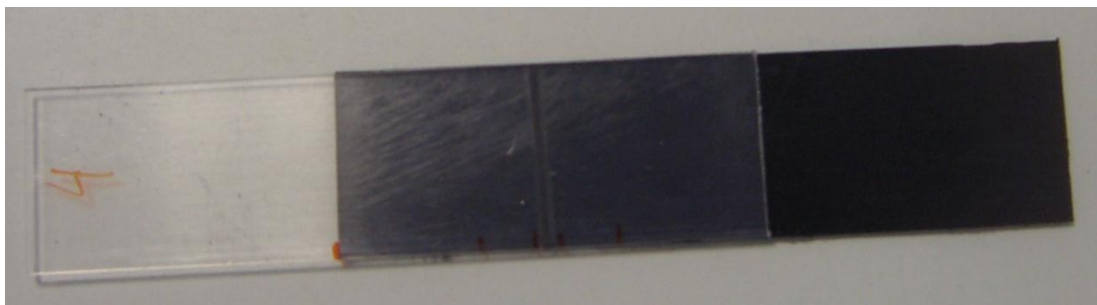


Figure 61 sample test welded by laser welding

#### 4.3.5 Mechanical tests results

After all the specimens had been welded the mechanical tests assessment was started. This assessment had the objective of determining which welding conditions are more suitable to produce a seam with higher resistance. The best welding conditions were used to join the two components of the component case study. The mechanical tests

were made on the specimens welded with the conditions presented in table 17 and 18. The mechanical tests were made in a universal test machine Shimadzu, from PIEP (Polo de Inovação em Engenharia de Polímeros). A displacement velocity of 1 mm/s was used. In the following figure 62 the test machine is presented demonstrating how the sample has been placed.



Figure 62 Testing machine

To calculate the maximum shear stress the following formula 28 was used.

$$\tau = \frac{F}{A} \quad (28)$$

The F represents the load applied by the machine and A is the welding area.

Deformation was determined according to equation 29.

$$\varepsilon = \frac{L - L_0}{L} \times 100 \quad (29)$$

Where L represents the length span of the samples grips after the application of the load and  $L_0$  represents the initial length span of the samples grips.

Firstly will be presented and discussed the results obtained for the seams of PC/PMMA. These tests were made in a room temperature of 23°C. The different welds were evaluated in terms of the maximum Shear Stress and maximum deformation. The

results for the mechanical resistance of the eight different welding conditions chosen are presented in the figure 63.

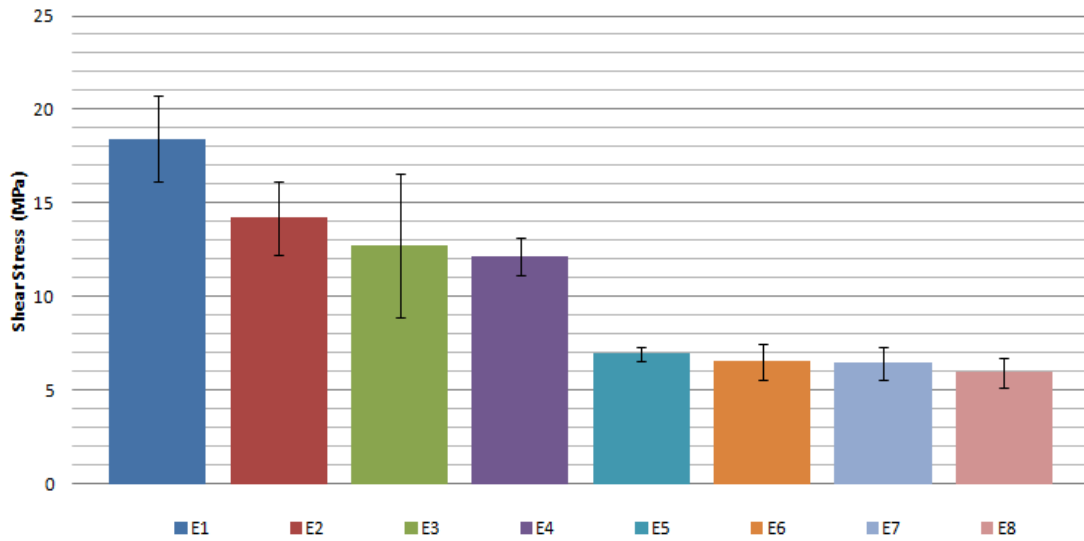


Figure 63 the Shear stress of the welded PC/PMMA specimens

The NIR analysis undertaken on the PMMA sample showed that this material present a high transparency to the laser used in the tests. The transparency is the factor that controls the amount of net energy that arrives at the welding zone. Moreover, this transparency will also influence the distribution of laser energy along the welding path. During the welding of these two materials temperatures near 700°C were registered. These temperatures were obtained when a laser power of 40W was applied. This temperature was measured mainly on the edge of the specimens and was obtained independently of the velocity used. In the zones where this temperature was measured smoke was observed; the smoke was later confirmed as evaporated material of the absorber material. The evaporation of this material created gaps in the final seam. Based on this observation a lower mechanical resistance of the seam was anticipated. This result was verified as a few specimens, when fixed to the clamps of the tensile machine, ruptured without the application of any force. Despite this problem it proved possible to test at least three specimens for each welding condition. With the results obtained the conclusion could be reached that the specimens that were welded with the lowest laser power, velocity and diameter were the specimens presenting the higher mechanical resistance values measured.



The other specimens – those welded with higher levels of power, velocity, diameter, etc. – all presented uniformly lower mechanical resistance values. Typically, these specimens presented seam resistance values averaging some 4 MPa lower than comparable specimens welded under condition 1. The specimens welded with a laser diameter of 2 mm presented a seam with a stress at rupture half that of the specimens welded with a laser beam of 1 mm. The welded materials presented a lower standard deviation on all welding conditions. The specimens that presented the smallest standard deviation, were the specimens welded with the conditions E4 (diameter 1 mm; velocity: 40 cm/min; Power: 40 Watts) and E5 (diameter 2 mm; velocity: 20 cm/min; Power: 20 Watts). The specimens welded with condition E3 (diameter 1 mm; velocity: 40 cm/min; Power: 20 Watts) were the specimens that presented higher variation.

The deformation results obtained of the different welding conditions are presented in the figure 64.

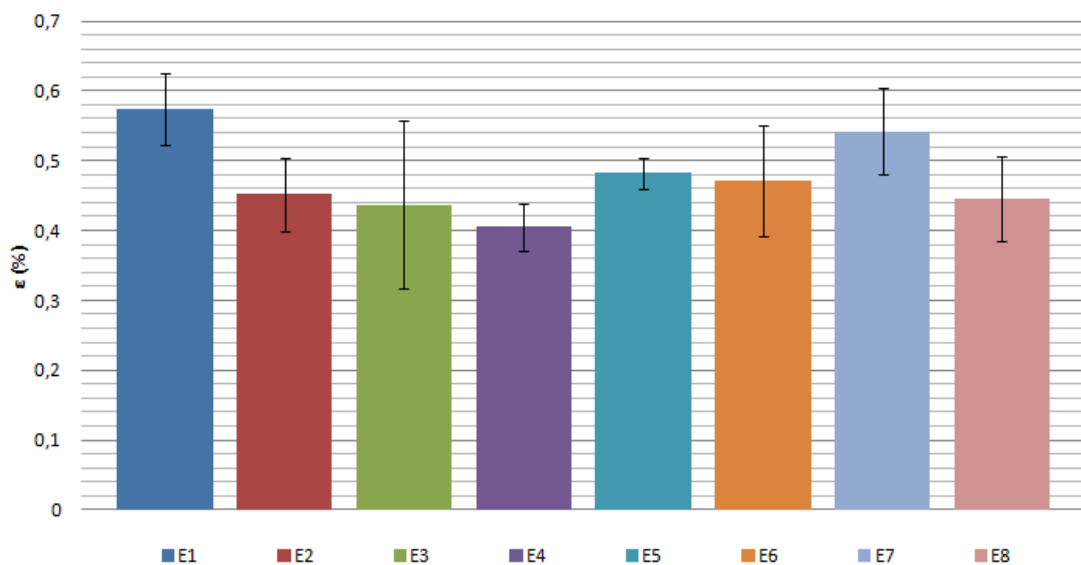


Figure 64 Deformation of the PC/PMMA specimens

The seams obtained were also evaluated in terms of deformation; the results presented above showed that all weld specimens presented an average deformation lower than 1%. The results also showed that maintaining the diameter and changing the other variable factors will reduce the final deformation of the specimen seam. The specimens welded with a laser beam with a diameter of 1 mm presented a reduction of maximum deformation, with increase of the power and the velocity. This behavior can be

explained due to the high temperatures measured during the welding process. The evaporation of the material had as consequence the reduction in the amount of net energy conducted between the two materials. This gap reduced the seam resistance and with this the deformation of the seam. In addition, the existence of a gap may have helped in the propagation of a crack when an external force was applied.

For the specimens welded with a laser of the diameter of 2mm the results were different. Here the deformation recorded did not decrease with increased laser power and velocity. The results showed a similar deformation between specimens welded with the maximum velocity and minimal power and those specimens welded with the lower weld values.

Overall, the standard deviation for deformation was similar to the results obtained for the seam resistance.

With the end of mechanical testing an evaluation through the DOE (design of experiences) was undertaken so as to bring out which factors are more important in terms of mechanical resistance of the seam. The results are presented in Table 17 below.

Table 17 DOE results for PMMA/PC

	Laser Diameter	Laser Velocity	Laser Power	Shear Stress (MPa)
E1	1	1	1	18,4
E2	1	1	2	14,2
E3	1	2	1	12,7
E4	1	2	2	12,2
E5	2	1	1	7,0
E6	2	1	2	6,6
E7	2	2	1	6,5
E8	2	2	2	6,0
-	14,4	11,6	11,2	
+	6,5	9,3	9,7	
effect	-7,9	-2,2	-1,4	

The results show the major influence of laser diameter (-7.90 MPa) on the final seam mechanical resistance values. The other two factors – laser velocity and laser power –

clearly have a degree of influence on the final resistance of the seam but far less when compared to that of laser diameter..

Evaluating these results with respect to the primary objective of deciding which condition will be used in the component case study it would seem that in terms of seam resistance condition E1 presented the higher stress levels at rupture. In terms of reliability, condition E5 presented the lower standard variation. Based on these results it was decided to use condition E1 since this was the condition yielding specimens presenting the higher seam resistance while registering a broadly comparable level of standard variation when compared to condition E5.

After this initial approach it was decided to evaluate other amorphous materials that are also transparent to laser. In this case it was decided to evaluate PC and PC mixed with different percentages of glass fibers. These tests had the objective of studying the influence of glass fibers and other amorphous materials in terms of final seam mechanical resistance and reliability. The different specimens were welded with condition E1 presented in table 12. In these new tests a laser material absorber was used, in this case PC mixed with 3% carbon black.

The shear stress levels at rupture of the various PC/glass fiber admixtures are presented in figure 65.

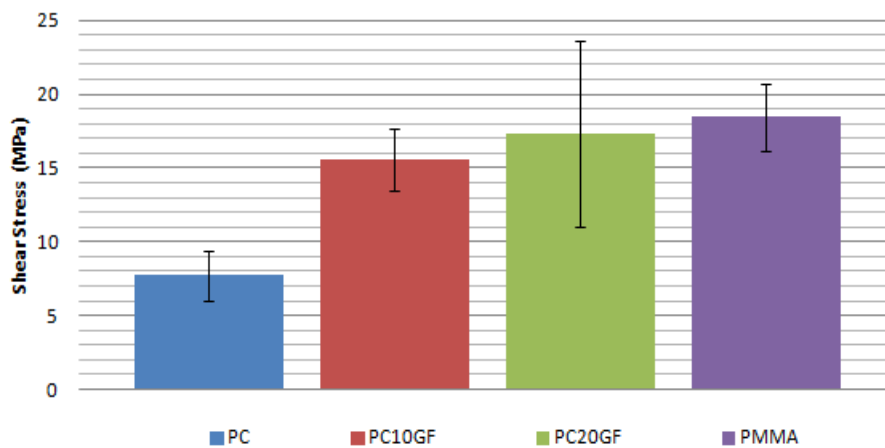


Figure 65 Shear Stress for the different amorphous materials

The mechanical tests showed that the PC (transparent) samples welded with the same conditions as the PMMA sample presented a uniformly lower seam resistance. The results also showed that the mixture of glass fiber with the PC increased the resistance of the seam. Considering that glass fibers have the capability of reflecting or refracting the laser beam, a lower seam resistance could have been expected. The results

showed that increasing the percentage of glass fiber increases the resistance of the seam. The specimens PC/PC were the specimens presenting the lowest mechanical resistance compared to the other materials. A higher level of seam resistance could well have been anticipated since the absorber layer and the transparent layer were of the same material and that no additives with the capability of adversely influencing the laser beam were present. The lower resistance values obtained can be explained by the high temperatures measured during the welding process; in some of the specimens temperatures near 500°C were measured which are close to the evaporation temperature of this material. As observed earlier, this would tend to create gaps between the two plates since the material that has the objective of absorbing the laser beam energy has evaporated.

In terms of standard deviation, the results obtained were in accord with what was expected - the higher the concentration of glass fiber, the higher the standard deviation registered. This is due to the capability that glass fibers have to affect the path of the laser beam. The materials without additives presented broadly similar patterns of standard deviation. The average deformation at rupture of the different materials tested is presented in figure 66.

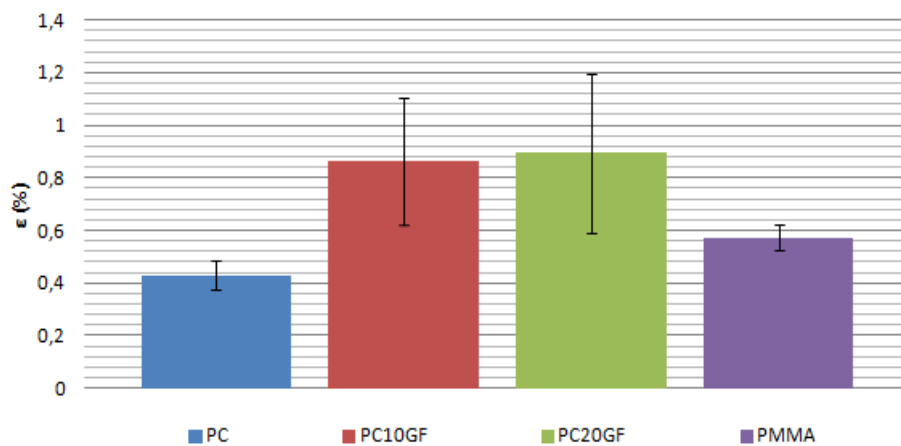


Figure 66 Deformation of the different amorphous materials

Relative to the deformation levels obtained, the results show interesting result. The PC with the highest percentage of glass fiber presented the highest deformation. Clearly, augmentation of the percentage of fibers increases the deformation of the material; the same material without additives presents a much lower level of deformation. The materials with added glass fiber continued to present a higher standard deviation. These results are explained by the influence that glass fiber has on reflection

and refraction of the laser beam. The PMMA and PC samples, despite differences in the relative levels of deformation, presented the lower levels of standard deviation.

While examination of the mechanical resistance and deformation of these amorphous materials has yielded satisfactory results, PMMA and PC are relatively expensive materials, particularly for the application envisioned. It is possible to find materials with lesser properties that are adequate for the application and that are available at lower cost. One of these materials is PP. For that reason it was decided to run the same tests as those done on the amorphous materials so as to better understand the comparable seam mechanical resistance properties of PP.

Initially, a pre-analysis of the welding process was undertaken with the objective of understanding how these materials can be joined under a laser beam. The results of the tests made in PP/PP seams are presented in figure 67.

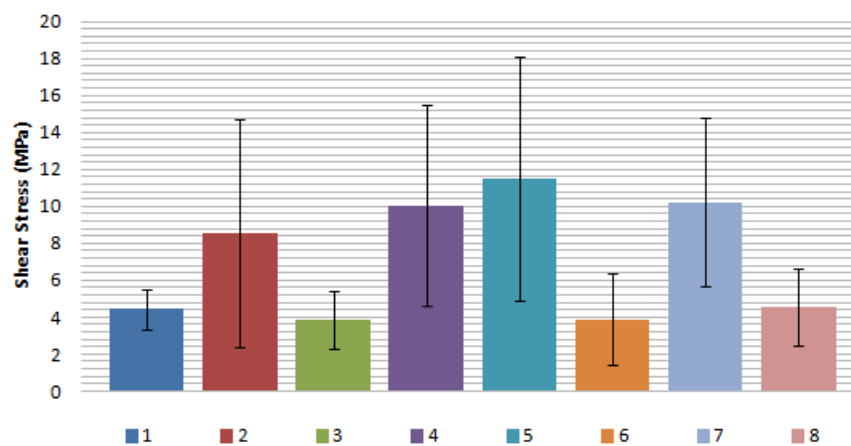


Figure 67 A new analysis to evaluate the Shear Stress of the PP/PP seam

This analysis also had the objective to better understand the influence that the formation of crystalline structures has on seam quality. To this end, the influence of various injection parameters was considered. In this analysis more homogeneous results were obtained compared to the initial PP/PP study. The results showed that the material with the higher power, higher velocity, higher laser diameter, higher cooling time and higher mold temperature had the lowest standard deviation. The weld that presented the higher seam resistance was obtained from the specimens welded and injected under condition 5 whereby specimens were injected with a lower mold temperature and a lower cooling time and welded with the lower welding velocity, the smaller diameter laser and with the higher laser power. Despite producing a seam with a higher resistance, the

specimens continued to show a higher standard deviation, since it proved possible to obtain seam resistance values varying from 5 MPa to 18MPa with the same apparently less reliable material. All in all, the high degree of influence of the processing conditions anticipated in these tests was verified.

The results also showed that the increase of laser beam diameter has a direct influence on the ultimate resistance of the seam. The specimens that were welded with a beam with a diameter of 2 mm presented a shear stress at rupture half that of the other specimens welded with the 1 mm diameter laser.

The results for the average deformation and standard deviation tests undertaken are presented in figure 68.

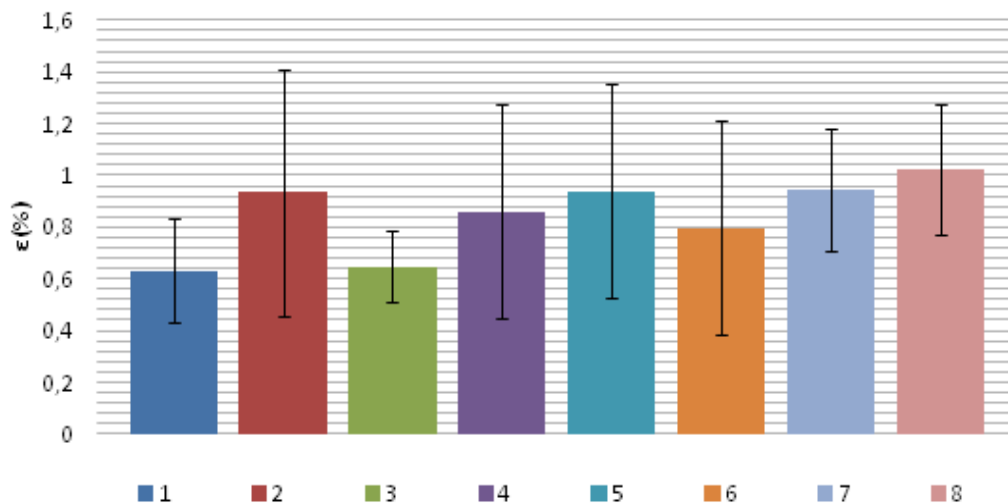


Figure 68 Seam deformation for laser welding PP/PP

As can be seen, specimens 1 and 3 were the specimens presenting the lowest deformation, near 0.8 %. At the same time they were the specimens presenting the smallest levels of standard deviation. With these results, it is possible to conclude that these two welding and injection conditions, are the most reliable to be used in future applications.

As observed in the seam resistance tests, mold temperature and cooling time did not appear to have directly influenced the deformation levels of the specimens. The DOE results are presented on table 18.

Table 18 DOE results for PP/PP

exp	Material	mold temperature	cooling time	laser Power	welding velocity	laser diameter	S (MPa)
1	2	2	2	2	2	2	4,4
2	2	2	2	1	1	1	8,5
3	1	2	1	2	2	2	3,9
4	1	2	1	1	1	1	10,0
5	2	1	1	1	1	1	11,5
6	2	1	1	1	2	2	3,9
7	1	1	2	2	1	1	10,2
8	1	1	2	1	1	2	4,5
1	7,2	7,5	7,3	6,7	10,1	10,1	
2	7,1	6,7	6,9	4,2	4,2	4,2	
Effect	-0,1	-0,8	-0,4	-2,6	-5,9	-5,9	

The DOE analysis for these tests showed that laser diameter (-5.89 MPa) and welding velocity (-5.86 MPa) represented the major influences on the final quality of the PP/PP seam recorded, these two variables having similar degrees of influence. Based on the results obtained, it is possible to conclude that the diameter factor represented the higher influence. Laser power (-2.57 MPa) was the other variable having a great influence on the final seam quality, the other variables showing much lower levels of influence.

Comparing the results obtained in the PMMA/PC tests, in the case of PP/PP tests broadly similar results were obtained.

Besides common PP, is possible to find PP mixed with different additives on the market, these materials normally being used to improve the mechanical properties of common PP. The most common additives used for this purpose are glass fibers (GF) and talc (TLC). In the market it is also possible to find other additives such as wood fibers (WF) and special additives for enhancing laser absorption such as Clearweld (CLW). Due the interesting properties of these materials, it was decided to evaluate them so as to understand the influence of the additives on the final mechanical resistance of the seam.

The seam resistance and the standard deviation for the different materials tested are presented in figure 69.

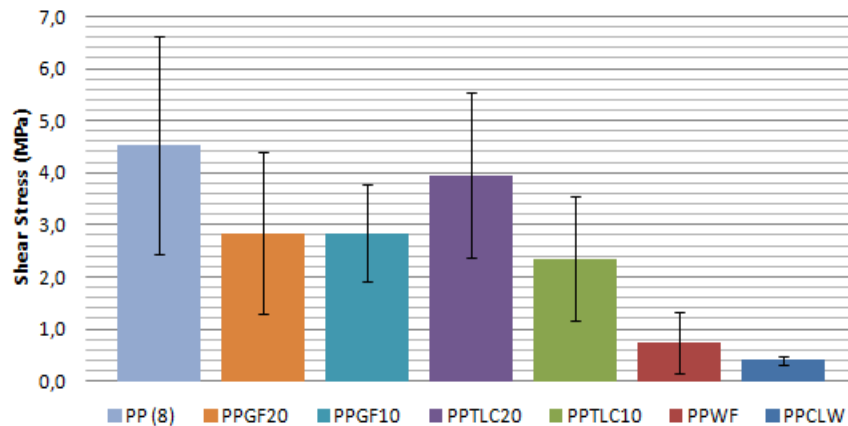


Figure 69 Comparison between PP / PP with additives

After a preliminary analysis of the material characteristics to hand, it was decided to weld the materials using the parameters detailed for condition number 8 as presented in Table 15. To verify the comparative influence that these additives have on the final quality of the seam proved problematic as it became apparent that it was not always possible to use the same conditions during the welding process. In some cases the high concentration of additives implied a corresponding increase in laser power to obtain a seam. One such example occurred in the weld made between PP with 20% of talc and PP mixed with 3% of carbon black. Due to the high concentration of talc, it was necessary to increase the power of the laser to obtain the weld. Increased laser power also proved necessary when attempting to weld PP597S (transparent) to a PP/wood fiber admixture. In this case, it was necessary to increase the laser power to 50W to obtain a joint of the two materials. The last case occurred when making the join between PP597S (transparent) with PP mixed with Clearweld. To obtain a seam between these two materials it proved necessary to increase laser power to the maximum possible, which was of 100 W.

The results presented in the figure 69, showed that the materials that used carbon black as the additive to promote laser beam absorption presented the higher resistances. The materials mixed with laser absorber enhancing additives such as wood fibers or Clearweld produced seams presenting with very low resistance values compared to those obtained from the materials with carbon black.



In terms of additive influence on the laser beam path, the results showed that talc showed more influence than glass fiber. In this case, the results showed that the increasing concentration of talc implied a corresponding increase in the laser power needed to weld. For example to weld PP with 20% of talc to PP with carbon black it was necessary to increase the laser power to 30W. This increase of in power increased the mechanical resistance of the seam, which was expected, since more energy is arriving at the welding zone. The PP/10% talc sample was the material that showed the lowest resistance values when compared to the other materials welded with the same laser power. As was expected, the PP sample without additives presented the seam with the higher resistance levels. The results obtained allow us to conclude that the simple presence of additives such as talc reduces the amount of energy that arrives at the welding zone. To overcome this problem, in future applications, where these additives are present, the diameter and the power from the laser should be increased. Besides lowering seam resistance, the presence of these additives increases the standard deviation. This result was expected, since these additives have the capability to reflect and/or refract the light, these interactions occurring between the laser beam and the additives invariably reduce the amount of energy arriving at the welding zone.

This analysis had another objective which was the study of the influence of additives that have the capability of absorbing laser beam energy. To this end, additives such as wood fiber and a special additive supplied by Clearweld were also examined. The seam obtained from a sample of PP welded with a PP/wood fiber mixture presented a lower mechanical resistance compared to specimens prepared using carbon black. These weldings presented an average shear stress of 7 MPa and a large standard deviation. The higher resistance was anticipated since this material presented a high level of energy absorbance in the laser wavelength during the NIR analysis undertaken earlier. During the welding of the two materials a high variation of temperature along the entire weld path was observed. This variation is due to distribution of the wood fibers that are responsible for absorbing the laser beam in the matrix. The large variations in temperature demonstrate that part of the energy of the laser beam is being absorbed by the fiber and part is passing through the specimen, the temperature fluctuations reflecting poor fiber distribution within the polymer matrix.

The additive supplied by Clearweld was also studied. To weld a PP/PP with Clearweld sample it was necessary to increase the laser power and reduce the diameter and velocity of the laser. To obtain the desired seam a power of 100W was needed to

join the two materials. The mechanical resistance and the standard deviation presented by the two seams tested was the lowest of all materials tested.

The Clearweld samples used as the absorber material presented the weakest seams overall. Indeed, it proved necessary to weld more than 10 plates of this material together to obtain 2 specimens capable of being mechanically tested. With the two analyses made, it is possible to conclude that is necessary to increase the concentration of Clearweld to obtain a good seam. Figure 70 presents analysis of the deformation levels obtained from the different samples tested.

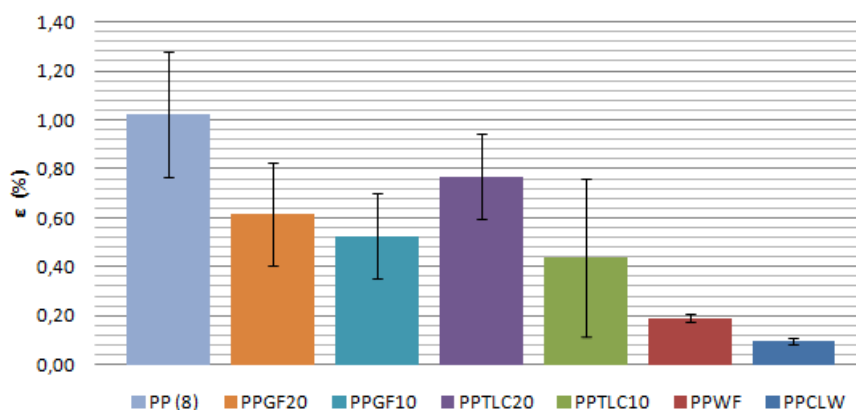


Figure 70 Deformation of the PP with different additives on their matrix

All the PP specimens with additives presented lower deformation when compared to the specimen with no additives, the PP sample with 20% of talc registering the higher level of deformation of all the specimens with additives.

In terms of the absorbent additives, the sample with the carbon black as an absorber was the material that presented the higher deformation, overall, when compared to the other additives. At the same time, the specimens that were welded using the carbon black absorber presented the higher levels of standard deviation.

#### 4.3.6 Visual inspection results

Having studied the mechanical behavior of the different welded materials, this section presents the results of a visual inspections of the seams of the different material combinations detailed in table 19 as well as the PC/PC welds and the PMMA/PC seams analysed above. This visual analysis had the objective of examining and verifying the degree of bonding and level of mixture occurring between the two materials after being

welded by laser. The visual inspection was made using a Lupe Stereoscopic Nikon SMZ-10 and a digital camera Olympus DP11 with four times of magnification. Due to the size of the welding path it was impossible to take a photo of the whole seam length and because of this it was decided to present two photos of each of the seams analyzed. One was taken near the middle of the seam and the other on the edge of the seam; the left-hand side photos shown below are always of the middle section while the right-hand side photos are always of the edge section.

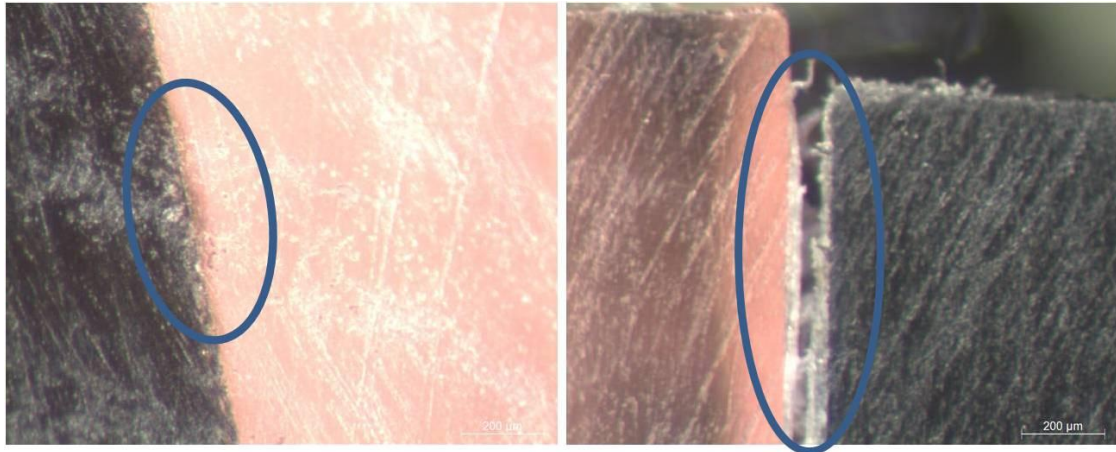


Figure 71 photos of the seam of the weld between PMMA with PC

In figure 71 in the middle section (left) it is possible to discern a small area of bonding between the PMMA and PC (inside the blue circle).

A continuous mixture of the two along the entire seam had been anticipated but this did not happen. The low pressure applied to keep the two materials connected can explain this result. At the same time, the image showed perfect contact between the two materials without the occurrence of any voids. The explanation for this comes from the low thermal levels exchanged between the two materials. In this case, the material that absorbed the laser energy did not exchange the necessary heat needed to form the seam.

The image taken at the edge of the weld path (figure 71 right) reveals a gap between the two materials (highlighted inside the blue circle). This defect is due to the low pressure applied to keep the two plates connected in the welding zone. Defects of this nature will be responsible for the initiation and the propagation of cracks when a load overcome the resistance of the seam.

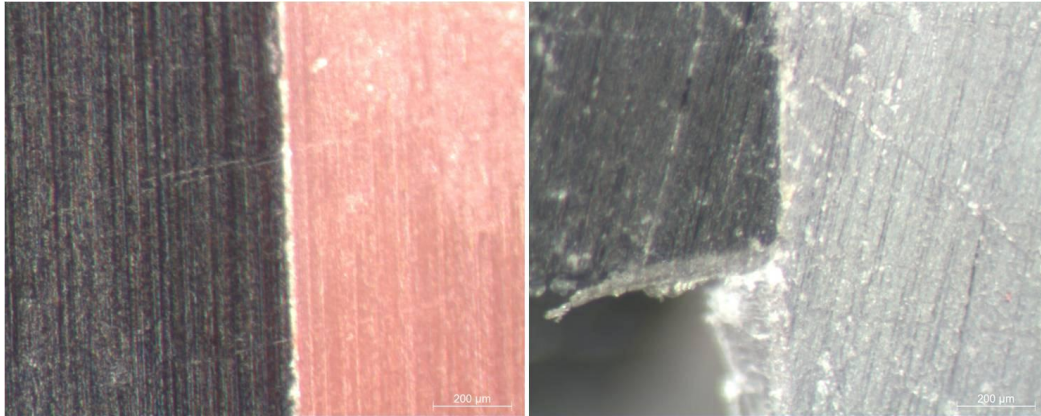


Figure 72 photos of the weld made between PC with PC

In figure 72 the photos taken of the welding zone of the PC/PC sample are presented. In the photos taken, it is possible to visualize a perfect contact between the two materials leading on to improved seam resistance when external loads are applied. No voids are discernable throughout the entire seam.

The following paragraphs analyze the PP/PP specimens welded according to table 16. The first specimen analyzed was the specimen welded with condition 1 of table 16. In the middle section of the weld (figure 73, left) an extensive bonding zone can be readily seen. The zone is clearly visible inside the blue circle. In this case, the material that absorbs the laser has blended well with the transparent material making it possible to obtain a good seam. No voids can be seen along the entire weld path.

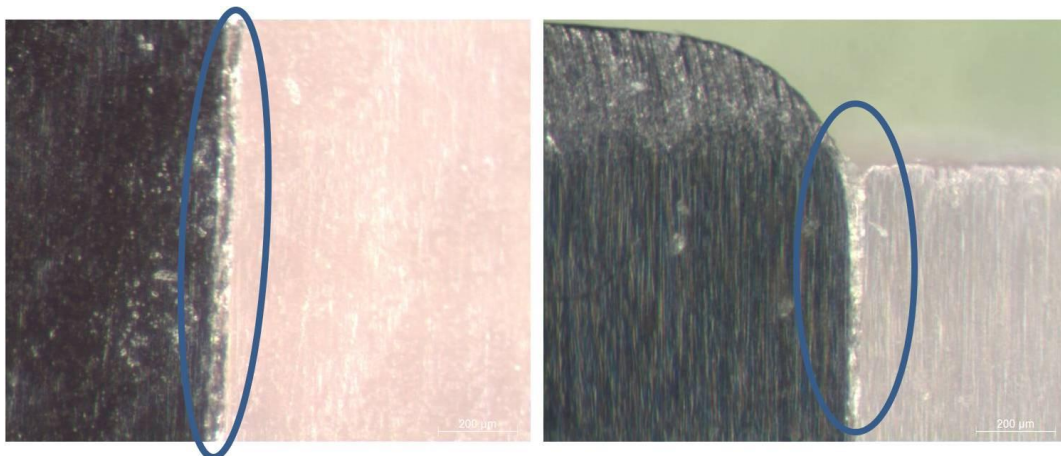


Figure 73 specimen welded and injected with condition 1

At the edge, (figure 73, right) of this specimen it was possible to identify a small area of defective bonding between the two materials (blue circle). This defect will decrease the resistance of the seam and it will be through this weak point that a crack propagates when the load limit is overcome.



Figure 74 shows the welding zone of the two PP plates joined with welding condition number two. The specimen analyzed exhibits a very visible mixture zone (blue circle) in the middle of the length of the seam. The zone analyzed does not present any voids, indicating an almost perfect contact between the two materials.

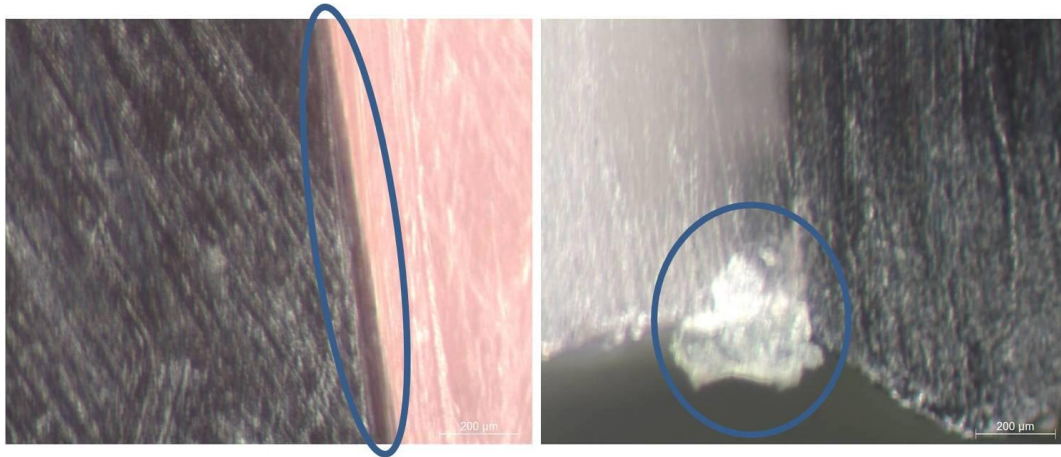


Figure 74 specimen welded and injected with conditions 2

At the edge of the specimen analyzed (figure 74 right) a large amount of burr material (blue circle) was visible. This can indicate two possible problems, the use of more pressure than was needed or too high a laser power. Taking into consideration the absence of voids, the explanation could be the use of a contact pressure higher than needed to join the two materials.

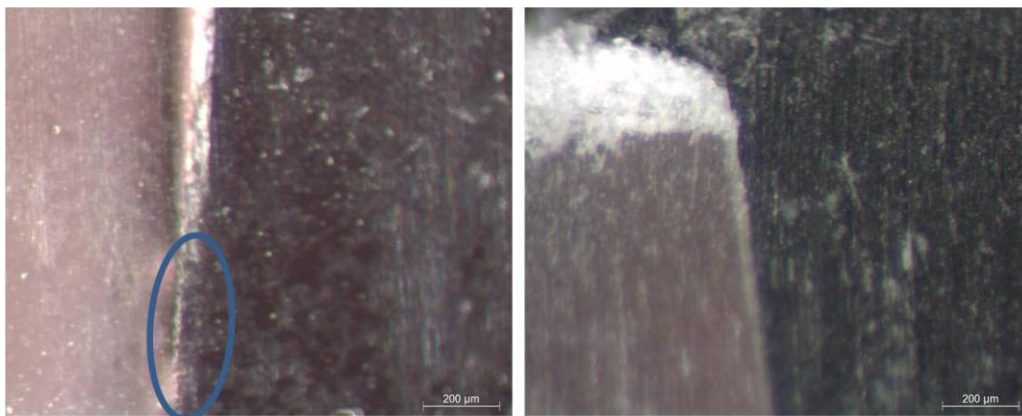


Figure 75 specimen welded and injected with conditions 3

The plates of PP welded with under condition 3 parameters (figure 75, above), showed a high level of mixture between the two materials (blue circle) and no visible voids were found along the weld path.

On the edge of the two plates an overlap of PP with carbon black was visible. This overlap indicates that more pressure than was needed to keep the two materials

connected during the weld process was applied. All the same, this over pressure can be advantageous because the mixture of more material is promoted, this more intimate level of bonding improving the mechanical resistance of the seam. The bright material discerned is burr material resulting from the steps needed to do this visual inspection.

The PP/PP specimen welded under condition 4 (Figure 76) shows a smaller welding area compared to preceding samples.

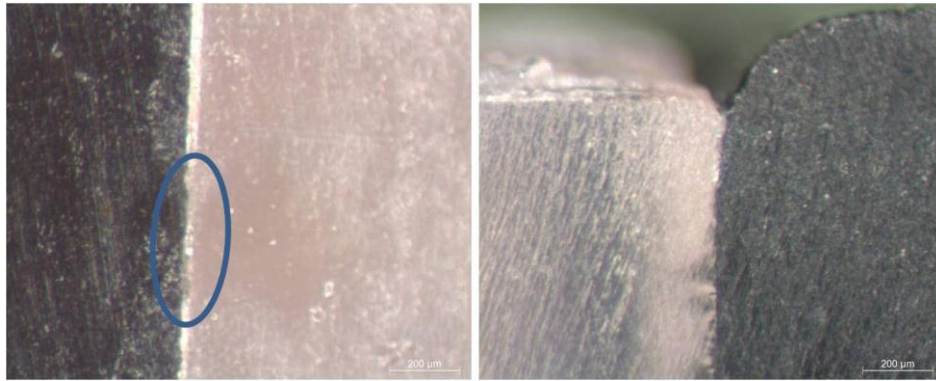


Figure 76 specimen welded and injected with conditions 4

Visual inspection reveals perfect contact along the entire length of the seam with no discernable voids. At the edge of the two plates the situation is the same with more or less perfect between the two materials.

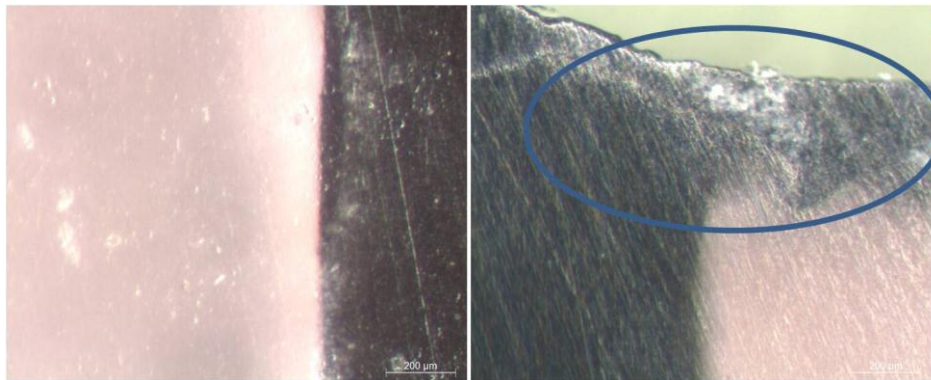


Figure 77 specimen welded and injected with conditions 5

For weld condition 5 the images show a perfect contact between the two plates with no visible voids (figure 77). The mixture between the two materials is not so visible along the entire length of the seam, being more pronounced at the edges. At the edge shown an enormous overlap of the carbon black material is seen, this being explicable in light of the use of high pressure to keep the two materials connected during the weld. The results obtaining at the edge of the seam can also stem from the application of high laser

power settings since a combination of high contact pressure with high laser power promotes the mixture of the two materials.

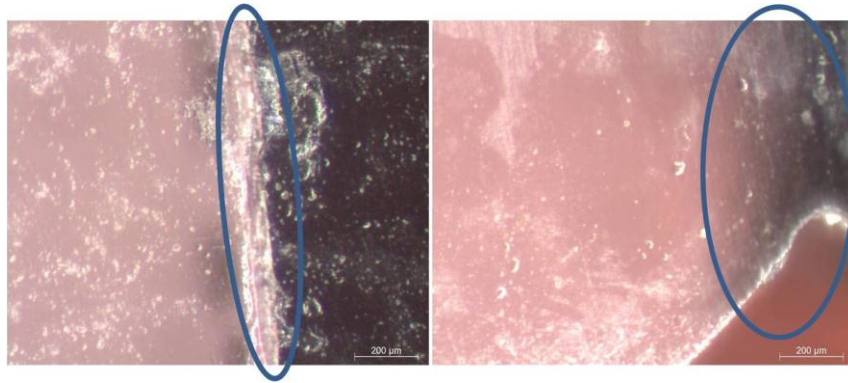


Figure 78 specimen welded and injected with conditions 6

In contrast to many other specimens, the plates welded with weld condition 6 (figure 78), presented a near perfect contact along the entire welding path, the images showing good mixture between the two materials throughout. The most interesting result comes from the image taken at the edge of the plates (figure 78, right). In this case the seam line disappears altogether indicating the formation of a perfect bond between the two materials.

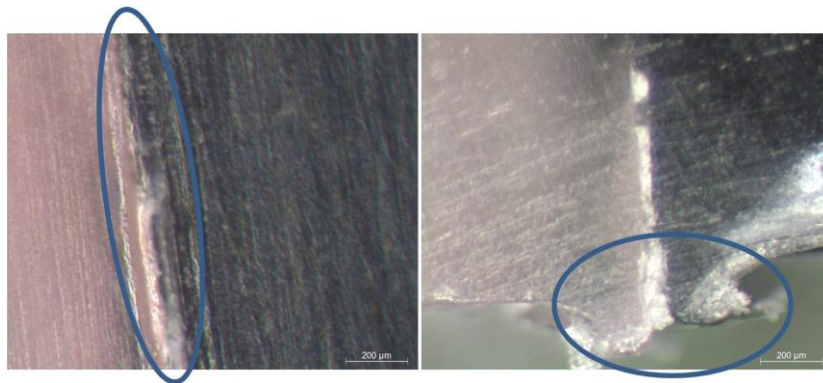


Figure 79 specimen welded and injected with conditions 7.

The specimen welded and injected according to the parameters detailed for condition 7 (figure 79), presented broadly similar results to those detailed for condition 6 above. Again, a zone of near perfect contact is visible without voids along the entire seam length. The specimen showed a zone of heat propagation, this area being larger on the black material than on the transparent material. Considering the photos, the specimen has more tendencies to break through the black material than the transparent.

On the edge of the specimen (figure 79, right), despite what is seen on the photo the contact between the two materials is good with no discernable voids. The bright material is, in fact, burr material from preparation of the sample.

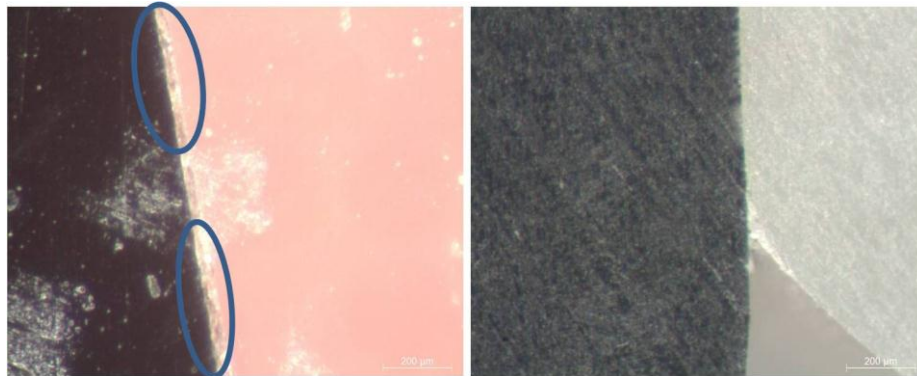


Figure 80 specimen welded and injected with conditions 8

The last specimen analyzed was the specimen welded and injected under condition number 8 (figure 80). On the middle length of the seam it is possible to see mixture between the two materials and no voids were found during the analysis of the entire seam.

On the edge of the two plates (figure 80 right) mixture between the two materials was not observed. This zone has more tendencies to initiate the propagation of cracks, at the same time showing the need to apply more laser power so as to increase bonding or mixture between the two materials.

#### 4.4 Concluding remarks

In this chapter the steps needed to design the rear lamp have been presented. The first task consisted in defining the minimum number of LEDs. Based on the legislation requirements it was found necessary to design a rear lamp with eleven LEDs. The following step consisted in designing the electric circuit. The circuit was initially designed with a PC mixed with 15% of metallic fibers. This material was unable to present the required conductivity when processed by injection molding. To overcome this weakness other materials like POM, PC and PP mixed with Carbon NanoTubes were considered. The carbon nanotubes were supplied by Nanocyl Masterbatch. The mixtures were analyzed in 3 percentages: 4%, 5% and 7%. The 4% of CNT was studied admixed with POM and PC. The 5% and 7% admixtures were studied with PC and PP.



Despite initially promising results, the POM melted after applying voltages higher than 12V. The PC didn't melt, but the amount of light intensity was not high enough for the applicable legislation. To increase the light intensity the percentage of CNT was increases by 1 percent. With this increase it was possible to obtain the desired results. The PP showed similar results but needed a higher percentage of CNT.

The second part of the chapter focused on study of the Laser welding process. Initially materials presently in use for this type of component subsystem were analysed, PC and PMMA. The two materials without additives presented a high transparency to the laser beam. The addition of glass fiber to the PC sample decreased the transparency of this material. A PP sample was also studied and the NIR analysis brought out the lower transparency of this material compared to the amorphous materials. The influence of additives such as talc and glass fiber was also examined. These additives were mixed in percentages of 10% and 20% with the PP. The result shows that the higher the percentages the lower the transparency. Of the two, the talc was seen to be the additive with the higher degree of influence on light transmittance within the various samples prepared. Other additives capable of enhancing absorption of laser beam energy were also studied - wood fibers and Clearweld. Both presented relatively high percentages of beam absorbance.

After the NIR analysis, it was decided to study different material combinations with the objective of analyzing their potential with regard to their possible use in the component case study. The first material combination analyzed was PC/PMMA. This combination presented a good seam resistance. The combination PC/PC was also evaluated; the samples prepared presented poor results compared to the previous material combination. To corroborate the results obtained in the NIR analysis, it was decided to study others material combination, namely PC/PC with glass fiber. Compared to the previous PC/PC combination, the PC with glass fiber presented a seam with a higher resistance.

Different PPs combination samples were also prepared for analysis. Across the board they presented seams with lower resistance values compared to comparable PC/PMMA combinations and all the combinations studied presented higher standard deviations. The incorporation of additives such as talc and glass fiber was accompanied by a decrease in seam resistance while of the absorber additives the carbon black presented the better results. While the use of wood fibers or Clearweld was seen to

promote enhanced absorption of beam energy, this proved insufficient to enable the production of a seam with a good resistance.

Seam quality was also analyzed by visual inspection. Various combinations of PC/PC, PMMA/PC and PP/PP with different processing conditions were prepared for the analysis. All the samples showed perfect contact. In the PMMA/PC samples a mixture between the two materials was visible. No mixture was visible within the PC/PC combinations under any of the weld/injection conditions used. In all the PP combinations a weld zone could readily be seen and some of the PP/PP samples presented high levels of mixture (conditions 6 & 7). Despite these results, the PP samples presented lower levels of mechanical resistance compared to the other combinations analysed.

The results also showed that reduction of the laser diameter increases the mechanical resistance of the final seam. With these results we can conclude that increasing the power per unit area leads to increasing amounts of material mixing or fusing - and consequently a higher shear stress capability at rupture.

## Chapter 5

---

In this chapter the tasks undertaken to design and to produce the tools needed to validate the process studied will be presented..

## 5 Prototype tool for in-mold assembling

To finalize the development of the process it was necessary to further develop the process concept, the simulation of the injection molding process and finally the development of the mold. In figure 81, a 3D model of the rear lamp component subsystem is shown.

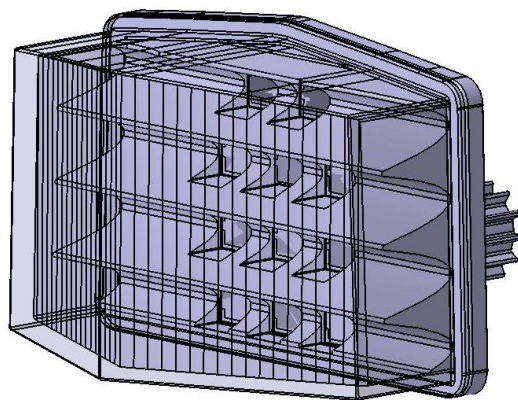


Figure 81 the final rear lamp.

The visualization of a 3D model is not always enough to verify possible problems that could appear during production. In such a complex subsystem as a rear lamp it is often easier to find prospective problems in a physical part than it is on a computer. Due to this consideration, a physical prototype was produced to verify some details that were not considered during the design phase.

The prototype was built with the Fused Deposition Modeling (FDM) technique in a Dimension SST 1200 machine. The material used to build the two parts was ABS (Acrylonitrile butadiene styrene). The following figure 82 presents the prototype of the housing and the crystal.

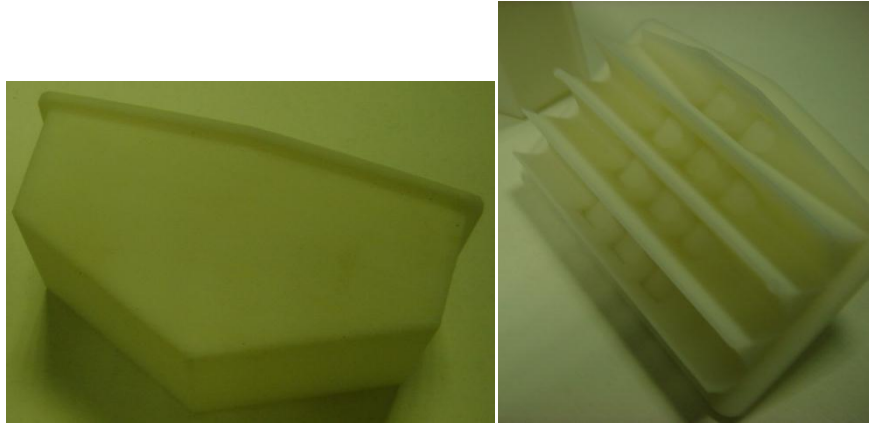


Figure 82 crystal and housing prototypes

Analysis of the prototype revealed the existence of thick zones in the area of the reflective cavities. The existence of these thick zones tends to presage the high probability of the appearance of defects such as voids, warpage or surface distortions. The existence of these surface defects will, in turn, influence the direction of light propagation. In order to analyze the possibility of these defects appearing in the final part, a Moldflow simulation was done.

### 5.1 Simulation of the injection molding process

The simulation of the process had the objective of enhancing understanding of the injection molding process to confirm that defect-free components can be produced via the process envisioned. This evaluation was made using Moldflow simulation software. The first component that was analyzed was the housing. Due to the complexity of the mold it was decided to make the injection of the housing in one point. Based on this input a simulation on Moldflow using the PC Lexan 123R was made.

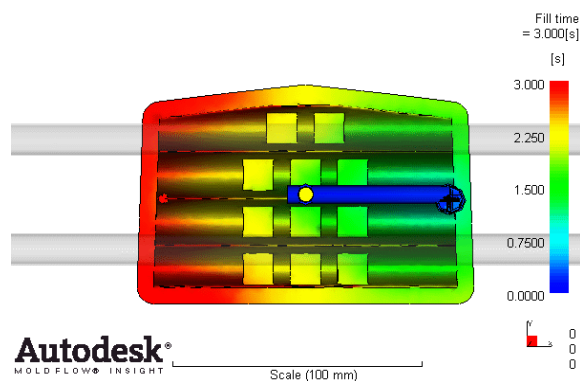


Figure 83 injection time for the fill the housing

Based on the analysis, 3 seconds was indicated as necessary to fill the entire housing. After the fill analysis, a volumetric shrinkage analysis was undertaken (figure 84).

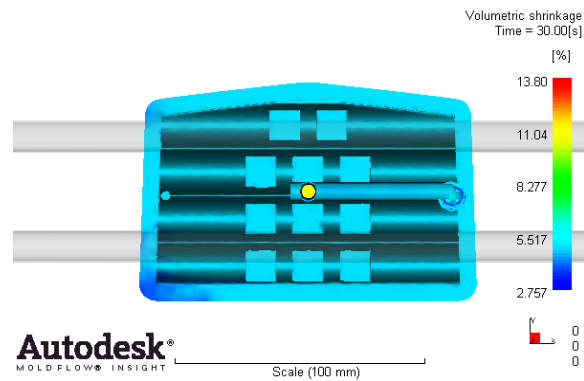


Figure 84 volumetric shrinkage of the housing

The housing presented a homogeneous volumetric shrinkage with an average value of 5.5%. The only exception appeared near the bottom of the left edge of the housing. In fact, this zone presented the smallest volumetric shrinkage of the entire component. Considering the difference in the volumetric shrinkage between this zone and the part remaining, it is possible that warpage problems could arise within the part. Despite this problem the injection point was not moved, since its modification created potential problems with light transmission.

The crystal was also studied and PMMA Plexiglas 8N was used in the simulation. The localization of the injection point was decided based on the requirements of the mold. The simulation showed that 2.3 seconds are needed to fill the entire part. Attempts were made to inject the component in the middle, but light transmission requirements obviated this. The fill phase of the crystal is presented in figure 85.

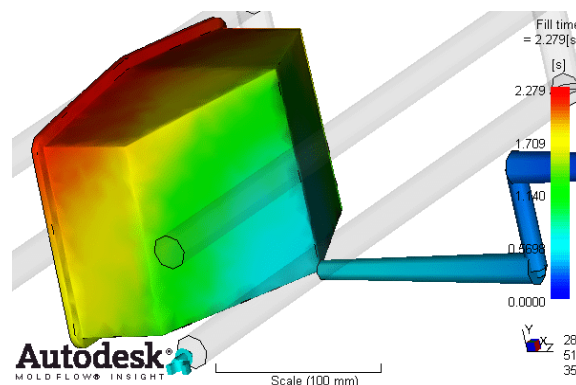


Figure 85 injection time of the crystal

Based on the analysis made, 2.279 seconds was needed to fill the entire crystal. The Volumetric shrinkage was also analyzed in the crystal component, figure 86.

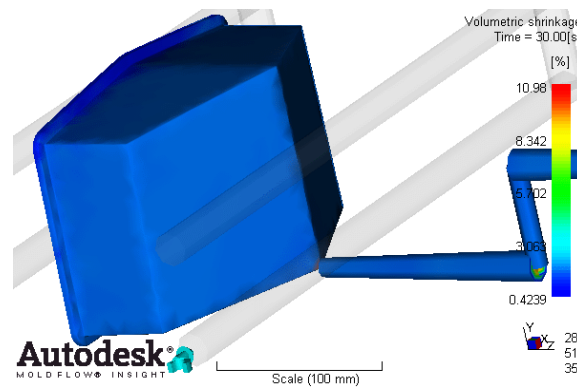


Figure 86 volumetric shrinkage of the crystal

The simulation showed that the crystal presented an average volumetric shrinkage of 0.429%, this result indicating that the component will come out of the mold with a low probability of deformation.

## 5.2 Mold concept

To develop the mold, it was necessary to define how the subsystem will be produced. The main objective, as indicated in the objectives of the thesis, was the production and assembling of all components using a single mold and process. To accomplish this objective a mold was developed with the capacity to:

- Produce the electric circuit, the housing and the crystal at the same time
- Assemble the different components.
- Be capable of supporting the overmolding process, in order to produce the housing over the electric circuit.
- Be capable of using the laser welding process

In the design of the mold the laser welding and the in-mold assembling processes had to be taken into account. To do these two processes in the same cycle it was necessary to design an assembly system. The system designed used two rotary plates with the objective of transporting the different parts to the assembly and welding

zones. The plates also had the objective to eject the final subsystem. In the following figure 87, the two halves of the mold design are presented. .

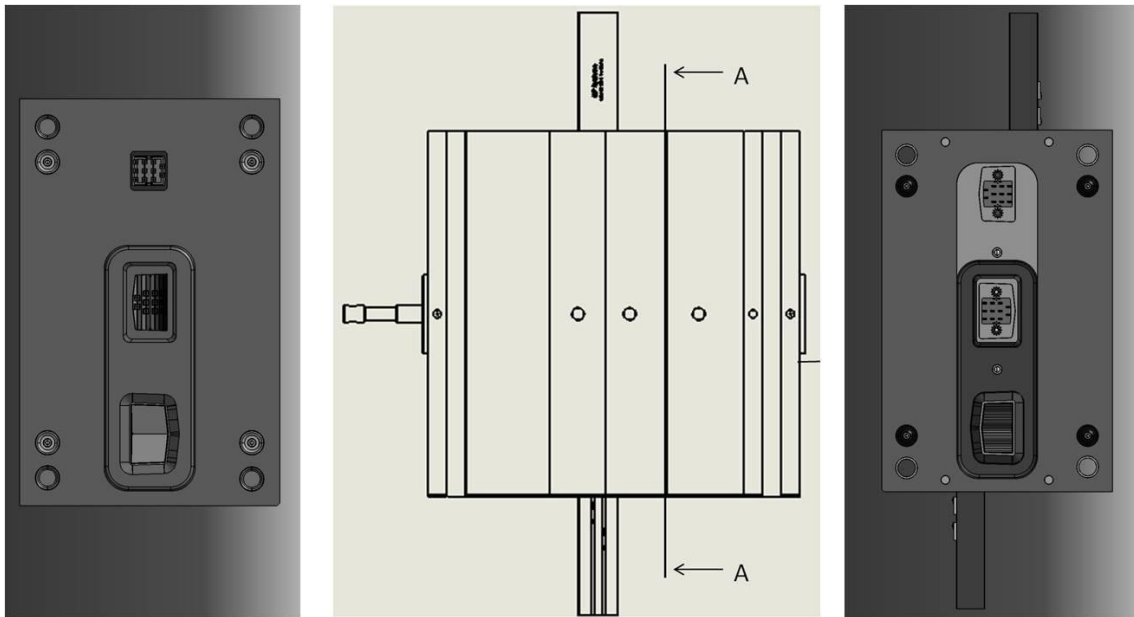


Figure 87 the mold

Inside the mold a system capable of maintaining the two parts in contact during the welding process was also created. This system consisted of a metallic ring that had the advantage of not creating gaps in the welding zone. In the following figure 88, the ring used to maintain the two parts in contact is illustrated.

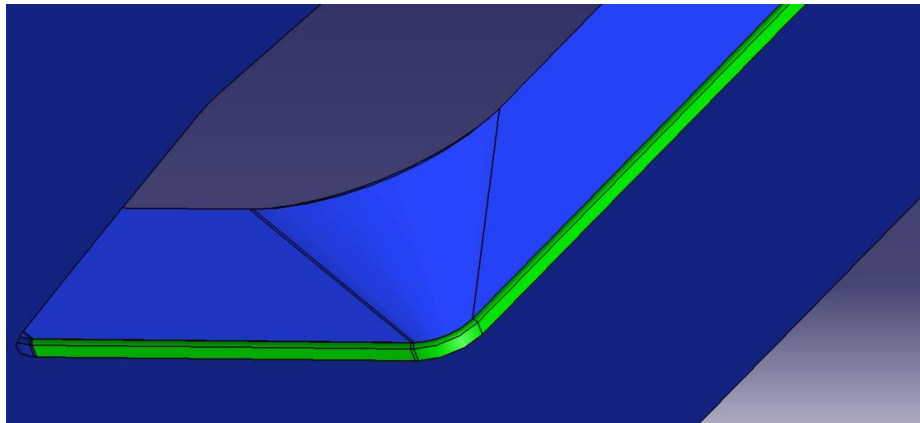


Figure 88 the metallic ring (green lines)

The next figure - 89 – illustrates the overall concept of the mold. The brown and blue plates are the rotary plates that control the process.



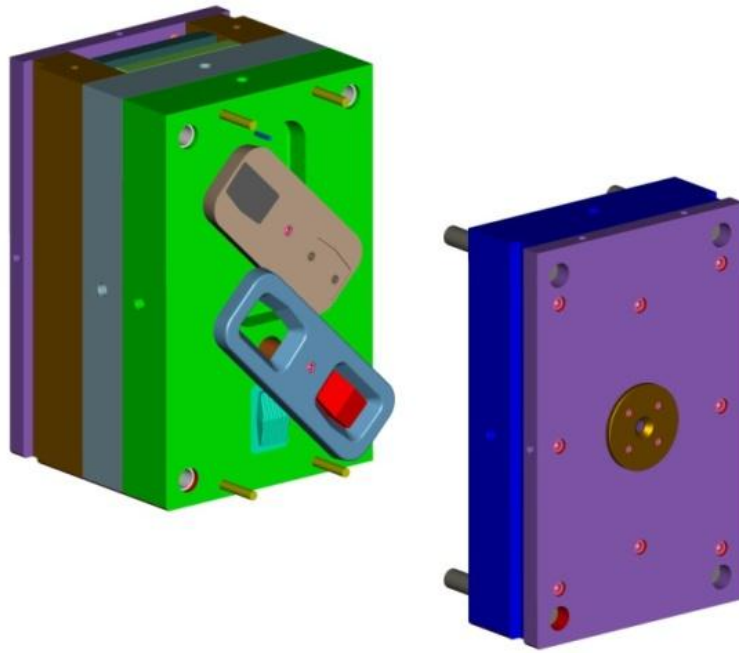


Figure 89 mold concept

### 5.3 The manufacturing cell

The main objective of this thesis was the development of a manufacturing cell with the capability of producing a complete and functional subsystem within the same molding cycle. To accomplish this objective several technologies were combined. The following figure 90 presents the equipment used in the manufacturing cell.

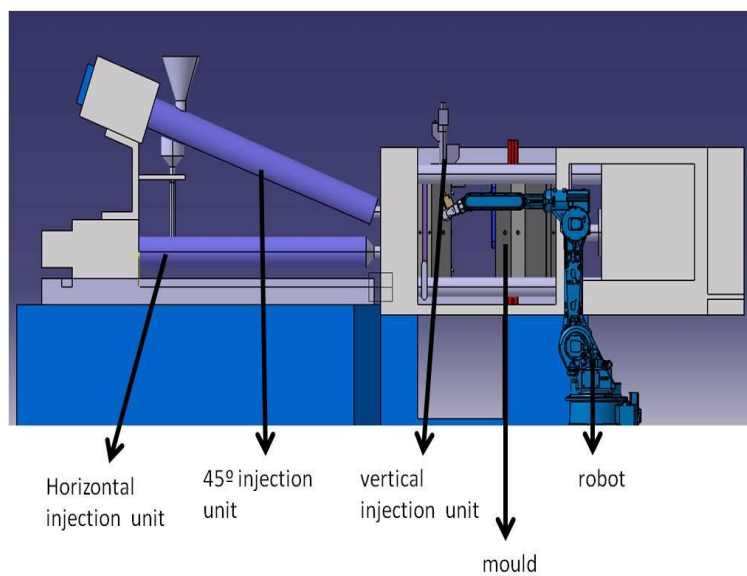


Figure 90 The Manufacturing cell

Figure 91 below shows the manufacturing cell from a different viewpoint.

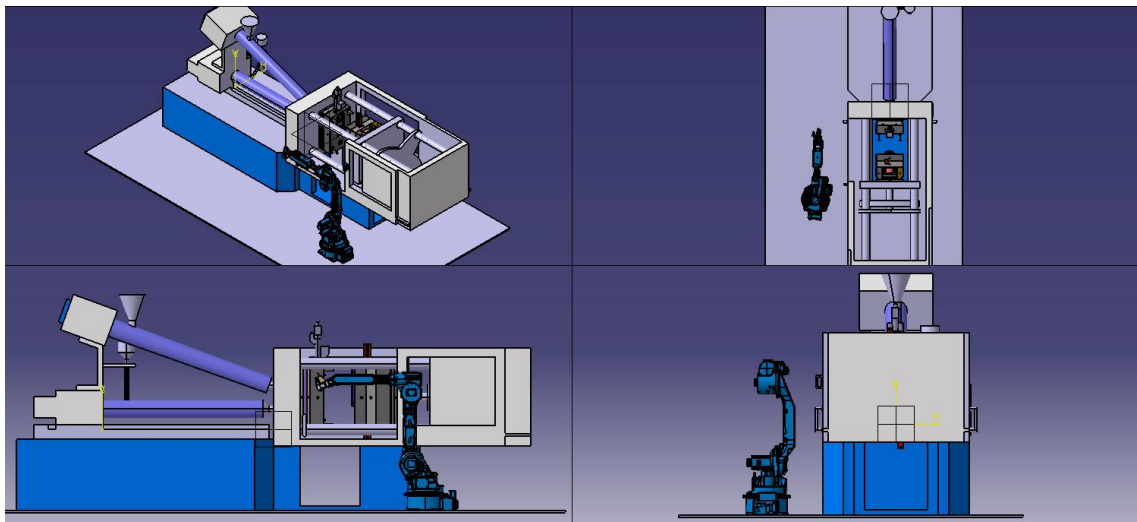


Figure 91 the manufacturing cell from a different perspective

Figure 92 presents a detailed view of the laser head within the manufacturing cell.

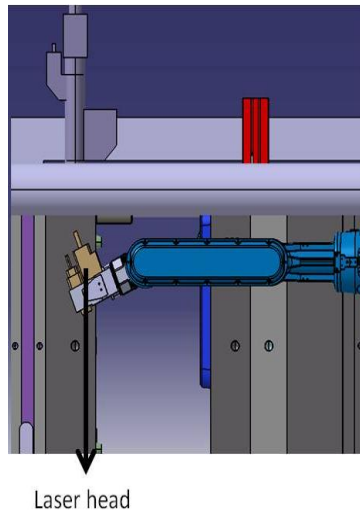


Figure 92 laser head in more detail

For the injection molding process a bi-material injection molding machine H150/470-200T (Billion Hercule) together with a Plasdan ELM - used to inject the conductive polymer for the electric circuit - were deployed. The Billion was used to

inject the housing (45° injection unit) and the crystal (horizontal injection unit). This equipment was also used to control the rotary plates of the mold, since it already had pre-installed software capable of controlling this type of movement. To inject the conductive material a vertical injection unit supplied by Plasdan was employed. The layout of these various equipment items is presented in the following figure 93.



Figure 93 Billion with the vertical unit and the laser protection

To integrate the vertical injection unit with the Billion® machine it was necessary to develop specific software. With this software it was possible to control simultaneously the injection process of all three injection units.

The temperature of the hot runners was done through an M series multizone controller from SISE Company. The temperature in the mold was controlled through a temperature control unit from Piovan Company. Due the specifications of the materials used for the housing and the crystal it was also necessary to employ a drying/dehumidifying unit. With this unit it proved possible to eliminate the humidity existent in these two materials.

The Piovan drying/dehumidifying unit utilized is presented in the following figure94.

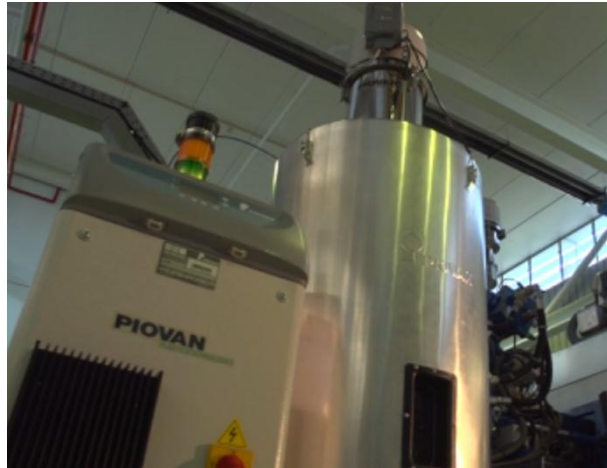


Figure 94the Piovan drying/dehumidifying unit

The manufacturing cell can be divided into two processes, the injection molding process and the laser welding process. To undertake the welding process an IA20 robot controlled by a control unit (NX100) and a diode laser LM100 (Mergenthaler Laser Technology) equipped with a pyrometer (LH500) were deployed. The laser source and the control system of the robot are presented in the following figure 95.



Figure 95 the laser and the NX100 robot control unit

The laser head was connected to the robot through a fixing system developed for specifically for the purpose. The robot, the laser head and the fixing system are presented in figure96 following.

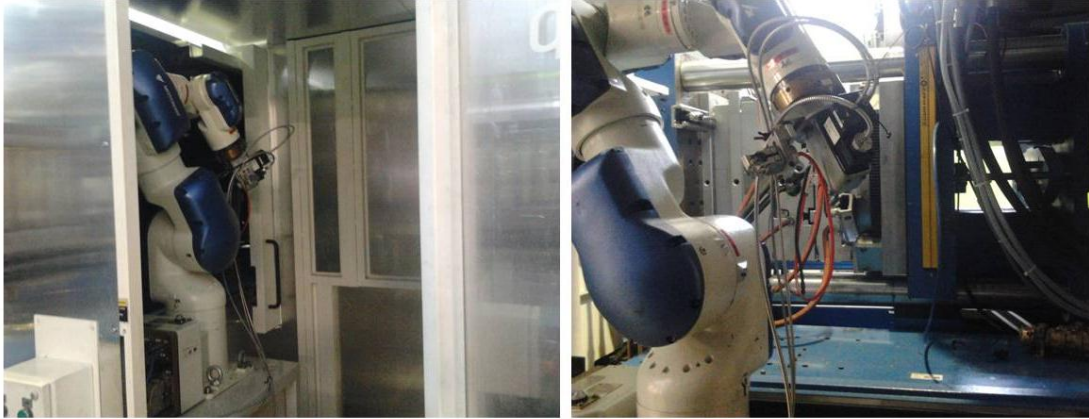


Figure 96 the robot the laser head

The use of the laser system implied the development of several safety procedures because the wavelength emitted by the laser constitutes a danger to the human eye. The main safety measure developed was the construction of a protective aluminum surround fitted to the injection molding machine. This protection system was developed according to guidelines obtained from the laser supplier and had a thickness of 1.5 mm. An inspection window fitted with a transparent material capable of absorbing the laser beam light was implemented within the protective system.

To accomplish the objective of this thesis it was necessary to integrate two processes, the laser system and the injection molding system. This integration was accomplished through the control unit of the robot (figure 97) and development of the requisite software programming needed to effect control of the robot.



Figure 97 robot control and robot console



### 5.3.1 The process tasks

To produce the functional subsystem in the same molding cycle several tasks were considered:

- 1- The LEDs are added with the help of a robot or a worker into the cavity where the electric circuit will be injected (Zone 6)

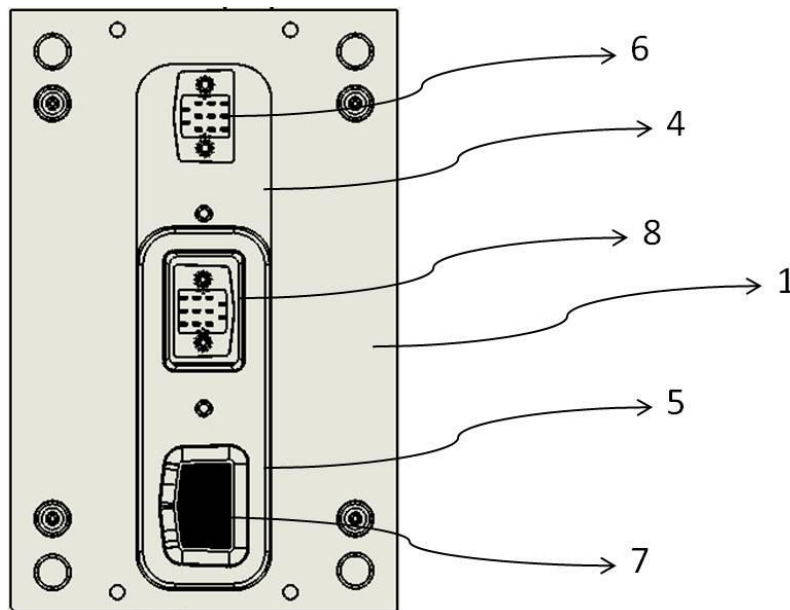


Figure 98 different sections of the mold used on the process

- 2- The mold closes
- 3- The electric circuit, housing (with electric circuit) and the crystal are injected (figure 99b)
- 4- The mold opens
- 5- The bottom plate (figure 99c) moves forward and rotates 180°. This movement transports the crystal to the assembly zone
- 6- The plate moves backward and assembles the crystal with the housing (figure 99d)

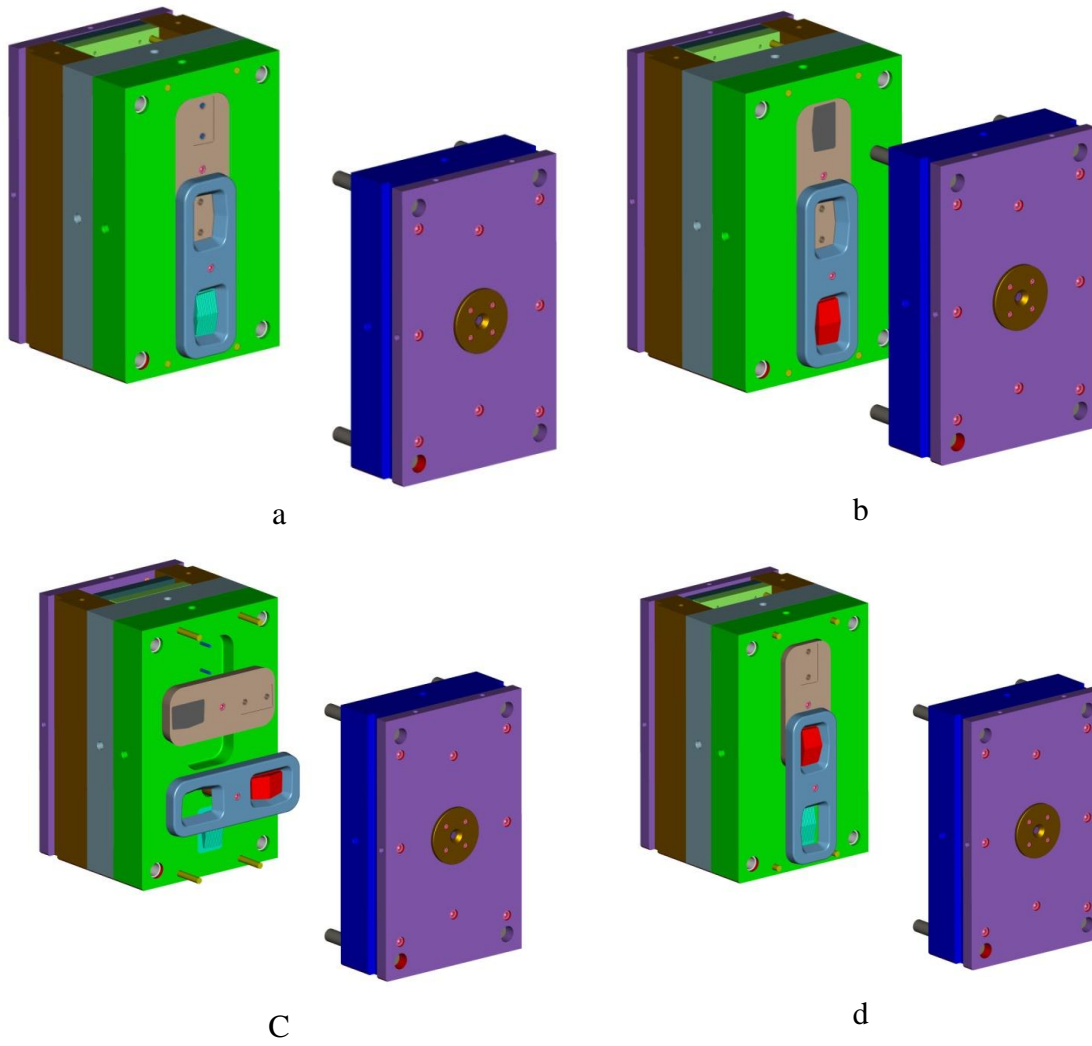


Figure 99 Process Tasks (a: mold open; b: injection of all components; c: rotation of the plates; d: in-mold assembly)

7- The laser welds the two parts (figure 100)



Figure 100 Laser Welding

8- The plates number 4 and 5 of figure 98 move forwards

9- The plate with the number 4 rotates 180° to the position indicated with the number 6 (figure 98)

10- The plate with number 5 (figure 98) rotates to the initial position

11- The two plates retreat and the subsystem is extracted ( figure 101)



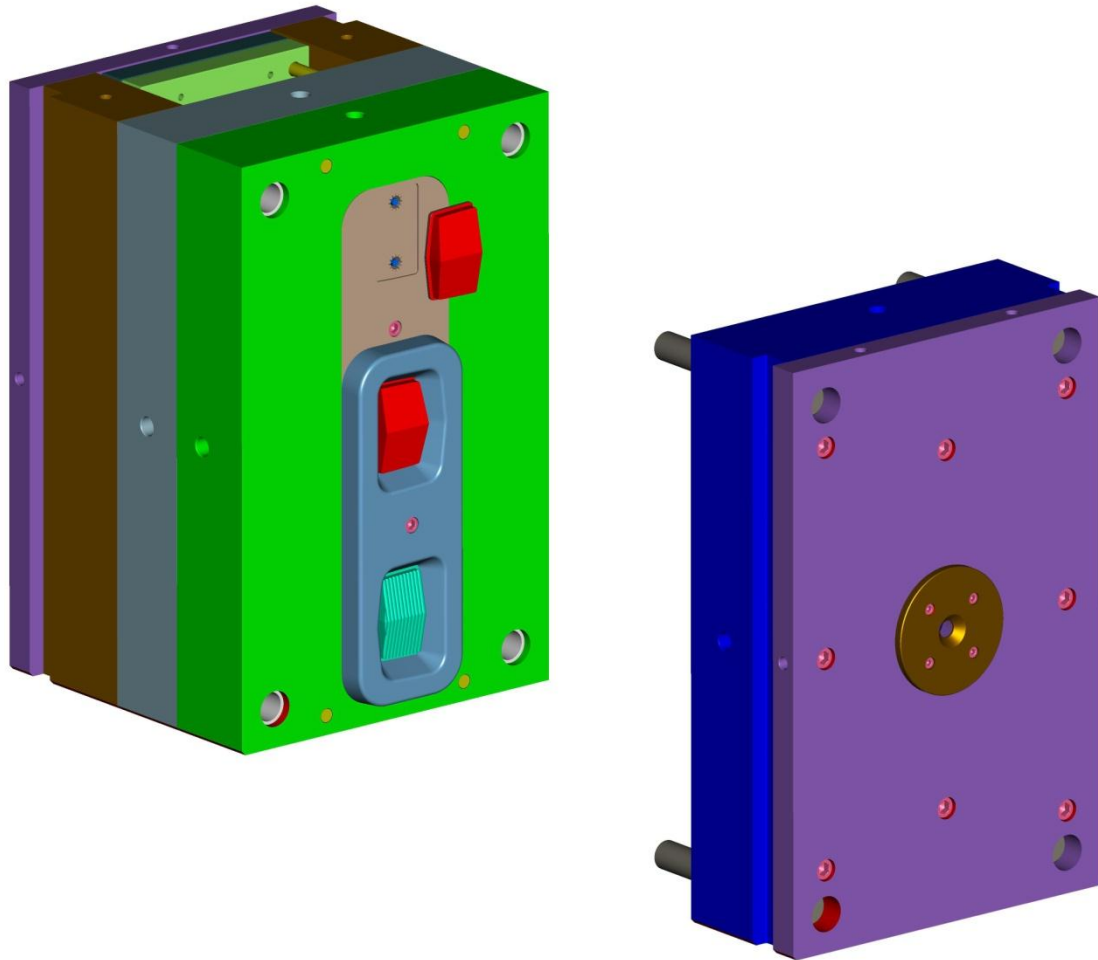


Figure 101 ejection of the final subsystem (red part)

12- The mold closes and the process restarts

With this solution, the assembly and the welding of the different parts become possible. The process will increase the cycle time, but at the same time the lead time will be substantially reduced.

#### **5.4 Results and process validation**

In previous chapters the different materials and processes and how they were integrated to accomplish the main goal of this thesis was presented and studied.

In this chapter the results obtained with the developed integrated mold incorporating the laser system and a robot will be presented.



Figure 102themold

The implementation of the integration process wasn't a simple task. Several challenges was found and solved

In order to integrate all the operations in the same mold and to guarantee the quality of each component of the sub-system it was decided to produce each component in an isolated way. After validation of the component's quality, the integration was implemented with the laser welding operation.

The first problem that was solved was the ejection system of the crystal. During the ejection cycle of this component several times the crystal remained in the core and didn't follow the ring plate that had the function to transport the crystal to the other cavity (figure 103).



Figure 103 ejection and transport of the crystal component

To overcome this problem it was necessary to design a texture in the metallic ring (figure 88) in order to increase the friction between the crystal and the metal ring. In the following figure104 the crystal is presented after production.

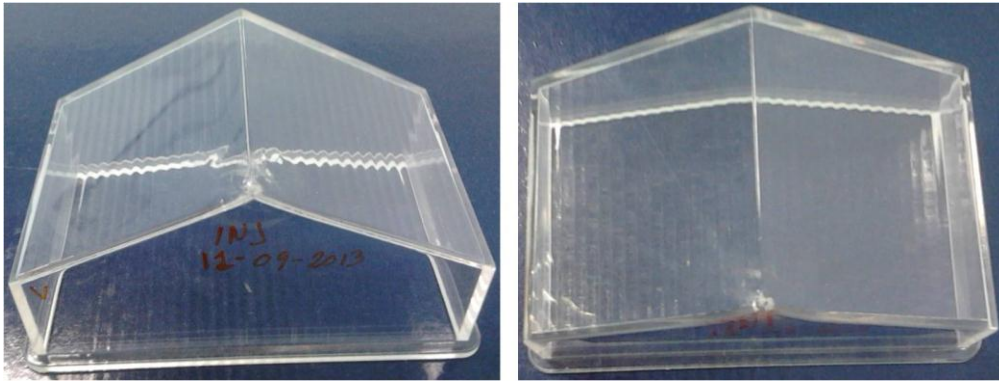


Figure 104the Crystal component

The housing was injected without the electric circuit according with the injection molding conditions presented in table 14. The housing presented some voids on the bottom surface and within the reflection cavities. These defects were eliminated with the processing of the electric circuit. In the following figure 105 the housing injected without the electric circuit is presented.

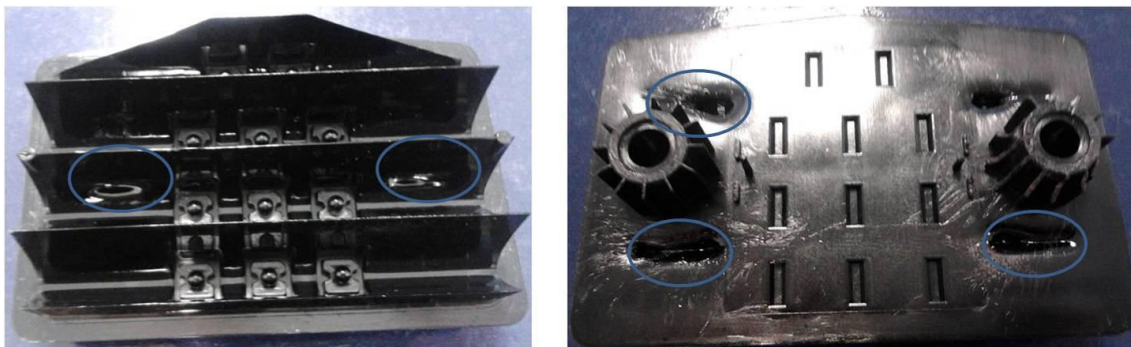


Figure 105 front and back side of the housing without the electric circuit

The last component to be processed was the electric circuit. The processing with the PC threw up several problems. One of them was the high temperatures measured inside the cavity. After injecting several electric circuits, it was verified that most of the LEDs were completely destroyed.

The high temperatures found in the cavity were due to the hot runner system used to eliminate the material present in the conventional runner systems. To overcome the high

temperature problem it was decided to change the PC material for PP with 7% of CNT. With this change the electric circuit was processed successfully and the LED's didn't show any damage.

The overmolding of the electric circuit with the housing was done using the processing conditions presented in table 6 and 8. The housing with the electric circuit is presented in figure 106.



Figure 106 the housing with the electric circuit

The overmolded product (housing with the electric circuit) was analyzed at microscopic level in the union regions. This analysis had the objective to study the adhesion between the two materials and to check for the existence of any overlap between the two materials.

The analyses were done using a microscope EMZ-TR of Meiji Techno UK Ltd and an Optika TB 3.0 with an augmentation of 0.5X. The initial results showed a perfect contact between the two materials. However in the pins zone (yellow box) an overlap of the PC was discernable. The overlap can be seen on the right image of figure 107.

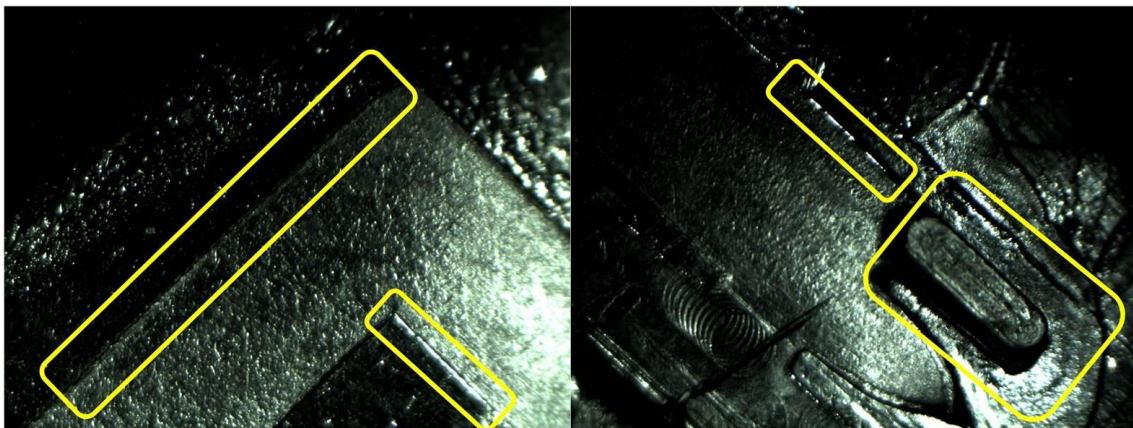


Figure 107 the interaction between the PC and PP



The image obtained through microscopy showed a good contact between the three components. The contact sections between the three components are shown inside the yellow boxes.

The last process to study was the laser welding of the housing with the crystal. The two components were welded according to condition 1 of the table 14. The welding process went as expected. The final rear lamp is presented in figure 108.

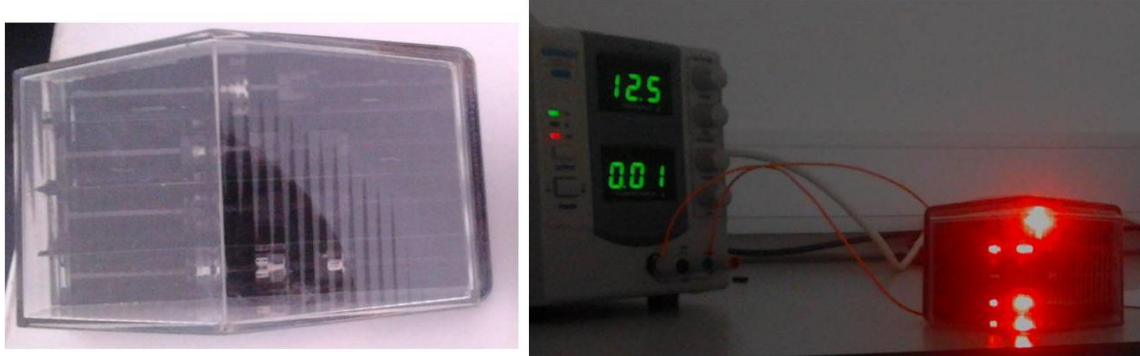


Figure 108the final rear lamp

## 5.5 Concluding remarks

The design of the mold and the process was the first step in starting production of the final prototype mold. To help in this first step, simulation of the injection molding process was done using a commercial software package, Moldflow. The results of the simulations showed that the components of the case study can be produced by the injection molding process and they didn't show any major defects.

Taking into consideration the need to assemble the different components of the case study, the design of the mold was built on the consideration of employing two rotary plates and the capability to support three injection points at the same time.

The process started with the placement of the LEDs, with the help of a robot or a worker, into the cavity where the electric circuit will be injected. After the mold closes the electric circuit housing (with electric circuit) and the crystal are injected. To make possible the assembling of these different components the rotary plate transports the crystal to the assembly zone where the laser welds the crystal to the housing. After this process is completed the rotary plates retreat and the subsystem is extracted. The mold closes and the process starts again.

Process testing and validation was the most important task for this part of the research project. Accordingly, the problematic crystal ejection system was updated with a textured finish imparted to the rotary ring so as to promote better ejection and transportation of the crystal. The voids presenting in the bottom and within the central reflection cavities of the housing were similarly addressed. These defects were not found on the simulations made for this component; they were corrected with design changes in the part.

The hot runner system used to inject all the components created several problems during the injection process. The main problem was the high temperatures measured in the electric circuit cavity. Here, temperatures higher than 160°C were recorded when PC was used; the temperature was so high that the LEDs melted. To overcome this problem it was decided to substitute the PC material with PP with 7% of CNT. With these changes it proved possible to inject the electric circuit.

The overmolding component was analyzed at the microscopic level. The analysis showed a perfect contact between the two materials.

The process of the laser welding was a success, and the welding between the housing and the crystal was successfully accomplished.

## Chapter 6

---

## 6 Cost analysis

In this chapter an economic analysis of the developed integrated process into the market and its potential economic benefit is presented.

The process presented in this thesis marks a response to the needs of companies producing rear lamps and head lamps. The actual process is too expensive to be implemented in Europe and assembly in China increases the lead-time. According to a research that was made [121], the actual assembly system is composed of at least five operations. The first operation is the injection of the different plastic components. After that they are stored in an appropriate space. The following operation consists of assembling the electric system and the lamp to the rear lamp. The last operation is the ultrasonic welding or screwing of the different plastic parts. With the subsystem completed, it is sent to the storage again where it will be shipped to the manufacturer's assembly plant. The actual process is presented in the following figure 109.

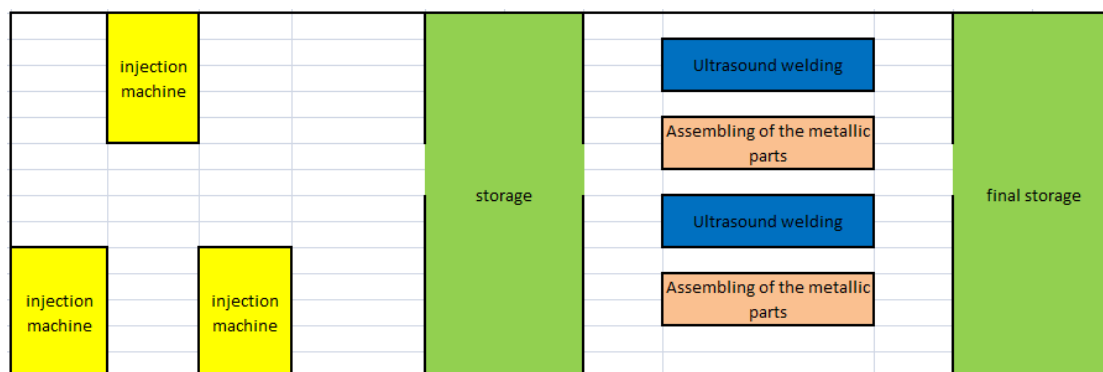


Figure 109 assumption of the actual factory assembly layout

As noted before, the actual production cost is too expensive to be implemented in Europe; to overcome this disadvantage the solution has passed to the development of a new process capable of decreasing to the minimum the requisite number of assembly tasks, namely by avoiding several intermediate tasks such as the assembly of the electric system and the welding of the different components. They were avoiding through the utilization of technologies such as laser welding and Multi-material injection molding.

The first technology mentioned, laser technology, is used to weld and cut different plastics. Besides that, this technology can be combined with robots, vacuum, compressed air systems and finally with injection molding machinery. The laser can



also be used to open holes and design channels where it is possible injecting another polymer material.

The multi material injection molding is used to inject sequentially or at the same time several materials in the same machine and with the same mold.

The main advantages, of this process are the reduction of the number of molds and injection machines. The current process needs two injection machines and two molds. This new process only needs one injection machine and one mold. Another advantage is the elimination of intermediate storage space. Transportation between the intermediate tasks is also eliminated. The number of workers is reduced as well, 4 workers to only 1 worker. The new assembling line is presented in the figure 110. As it is shown in the figure, it proved possible to reduce the factory size. Each injection machine/laser is capable of producing a complete subsystem.

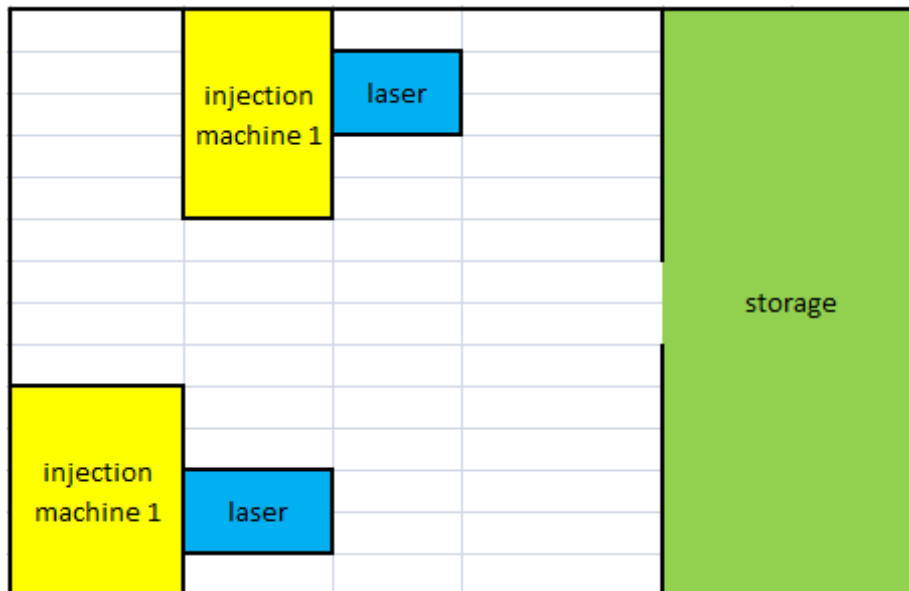


Figure 110 the new production site

## 6.1 Cost analysis

In the business model developed to the process it was assumed that some of the tests will be made in Olesa facilities. For that reason, the company will do an initial investment. The major investments will be made in a room to do the laser tests (10 k€), an injection molding machine with 3 plasticization units (190 k€), a robot (60 k€) and finally a laser (40 k€). The total initial investment to do the tests is 400 k€. On this

initial approach it was assumed a building that already exists. The price of the mold was not considered.

As noted earlier, the process will be initially sold to the companies that produce headlights. The target markets are companies producing this type of product to European and Indian automotive manufacturers. Based on the information gathered, these two markets have a sales potential of 30.4 million vehicles per annum (motorcycles and automobiles).

Before initiating the sale prediction, it is essential to understand if the new process presents a lower production cost when compared to the current one. The financial analysis showed that this new process has a higher production rate than the current process. The price of subsystem is also lower when compared to the current one.

In these calculi (see Annex) a 2% defect rate was assumed together with a 15% profit for each subsystem produced. In the new process a mold with an estimated price of 70 000€ was used; in the current process a mold with a price of 20000€ was used. Despite the low price of the mold of the existing process, two molds and two injection molding machines are necessary. The other inputs used in the calculi are presented in the annexes. In figure 114 the variation of the subsystem price according to the demand size of the two processes is presented.

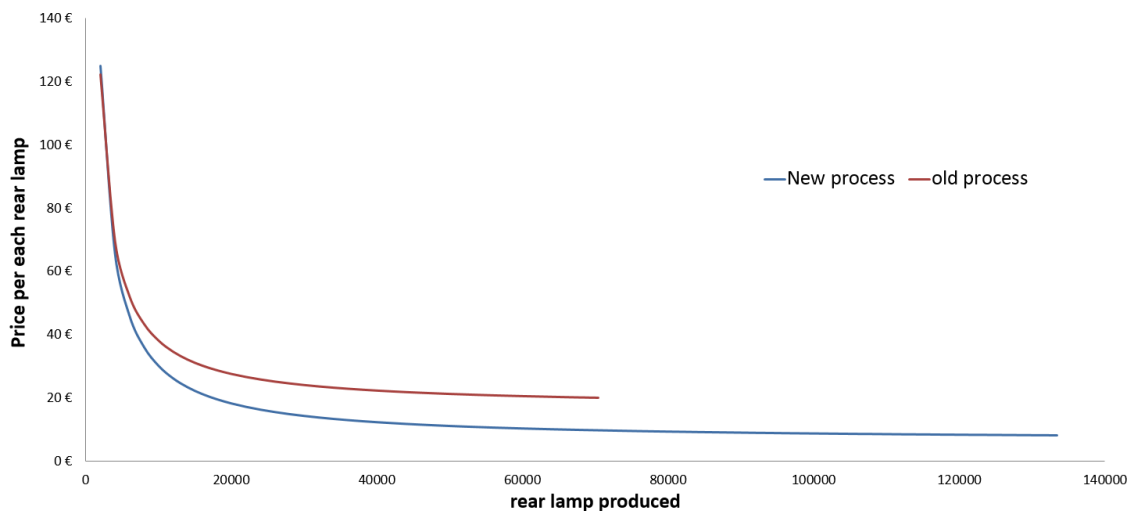


Figure 111 Comparison between the new and the old process

In this first analysis the process developed in this thesis and the existing process were compared. The following paragraph presents a cost analysis between the process studied in this thesis and a variant based on contra cycle operation. This comparison assumes an assembly process similar to the one studied herein while the new variant

process, as presently envisioned, is predicated on the employment of two injection machines, one robot and one laser. To optimize the process it has been decided to put the two injection machines working in contra cycle. This means that when the injection process is occurring in one injection machine, the mould is open and the welding process is happening on the other.

In this comparison it was decided to maintain the same number of workers, working in the same building, the only difference is on the number of injections machines and the mould. With this new process, it was possible to double production over the same time frame. Relative to the costs of production under the process developed for this thesis, this variation produces subsystems with a higher cost for productions volumes lower then 150 000 rear lamps. Above this amount it is possible to achieve similar subsystem costs as established for the process studied herein. The comparison in terms of final price between the two processes is presented in figure 112.

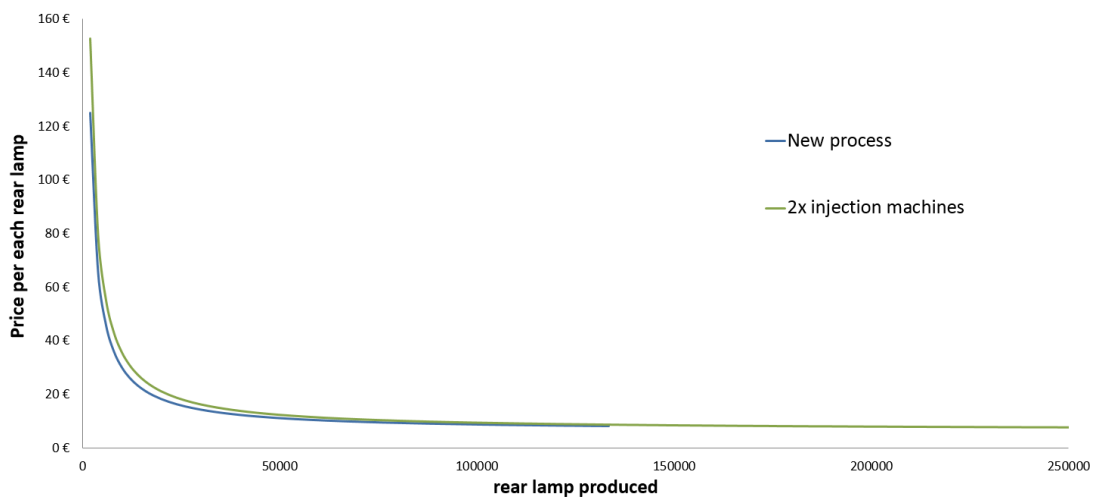


Figure 112 comparison between the process studied and variation

The difference in final price in the current process considered the building cost is presented in figure 113.

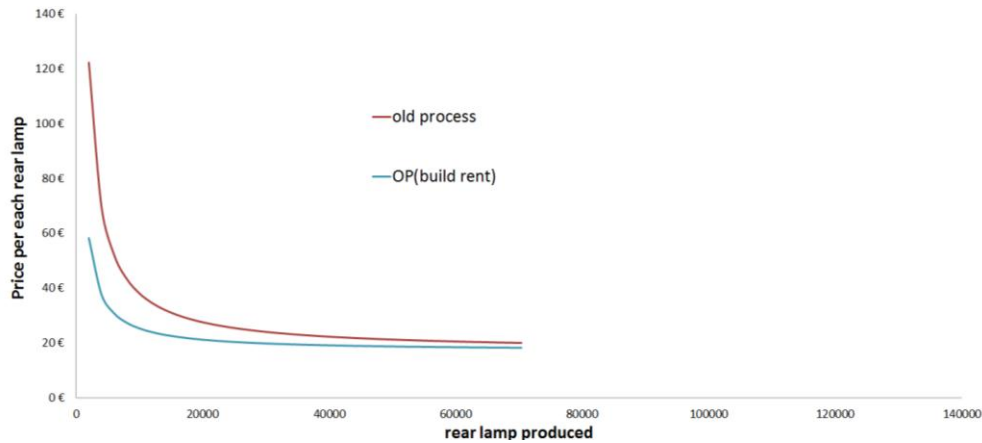


Figure 113 comparison between the old process with and without the rent

In this cost analysis an attempt has been made to try to understand which factors have more influence on the final price of the component subsystem. One of the initial considerations was the acquisition of a building with a cost of 700 000€. Due to the high cost of this investment it was decided to rent a building with the same characteristics rather than buying it outright. To rent the building an initial rent of 1200€ was assumed, with an augmentation of rent of 3% per year. With this modification it has proved possible to substantially reduce the final price of the rear lamp in all the processes studied in this analysis. In the case of the current assembly process it was possible to reduce the final price of a production batch of 20 000 units from 40 euros per subsystem to a production cost of 20 euros per subsystem.

The comparison between the prices of buying or renting the building for the process is presented in the following figure 114.

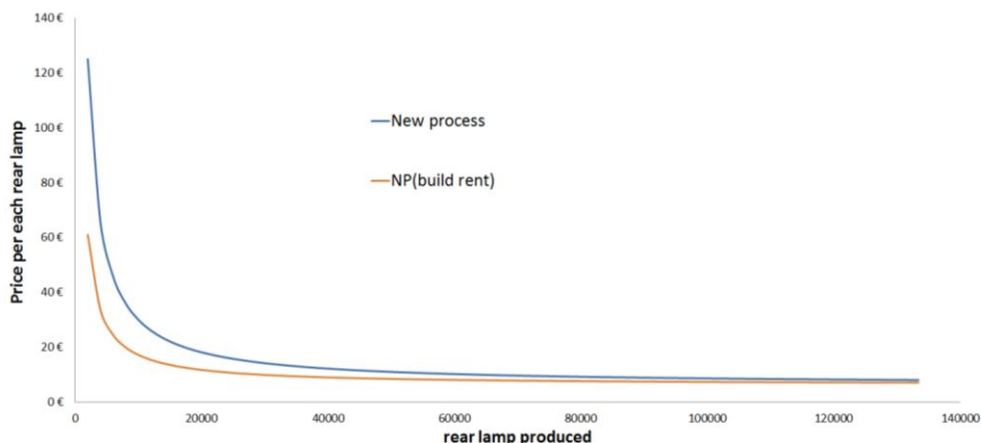


Figure 114 comparison between the new process with and without the rent

The same comparison for the process studied in this thesis was made. The result was very similar; the process studied has the capacity of producing near 140 000 subsystems per year, the results showing that for production volumes higher than 100 000 subsystems per year, the acquisition of the building or the rent does not significantly influence the final price of the component subsystem.

A comparison between the acquisition of the building and the rent for the contra cycle injection machine variant is presented in the following figure 115.

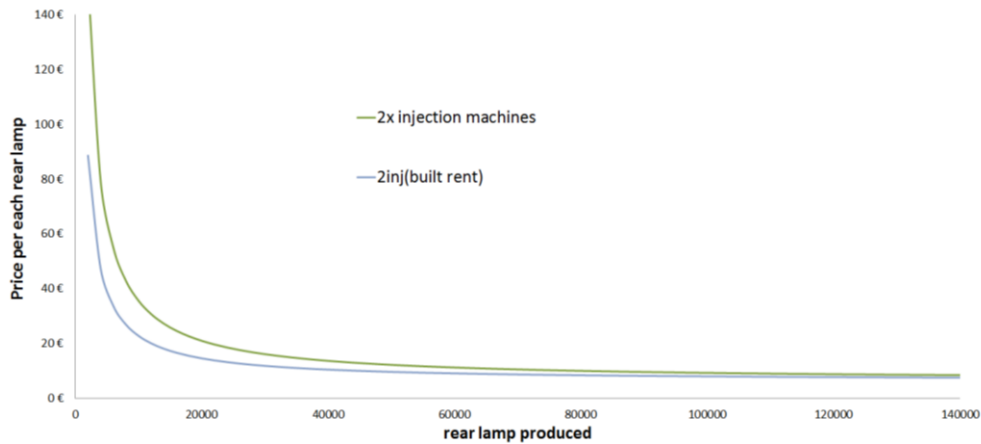


Figure 115 comparison between the new process variation with and without the rent

The variant process studied whereby two injection machines are operated in contra cycle was also evaluated with regard to the influence of the acquisition of building against renting the same building. The results were similar to those obtained in the figure 114. In this case for higher batch volumes the building has a relatively low influence on the final cost of the subsystem.

## 6.2 Conclusion

In this chapter a cost comparison between the current process and the process studied in this thesis has been undertaken. The current process present a cost similar to the process studied for production batches smaller than 2800 units. For larger production volumes, the new process produces subsystem at a lower price.

Considering a capital cost of 700 000€ for the factory building, it was decided to study and evaluate the influence of this factor in the final cost of the subsystem. The three processes evaluated showed that renting the building has more advantages than the acquisition of the building.



## Chapter 7

---

## 7 Conclusion

This chapter summarizes the conclusions of the present thesis, in respect to each of the chapters. This thesis starts with five main questions. These questions have the objective to define the research path to follow all the research process.

*The first objective achieved was “Which subsystem can be assembled using this combination of technologies?”*

The market analysis showed the negative influence of the worldwide economic crisis on all the main automotive markets. The established major markets in Europe, North America and Japan have all witnessed a decline in the sales of automobile and motorcycle. The only exception has been the emergent Indian market. This market presented an increase in sales in the period analyzed.

Two case studies were analyzed (door trim and lamps). Based on the market research, the case study that presented the higher market potential was the lamps, simply because they can be applied to automobiles and motorcycles.

In addition, the research showed that in all markets analyzed the sales of motorcycle suffered less with the economic crisis. For that reason it was concluded that motorcycle head lamps or rear lamps have more potential in terms of sales.

The best subsystem to be studied was the rear lamp since these have less complexity when compared to a headlamp.

*The second objective achieved in this thesis was “How can this integration be made?”. To be more precise how can a complete subsystem such as a motorcycle rear lamp be assembled in only one process.*

The best processes to produce several components in one process are multi material injection molding and in-mold operation. With these techniques it is possible to eliminate work-in-progress inventories and ensure correct registration or alignment of the different parts in the assembly.



To reduce the complexity of the final subsystem, the best joining technology is laser welding. Since this joining process doesn't produce a visible seam, the joint designs are simple flat to flat surfaces and the seams are hermetic.

These two processes have also the advantage of being highly automated processes.

To produce a complete subsystem in one process it was necessary to exchange the existing electric circuit technologies for new ones – conductive polymers and LEDs.

This new process started with the assembling of the LEDs, with the help of a robot or a worker, into the cavity where the electric circuit will be injected. After the mold closes, the electric circuit, the housing (with electric circuit) and the crystal are injected. To make possible the assembling of these different components the rotary plates transport the crystal to the assembly zone and the laser welds the crystal to the housing. After the process is completed the rotary plates retreat and the subsystem is extracted. The mold closes and the process starts again. With this new process we can produce a complex subsystem in one production cycle.

*The third objective achieved in this thesis was “Are there conductive polymers appropriate to be used in this process?”.*

Two electric conductive additives were tested, and the best were carbon nanotubes (CNT). The tests also showed the improvement of their conductive properties with the reduction of velocity of injection. The results also showed that for this application the best material is a mixture of 5% of CNT with PC. The PP/CNT material can also be considered although the PP/CNT admixture required 2% more CNT to obtain the same result when compared to the PC/CNT material

The study also demonstrated that these materials are capable of supporting the overmolding process, without losing electrical conductivity.

*The fourth objective achieved was related to the laser process, in this case “Which are the best laser welding properties, for joining the different components of the subsystem?”.*

Several materials were welded and the join that presented the best seam resistance was the PMMA (transparent) with the PC (absorber)

The admixture polymers with additives such as talc and glass fiber, reduced the transparency of these materials to the laser beam. The mixture of wood fibers with a polymer also reduces the transparency of this material to laser energy.

The laser welding of amorphous materials is more reliable when compared to the semi-crystalline polymers. The amorphous materials presented the seams with higher mechanical resistance.

The DOE analysis showed that the factor that has the greater influence on seam resistance is laser diameter. The results showed that reduction of the laser diameter increases the mechanical resistance of the final seam. This results means that increased laser power per unit area leads to an increase in the amount of material mixed/bonded and with this comes a higher shear stress value at rupture.

In the case study the best welding conditions obtaining are the lowest laser velocity, the lowest laser diameter and the lowest power.

*The fifth objective achieved in this thesis was “Is it possible to produce components, with a lower cost compared to the current assembling process for this case study*

This new process needs less space, fewer injection machines and fewer workers to produce a complete functional subsystem. At the same time it needs less storage capability. With this process it is also possible to reduce the factory area and to reduce the complete production time. These advantages will all reduce the final cost of the component subsystem.

Finally, a cost analysis between the current assembling process and the process studied was undertaken. The current process presented a lower cost per subsystem for production batches smaller than 2800 units; above this level of production the new process studied presented lower production costs. A variation of the process studied in this thesis was also evaluated. In this case, the possibility of working with two injection machines in contra cycle with one laser and robot was analysed. This variant is capable of producing subsystems with a lower cost compared to the process studied herein and at double the rate of production.

## Chapter 8

---

## 8 Future work

The work presented in this document does not end here and much more can be done as to;

- Study the influence of crystalline properties on the final seam quality
- Development of a mathematical model, more reliable for applying in FEM elements software
- Optimization of the electric system, with the objective of reducing the thickness and the size
- Optimization of the reflective structures, with the objective of reducing the thickness.
- Applying this process to door trims or other complex subsystem
- Studying utilization of lasers to cut and weld in the same injection process
- Optimization of the process studied in this document

## Chapter 9

---

## Bibliography

- [1] - FEENSTRA, ROBERT C. - Integration of Trade and Disintegration of Production in the Global Economy. **The Journal of Economic Perspectives**, Vol. 12, No. 4 (Autumn, 1998), pp. 31-50
- [2] - NEVES, FERNANDO. As Dez Maiores Fabricantes de Carros do Mundo”. Website founded in 13-08-2010, <http://rankz.wordpress.com/2008/08/13/as-dez-maiores-fabricantes-de-carros-do-mundo/>
- [3] - Source Wikipedia, LLC Books. - **Motorcycle Manufacturers: Moped Manufacturers, Scooter Manufacturers, Birmingham Small Arms Company, Peugeot, Honda, Ducati, Aprilia, Vespa**. LLC Books, ISBN 1157883478
- [4] - VELOSO, FRANCISCO; KUMAR, RAJIV - "The Automotive Supply Chain: Global Trends and Asian Perspectives". **Department of Engineering and Public Policy**, 2002, Paper 134.
- [5] - webbikeworld. “Motorcycle Sales Statistics, News and Information”. Website founded in 21-08-2010, Motorcycle Manufacturers: Moped Manufacturers, Scooter Manufacturers, Birmingham Small Arms Company, Peugeot, Honda, Ducati, Aprilia, Vespa <http://www.webbikeworld.com/motorcycle-news/statistics/motorcycle-sales-statistics.htm>
- [6] - Association des Constructeurs Européens de Motocycles (ACEM). “ACEM”. Website founded in 27-09-2010, <http://www.acem.eu/cms/marketfigures.php>
- [7] - Society of Indian Automobile Manufacturers (SIAM). “Domestic Sales Trend”. Website founded in 27-01-2013, <http://www.siamindia.com/scripts/domestic-sales-trend.aspx>
- [8] - Japan Automobile Manufacturers Association. Forecast for Japan's Motor Vehicle Demand. Website founded in 01-01-2013, <http://www.jama-english.jp/statistics/forecast/2012/120201.html>
- [9] - ACEA (European Automobile Manufacturers' Association). “Passenger Cars: 2009 Registrations down 1.6% compared to 2008”. Website founded in 2-08-2010, [http://www.acea.be/index.php/news/news\\_detail/passenger\\_cars\\_2009\\_registrations\\_down\\_16\\_compared\\_to\\_2008](http://www.acea.be/index.php/news/news_detail/passenger_cars_2009_registrations_down_16_compared_to_2008)

- [10] - Motor Intelligence. "SAAR Data". Website founded in 27-01-2013, [http://www.motorintelligence.com/m\\_frameset.html](http://www.motorintelligence.com/m_frameset.html)
- [11] - Japan Automobile Manufacturers Association, Inc. "Active Matrix Database System". Website founded in 27-01-2013, <http://jamaserv.jama.or.jp/newdb/eng/index.html>
- [12] - AML (peças auto). "Farol principal Audi A3 8P1". Website founded in 25-09-2010, <http://pecasautopt.com/audi-a3/18-farol-principal-alfa-romeo-audi-a3-8p1.html>
- [13] - Valeo service." Lighting and Signaling". Website founded in 25-09-2010, [http://www.valeoservice.com/html/unitedkingdom/en/products.gammesdetail-lighting\\_and\\_signaling-3223504834374DB50EF42C.html](http://www.valeoservice.com/html/unitedkingdom/en/products.gammesdetail-lighting_and_signaling-3223504834374DB50EF42C.html)
- [14] - Wipac. "lightning". Website founded in 25-09-2010, <http://www.wipac.com/products/lighting.aspx>
- [15] - Anzo USA. "Tail Lights". Website founded in 25-09-2010, <http://www.anzousa.com/azcatalog/category/view/id/4/>
- [16] - Inprocarwear. "Crystal eyes product lineup". Website founded in 25-09-2010, <http://www.inprocarwear.com/>
- [17] - Alibaba. "cn-mingzhen.e". Website founded in 22-09-2010, [http://cn-mingzhen.en.alibaba.com/productgrouplist-210416450/HID\\_Projector\\_Headlight.html](http://cn-mingzhen.en.alibaba.com/productgrouplist-210416450/HID_Projector_Headlight.html)
- [18] - Jiangsu Tianju Lamp Industrial co., ltd. "New products". Website founded in 29-09-2010, <http://www.cntianju.com/ProductShow.asp?ID=199>
- [19] - Motostrano. "Acerbis Vision Headlight". Website founded in 28-09-2010, <http://www.motostrano.com/acerbisvision.html>
- [20] - Moto lumé. "clear alternatives". Website founded in 22-09-2010, <http://clearalternatives.com/>
- [21] - Motorcycle Superstore Inc. "Moose Racing Road Warrior Headlight". Website founded in 30-04-2013, [http://www.motorcycle-superstore.com/2/9/195/34353/ITEM/Moose-Racing-Road-Warrior-Headlight.aspx?SiteID=SLI|Moose%20Racing%20Lights&WT.MC\\_ID=10010](http://www.motorcycle-superstore.com/2/9/195/34353/ITEM/Moose-Racing-Road-Warrior-Headlight.aspx?SiteID=SLI|Moose%20Racing%20Lights&WT.MC_ID=10010)
- [22] - Bikebiz. "Polisport EMX Headlight". Website founded in 1-09-2010, <http://www.bikebiz.com.au/products/Polisport-EMX-Headlight.html>
- [23] - UK bike parts. "Fairings". Website founded in 1-09-2010, <http://www.ukbikeparts.net/acatalog/Fairings.html>

- [24] - Alba action.com. "Product". Website founded in 22-09-2010, <http://www.albaaction.com/productdetail.htm?productId=8790637&catalogId=&searchProducts=headlights>
- [25] - Rinder. "Products". Website founded in 12-10-2010, <http://www.rinder.com/contenido.php?id=68&sec=1>
- [26] - Alibaba. "Changzhou Xufengzhixiu Vehicle Lamp Co., Ltd." Website founded in 26-10-2010, [http://www.alibaba.com/product-gs/257113862/front\\_lamp\\_headlamp\\_head\\_lightings\\_suit/showimage.html](http://www.alibaba.com/product-gs/257113862/front_lamp_headlamp_head_lightings_suit/showimage.html)
- [27] - Automobile Association Developments Ltd. "Daytime Running Lights (DRL)". Website founded in 08-11-2014, [http://www.theaa.com/motoring\\_advice/safety/daytime-running-lights.html](http://www.theaa.com/motoring_advice/safety/daytime-running-lights.html)
- [28] - PAINE, MICHAEL. "Review of Daytime Running Lights". Australia: NRMA Motoring & Services and RACV, 2003.
- [29] - Q&As: Daytime running lights. "Daytime running lights Insurance Institute for Highway Safety, Highway Loss Data Institute". Website founded in 12-10-2010, <http://www.iihs.org/research/qanda/drl.html>
- [30] - National Motorists Association." Daytime Running Lights" Website founded in 12-10-2010, <http://www.motorists.org/drl/>
- [31] - Faurecia. "Faurecia interior systems". Website founded in 15-1-2010, <http://www.faurecia.com/expertise-innovation/automotive-equipment/car-interior-seating/Pages/car-doors.aspx>
- [32] - Magna. "Magna Exteriors and Interiors". Website founded in 15-1-2010, [http://www.magna.com/xchg/interior\\_systems](http://www.magna.com/xchg/interior_systems)
- [33] - Johnson Controls. "Door Panels". Website founded in 15-1-2010, [http://www.johnsoncontrols.com/publish/us/en/products/automotive\\_experience/interiors/door-panels.html](http://www.johnsoncontrols.com/publish/us/en/products/automotive_experience/interiors/door-panels.html)
- [34] - Peguform. "Interiors". Website founded in 15-1-2010, <http://www.peguform.de/interiors0.html?&L=0>
- [35] - Antolin. "DTM Door Trim Module". Website founded in 15-1-2010, <http://www.grupoantolin.com/contenido1.asp?idioma=EN>
- [36] - Visteon. "Door Trim". Website founded in 08-11-2014, <http://www.visteon.com/products/interiors/index.html>
- [37] - Draexlmaier. "Door Panels". Website founded in 08-11-2014, <https://www.draexlmaier.com/en/products/door-and-cockpit-modules.html>



- [38] - Kasai Kogyo Co. Ltd. "Cabin Trim". Website founded in 18-1-2010, <http://www.kasai.co.jp/english/products/cabintrim.html>
- [39] - Gemini Group, Inc. "Vacuum Forming". Website founded in 08-11-2014, <http://geminigroup.net/plastics-interior-trim-vacuum-forming>
- [40] - Röchling-Group - Proficiency in Plastics. "Door and Side Panels". Website founded in 18-1-2010, <http://www.roechling.com/en/automotive-plastics/products/passenger-compartment/door-and-side-panels.html>
- [41] - International Automotive Components Group North America. "Interior trim". Website founded in 18-1-2010, <http://www.iacgroup.com/door-and-trim-systems;jsessionid=170A1AB3ED79D89D17659873CF795267>
- [42] - Simoldes Plastic Division. "Products". Website founded in 19-1-2010, <http://www.simoldes.com/plastics/products1.html#>
- [43] - TROUGHTON, MICHAEL. - **Handbook of Plastics Joining: A Practical Guide**. William Andrew Inc., 2008, ISBN: 9780815515814, pp. 78-93
- [44] - ROTHEISER, JORDAN- **Joining of Plastics: Handbook for Designers and Engineers**. 2 ed., Hanser Gardner Pubns, 2004. ISBN-10: 1569903549. Pp.520-542
- [45] - MACKWOOD, A.P. - **Thermal modelling of laser welding and related processes: a literature review**. **Optics & Laser Technology**, vol.37, 2005, p. 99 – 115
- [46] - JONES, IAN - Laser welding for plastic components. **Assembly Automation**, Vol. 22, n° 2, 2002, pp. 129–135
- [47] - SILFVAST, WILLIAM T.- **Laser Fundamentals**. Cambridge University press, 2° edition, pp. 1-5, 511-515,545, 550-554, 570-572, 576-597; 2004; ISBN 0 521 83345 0
- [48] - KOECHNER, WALTER- **Solid-State Laser Engineering**. Springer; Sixth Revised and Updated Edition; pp. 210-297,300, 488; ISBN-13: 978-0387-29094-2
- [49] - READY, JOHN F.; FARSON, DAVE F.-**LIA Handbook of Laser Materials Processing**. Laser Institute of America, 2001, ISBN : 9780912035154, pp.1-10
- [50] - COELHO, J.P.; ABREU, M.A.; PIRES M.C.- High-speed laser welding of plastic films. **Optics and Lasers in Engineering**, Elsevier Ltd; vol. 34; 2000; pp. 385-395

- [51] - SPEKA, MARYNA; MATTEI, SIMONE; PILLOZ, MICHEL; ILIE, MARIANA - The infrared thermography control of the laser welding of amorphous polymers. **NDT&E International**; Elsevier Ltd; vol.41; 2008; pp. 178–183
- [52] - CASALINO, GIUSEPP; GHORBEL, ELHEM-Numerical model of CO2 laser welding of thermoplastic polymers. **journal of materials processing technology**, Elsevier BV, vol. 207, 2008, pp. 63–71
- [53] - ACHERJEE, BAPPA; et al. - Experimental investigation on laser transmission welding of PMMA to ABS via response surface modeling. **Optics & Laser Technology**, vol. 44, 2012, p. 1372–1383
- [54] - ILIE, M.; *et al.* “Diode laser welding of ABS: Experiments and process modeling”. **Optics & Laser Technology**, Elsevier Ltd, vol.41, 2009, pp. 608–614
- [55] - KNEIP, J.C.; *et al* - Heat transfer in semi-transparent materials during laser interaction”. **Journal of Materials Processing Technology**, Elsevier Ltd, vol: 155–156; 2004;pp. 1805–1809
- [56] - COELHO, JOÃO M.P.; *et al* - Modelling the spot shape influence on high-speed transmission lap welding of thermoplastics films. **Optics and Lasers in Engineering**, vol. 46, 2008, p. 55–61.
- [57] - “Welding plastics without adhesives”. **Industrial laser solutions**; Penn Well Publishing Co.; September 2009; pp. 2.
- [58] - ZAK, G.; MAYBONDI L., *et al* - Weld line transverse energy density distribution measurement in laser transmission welding of thermoplastics; **Journal of Materials Processing Technology**; Elsevier Ltd; vol. 210; 2010; pp. 24–31
- [59] - ACHERJEE, BAPPA; *et al* - Effect of carbon black on temperature field and weld profile during laser transmission welding of polymers: A FEM study. **Optics & Laser Technology**, vol. 44, 2012, p.514–521
- [60] - GHORBEL, ELHEM; *et al* - Laser diode transmission welding of polypropylene: Geometrica and microstructure characterization of weld”. **Materials and Design**, vol. 30, 2009, p. 2745–2751
- [61] - MONTALVO-URQUIZO, J.; *et al* - Adaptive finite element models applied to the laser welding problem. **Computational Materials Science**, vol. 46, 2009, p. 245–254.

- [62] - TOURKI, ZOUBEIR; *et al* - Numerical study of laser diode transmission welding of a polypropylene mini-tank: Temperature field and residual stresses distribution. **Polymer Testing**, vol. 30, 2011, p. 23–34
- [63] - ACHERJEE, BAPPA; *et al.* - Prediction of weld strength and seam width for laser transmission welding of thermoplastic using response surface methodology. **Optics & Laser Technology**, vol. 41, 2009, p. 956–967
- [64] - JIMIN, CHEN; *et al.* - Parameter optimization of non-vertical laser cutting. **Int J Adv Manuf Technol**; 2007 vol.33; pp.469–473.
- [65] - VAN DE VEM, JAMES D.; *et al.* - Laser Transmission Welding of Thermoplastics—Part I: Temperature and Pressure Modeling. **Journal of Manufacturing Science and Engineering**, Vol. 129, October 2007, p. 849-858
- [66] - SULTANA, T.; *et al* - Study of two different thin film coating methods in transmission laser micro-joining of thin Ti-film coated glass and polyimide for biomedical applications . **Journal of the mechanical behavior of biomedical materials**, Elsevier Ltd, vol.2, 2009, pp. 237- 242.
- [67] - MATTEI, SIMONE; *et al* - Using infrared thermography in order to compare laser and hybrid (laser+MIG) welding processes ; **Optics & Laser Technology**; Elsevier Ltd; vol. 41; 2009; pp. 665–670
- [68] - WILD, M.J.; *et al.* - Locally selective bonding of silicon and glass with laser; **Sensors and Actuators. Elsevier Ltd**; vol. 93; 2001; pp. 63-69
- [69] - BOGLEA, ANDREI; *et al.* - Fibre laser welding for packaging of disposable polymeric microfluidic-biochips. **Applied Surface Science**; Elsevier B.V.; vol. 254; 2007; pp.1174–1178
- [70] - CHOUDHURY I.A.; SHIRLEY S. - Laser cutting of polymeric materials: An experimental investigation; **Optics & Laser Technology**; vol. 42; 2010; pp. 503–508
- [71] - CAIAZZO, F.; CURCIO, F.; DAURELIO, G.; MINUTOLO, F.; MEMOLA, CAPECE - Laser cutting of different polymeric plastics (PE, PP and PC) by a CO2 laser beam. **Journal of Materials Processing Technology**; vol. 159; 2005; pp. 279–285
- [72] - ROOKS, BRIAN - Laser processing of plastics. **Industrial Robot: An International Journal**, Volume 31, Number 4, 2004, pp. 338–342

- [73] - KURIK, M. V. - Accuracy of the Determination of absorption and reflection coefficients in absorbing media. **Zhurnal Prikladnoi Spektroskopii**, Vol. 4, No, 3, 1966, pp. 275-278.
- [74] - BERG, M.J.; et al. - Explanation of the patterns in Mie theory . **Journal of Quantitative Spectroscopy & Radiative Transfer**, vol. 111, 2010, p.782–794
- [75] - GOUESBET, G. - Cross-sections in Lorenz–Mie theory and quantum scattering: formal analogies. **Optics Communications**, vol. 231, 2004, p. 9–15.
- [76] - LOCK, JAMES - Generalized Lorenz–Mie theory and applications. **Journal of Quantitative Spectroscopy & Radiative Transfer**, vol. 110, 2009, p. 800–807
- [77] - LI, XINGCAI; et al. - The comparison between the Mie theory and the Rayleigh approximation to calculate the EM scattering by partially charged sand. **Journal of Quantitative Spectroscopy & Radiative Transfer**, vol. 113, 2012, p. 251–258.
- [78] - TRIVIC, D.N.; et al. Modeling the radiation of anisotropically scattering media by coupling Mie theory with finite volume method. **International Journal of Heat and Mass Transfer**, vol. 47, 2004, p. 5765–5780.
- [79] - ACHERJEE, BAPPA; et al. - Modeling and analysis of simultaneous laser transmission welding of polycarbonates using an FEM and RSM combined approach. **Optics & Laser Technology**, vol. 44, 2012, 995–1006
- [80] - ACHERJEE, BAPPA; et al. - Modeling of laser transmission contour welding process using FEA and DoE. **Optics & Laser Technology**, vol.44, 2012, 1281–1289.
- [81] - GLS Corporation. “Overmolding Guide”. Website founded in 21-08-2011, [www.glstpes.com/pdf/om.pdf](http://www.glstpes.com/pdf/om.pdf)
- [82] - CUNHA, A. M., PONTES, A.J., – **Non-conventional injection molds**. In *Injection molding: Fundamentals and application*, Chapter 4. M. R. Kamal, A. Isayev, and S.-H. Liu (eds), Hanser publishers, Munich, 2009. 21 Chapters, p. 926, ISBN: 978-1-56990-434-3
- [83] - KNIGHTS, MIKELL. “In-mold assembling: the new frontier for multi-shot molding”, website founded in 20-03-2012, <http://www.ptonline.com/articles/in-mold-assembly-the-new-frontier-for-multi-shot-molding>
- [84] - CUNHA, ANTÓNIO; et al – técnicas não convencionais. In *Centimfe – Manual do projectista para moldes de injeção de plástico*. Marinha Grande: Centimfe, 2004, ISBN 972-98872-1-7, pp. 13-35.

- [85] - GOODSHIP V. ; Love, J.C. - **Multi-Material Injection Molding**. Rapra Technology Limited, Shawbury, Shrewsbury, Shropshire SY4 4NR, United Kingdom, report 145, Volume 13, Number 1, 2002. ISSN: 0889-3144
- [86] - Ferromatik Milacron GmbH. “in mold labeling”. Website founded in 30-03-2013, <http://www.ferromatik.com/en/anwendungstechnik/in-mold-labeling.php>
- [87] - DEVLIN, ROBERT et al., Inventor; Devlinks, Ltd. “In-Mold Labeling”. US20130258034 A1 - 3 Out 2013
- [88] - Nissha Printing Co., Ltd.-“IMD” website founded in 24-02-2014, [http://www.nissha.com/english/products/industrial\\_m/imd/index-exposition.html](http://www.nissha.com/english/products/industrial_m/imd/index-exposition.html)
- [89] - Plas-Tech Engineering. “MOLDING - DIE SLIDE INJECTION”. website founded in 20-03-2012, <http://www.plastechengineering.com/Molding/dsi.asp>
- [90] - Ferromatik Milacron. “Ice Cold Trick”, website founded in 20-03-2012, <http://www.ferromatik.com/en/technologie/verfahrenstechniken/mehrkomponenten/index.php>
- [91] - Styner-bienz. “FOBOHA twin cube technology”. website founded in 20-03-2012, <http://styner-bienz.com/technologies/injection-molding-technology-plastics/fobo-ha-stack-turning-technology/fobo-ha-twin-cube-technology.html>
- [92] - Plasdan - New Concepts in tooling for integrated manufacturing. Website founded in 24-02-2014, <http://www.kunststoffenbeurs.nl/assets/Uploads/29-9-Hacoplast.pdf>
- [93] - Hearst Business Communications, Inc. “LEDs for More Efficient Automotive Lighting Solutions”. Website founded in 13-10-2010, [http://www.semiapps.com/LEDs\\_For\\_More\\_Efficient\\_Automotive\\_Lighting\\_Solutions.aspx](http://www.semiapps.com/LEDs_For_More_Efficient_Automotive_Lighting_Solutions.aspx).
- [94] - V., STEELE ROBERT. - OptoIQ - Gateway to the application of light.” Website founded in 13-10-2010, <http://www.optoiq.com/index/photronics-technologies-applications/lfw-display/lfw-article-display/241158/articles/laser-focus-world/volume-41/issue-11/features/high-brightness-leds-led-automotive-headlamps-move-closer-to-market.html>
- [95] - MUTHU, SUBRAMANIAN; SCHUURMANS, FRANK J.; PASHLEY MICHAEL. “Red, Green, and Blue LED based white light”. **IEEE**, 2002, p. 327-333
- [96] - Hearst Business Communications, Inc. “LEDs for More Efficient Automotive Lighting Solutions”. Website founded in 13-10-2010,

[http://www.semiapps.com/LEDs\\_For\\_More\\_Efficient\\_Automotive\\_Lighting\\_Solutions.aspx](http://www.semiapps.com/LEDs_For_More_Efficient_Automotive_Lighting_Solutions.aspx).

- [97] - HELD, GILBERT. **Introduction to Light Emitting Diode Technology and Applications**. Auerbach Publication, 2009, pp. 1-22, ISBN-13: 978-1420076622
- [98] - Pratt, Colin. "Applications of conductive polymers". Website founded in 12-10-2010, <http://homepage.ntlworld.com/colin.pratt/applcp.htm>
- [99] - MORALES, G.; BARRENA M.I.; et al. - "Conductive CNF-reinforced hybrid composites by injection molding". **Composite Structures**, vol. 92, 2010, p. 1416–1422.
- [100] - VAN HATTUM, F. - "Conductive long fibre reinforced thermoplastics by using carbon nanofibres". **Plastics, Rubber and Composites**, Vol 35, n° 6, 2006.
- [101] - HIGGINS, BERNADETTE A.; et al. - "Polycarbonate carbon nanofiber composites". **European Polymer Journal**, vol.41, 2005, p. 889–893
- [102] - ZENG, JIJUN; et al. - "Processing and properties of poly(methyl methacrylate)/carbon nanofiber composites". **Composites: Part B**, vol.35, 2004,p. 245–249.
- [103] - MALLETT, J. G.; et al. - "Carbon Black Filled PET/PMMA Blends: Electrical and Morphological Studies". **Polymer Engineering and science**, Vol. 40, October 2000, No. 10, p.2272-2278.
- [104] - MORALES, G.; BARRENA, M.I.; et al. - "Conductive CNF-reinforced hybrid composites by injection molding". **Composite Structures**, vol. 92, 2010, p. 1416–1422.
- [105] - JANA, SADHAN C. - "Loss of Surface and Volume Electrical Conductivities in Polymer Compounds Due to Shear-Induced Migration of Conductive Particles". **Polymer Engineering and Science**, Vol. 43, March 2003, n°. 3, p.570-579
- [106] - AL-SALEH, MOHAMMED H.; et al. - "Electrically conductive carbon nanofiber/polyethylene composite: effect of melt mixing conditions". **Polym. Adv. Technol.**, Vol. 22, 2011, p. 246–253.
- [107] - WEBER, MARK; et al. - "Estimation of the Volume Resistivity of Electrically Conductive Composites". **Polymer Composites**, Vol. 18, December, 1997, n°. 6, p.711-725
- [108] - VILLMOW, TOBIAS; et al. - "Influence of injection molding parameters on the electrical resistivity of polycarbonate filled with multi-walled carbon nanotubes". **Composites Science and Technology**, vol. 68, 2008, p. 777–789.

- [109] - HONG, CHANG-MIN; et al. - Shear-Induced Migration of Conductive Fillers in Injection Molding. **Polymer Engineering and Science**, Vol. 44, November 2004, nº11, p.2101-2109
- [110] - CHANDRA, ALEXANDER; et al. - **Effect of injection molding parameters on the electrical conductivity of polycarbonate/carbon nanotube nanocomposites**. Antec, 2007, p.2184-2188
- [111] - MAHMOODI, MEHDI; et al. - The electrical conductivity and electromagnetic interference shielding of injection molded multi-walled carbon nanotube/polystyrene composites. **Carbon**. Vol. 50, 2012, p. 1455–1464.
- [112] - UNECE Vehicle Regulations - 1958 Agreement; Regulation No. 50 - Rev.2 - Position lamps, stop lamps, direction indicators for motor cycles
- [113] - Vehicle inspection requirements manual In-service certification; vol2; Version 4; NZ Transport Agency; April 2010; pp. 4-1-1to 4-11-1
- [114] - Invicta escola de condução. “O condutor e o Veículo”. 2001, Website founded in 12-10-2010, <<http://www.invicta.com.pt/codigo/iluminacao.asp>>
- [115] - Lumileds Lighting U.S. LLC. AB20-1 Using SuperFlux LEDs In Automotive Signal Lamps, website, website founded in 20-06- 2011, <[www.philipslumileds.com/uploads/207/AB20-1-PDF](http://www.philipslumileds.com/uploads/207/AB20-1-PDF)>
- [116] - Lumileds Lighting U.S. LLC. AB20-4 Thermal Management Considerations for SuperFlux LEDs, website founded in 20-06-2011,<[www.philipslumileds.com/uploads/226/AB20-4-PDF](http://www.philipslumileds.com/uploads/226/AB20-4-PDF)>
- [117] - Lawrence, Mark. “Motorcycle Headlights and Tail Lights”.Website founded in20-6-2011, <<http://motorcycleinfo.calsci.com/Lights.html>>
- [118] - Lumileds Lighting U.S. LLC. AB20-3 Electrical Design Considerations for SuperFlux LEDs, website founded in 20-06-2011,<[www.philipslumileds.com/uploads/208/AB20-3-pdf](http://www.philipslumileds.com/uploads/208/AB20-3-pdf)>
- [119] - Nanocyl s.a. “Nanocyl™ NC 7000 Thin Multiwall Carbon Nanotubes”. Website founded in 12-4-2012, <http://www.nanocyl.com/en/Products-Solutions/Products/Nanocyl-NC-7000-Thin-Multiwall-Carbon-Nanotubes>
- [120] - Lumileds Lighting U.S. LLC. AB20-5 Secondary Optics Design Considerations for SuperFlux LEDs, website founded in 20-06- 2011, [www.philipslumileds.com/uploads/227/AB20-5-PDF](http://www.philipslumileds.com/uploads/227/AB20-5-PDF)

[121] - TOMINAGA, MOTONORI; et al, Inventor; Denso Corporation - Vehicle headlamp assembly with convection airflow controlling plate. US 8678631 B2 - 25 Mar 2014.



# Annexes

---



